ANTITUMOR AND ANTIOXIDANT ACTIVITY OF *ESCHERICHIA COLI* IS ACCOMPANIED BY CHANGES IN THE L-ARGININE DICHOTOMOUS PATHWAYS IN PERITONEAL AND BLOOD LEUKOCYTES FOLLOWING EHRLICH ASCITES CARCINOMA

N. Kh. Alchujyan[a]*, H. A. Movsesyan[a], A. A. Aghababova[a], A. G. Guevorkyan[b], N. H. Movsesyan[a], H. F. Khachatryan[a], V. H. Barseghyan[a], H. L. Hairapetyan[a], L. S. Sahakyan[c], L. G. Avanesyan[d], L. H. Melkonyan[a], K. A. Barseghyan[a] and G. A. Kevorkian[a]

Keywords: arginase, cytoplasm, Ehrlich ascites carcinoma, *Escherichia coli*, leukocyte, lipid peroxidation, mitochondria, nitric oxide synthase.

The effectiveness and mechanisms of antitumor activity of non-pathogenic *Escherichia coli* EM0 strain using mouse model of Ehrlich ascites carcinoma (EAC) is studied. 48 h after inoculating EAC cells, a single noninvasive treatment of the 2-month-old male white mice's eyes and mouths with live *E. coli* isolate increased the life span by 75% (P<0.001). Furthermore, a significant decrease in the volume of ascites fluid (66.5 %, P<0.01) was determined, accompanied by down-regulation of EAC-activated lipid peroxidation processes and changes in the L-arginine metabolic profile in leukocytes as early as within 9 days of post-treatment compared to non-treated EAC-bearing mice. We found EAC-induced stimulation of arginase and nitric oxide synthase (NOS) activity correlated with the levels of their common substrate, L-arginine and products (arginase-derived L-ornithine and NOS-derived NO and L-citrulline) in the cytoplasm and mitochondria of peritoneal and blood leukocytes. The biochemical pattern was differentially modulated by *E.coli* treatment depending on whether leukocytes were localized in the ascitic fluid or the peripheral blood. *E. coli* concentrated in the ascitic fluid directly affected the surrounding cells including peritoneal leukocyte in which it decreased the activity of two arginase isoforms and a total NOS in the cytoplasm. Negligible number of *E coli* at sites remote of tumor suggests its indirect effects particularly via stimulation of LPS-mediated non-specific immune response associated with activation of arginase and NOS in the cytoplasm of blood leukocytes. The data obtained should be taken into account in the further study aimed to use non-pathogenic *E. coli* strains in the adjuvant therapy of ascites tumors.

* Corresponding Authors
E-mail: alchujyan@mail.ru
[a] H. Buniatian Institute of Biochemistry NAS RA, 5/1 P. Sevak St., 0014, Yerevan, Republic of Armenia
[b] Yerevan State Medical University after M. Heratsi (YSMU)
[c] R. O. Eolyan Hematology Center, MH RA (HC)
[d] Kh. Abovyan Armenian State Pedagogical University (ASPU)

INTRODUCTION

Although conventional anticancer treatment methodologies are effectively used, but for about half of cancer patients these are ineffective.[1] Outcomes of cancer treatments depend on plenty of factors, many of which are still unknown. Leukocytes infiltrate and interact with tumor and can cause either destruction of the tumor or promotion of malignancy.[2] Understanding the metabolic interplay between tumor and immune system will guide the development of optimal metabolic interventions on cancer.[3] Recent findings in tumor bearing mice and most human cancers indicate that accumulation of myeloid-derived suppressor cells (MDSC), heterogeneous cell population consisted of granulocyte, and mononuclear cells play a significant role in tumor-associated inflammation and immunosuppression.[4] Myeloid-derived cell immuno-suppressive activity is provided by production of reactive oxygen species, and over-expression of cytoplasmic arginase (ARG1) and inducible NO synthase (iNOS).[5] The critical interplay between arginase and NOS sharing a common substrate, L-arginine is involved in the cellular immune response and outcome of several pathologic conditions by modulating either the amount of NO produced or metabolic intermediates of the arginase pathway comprising L-ornithine, the precursor of polyamines essential for cell proliferation and urea which participates in detoxification of protein degradation.[6] Up-regulation ARG1 and iNOS expression is implicated in the suppression of T cell proliferation and IFN-γ production by MDSCs.[7] Inversely, inhibition of suppressive effects of CD11b+/Gr-1+ MDSCs is associated with a down-regulation of the mentioned enzymes, accompanied by enhanced T cell infiltration of the tumor and reduction of tumor growth.[8] Modulation of expression and activity of both arginase and NOS by various pathogenic microbes has been reported.[9,10] At the same time certain bacteria could be used for treatment of neoplasia.[11] They accumulate in the tumor microenvironment and induce specific and non-specific antitumor immune response, inhibiting carcinogenesis and thus offering a potential tool for cancer therapy.[12]

Previous findings suggest that administration of *E. coli* (a gram-negative facultative anaerobe of the intestine of healthy people and animals) or priming with

lipopolysaccharide (LPS) (the major component of the cell wall of gram-negative bacteria) cause a production of tumor necrosis factor by activated macrophages, which suppresses proliferation of tumor cells prolonging a survival time of mice in Ehrlich ascites carcinoma (EAC).[13,14] Phagelysates of *E. coli* potentiate antitumor effects of drugs (combination of doxorubicin, cyclophosphan, and fluorouracil) elevating the intrinsic resistance to a cytotoxicity of EAC cells, and inhibiting a selective growth advantage of tumor cells over normal cells by 80-90% without apparent side effects.[15] Nevertheless, the impact of *E. coli* on the tumor-induced molecular changes in the immune cells is not fully elucidated. Notably, *E. coli* could be eliminated by iNOS-derived nitric oxide (NO), the central component of innate immunity contributed to antibacterial activity in the host.[16] Peritoneal macrophages has shown express high levels of the iNOS, and released substantial amounts of NO in ascitic fluid of tumor-bearing animals.[17] As a consequence, the occurred *E. coli* deficit may contribute to alterations in microbiota that should affect various metabolic pathways including those of L-arginine.[9] This could be prevented by administration of *E. coli,* which plays a selective role in regional gut immunity via transient modulation of the host intestinal microflora and the capacity to interact with the immune system directly or mediated by the autochthonous microflora.[18] We propose that *E. coli* could affect reactive oxygen species production and arginine metabolizing enzymes considered as therapeutic targets in cancer treatment. This study was undertaken to evaluate the effectiveness and mechanisms of antitumor activity of *E. coli* using well-established mouse model of EAC.

EXPERIMENTAL

Materials

Dulbecco's modified Eagle medium (DMEM) was from Serva (Heidelberg, Germany). Bovine serum albumin was from Carl Roth (GmbH, Karlsruhe). N^G-monomethyl-L-arginine hydrochloride was obtained from Calbiochem (La Jolla, CA). All other reagents were purchased from Sigma-Aldrich (St. Louis, MO, USA).

Animals and treatments

All procedures involving animals were in accordance with the International Laboratory Animal Care and the European Communities Council Directive (86/809/EEC) and approved by the respective local committee on biomedical ethics (H. Buniatyan institute of biochemistry, Yerevan, RA). 2-month-old male white mice weighing 20.3 ± 0.2 g from our breeding colony were used. All animals were maintained on a 12 h light/dark cycle at normal room temperature and housed in groups of 6/cage with free access to food and tap water.

Experimental design

The animals were divided into groups (n = 18 mice/group): control group - native mice; the first experimental group - mice inoculated intraperitoneally (*ip*) with EAC cells (0.2 ml of 1.5 × 10^7 cells); the second experimental group - mice treated with *E. coli* (10^9 CFU/ml) 48 h after EAC inoculation. A single non-invasive treatment of eyes and mouth of mice with live bacteria was performed. On the 11^{th} day after tumor implantation, all the experimental animals were sacrificed by decapitation and the ascitic fluid was collected for measuring the volume and leukocyte separation.

Bacteria. The *E. coli* strain EM0 isolated from the fecal flora of a healthy human volunteer was kindly supplied by Dr. I. Hakobyan ("Armenicum", Clinical Center, Armenia). Commensal *E coli* isolate were propagated in Luria-Bertani broth (Difco Lab., Detroit, MI, USA) for 18-24 h at 37 °C under aerobic conditions, and suspended after centrifugation and adjusted to the appropriate concentration in sterile 20 mM HEPES buffer (pH 7.4).

Determination of survival time. Two groups of male white mice (18/group) were used. EAC cells were inoculated to each group of mice and treatment with *E. coli* was performed 48 h after tumor cells inoculation. Host survival was recorded and expressed as mean survival time (MST, in days) and percent of increase in life span (ILS) was calculated by the following formula: MST = (Day of first death + Day of last death) / 2; ILS = [(MST of EAC/E. coli group/MST of EAC group) –1] × 100.[19]

Isolation of resident peritoneal cells. After decapitation, healthy control mice were fixed and 20 mM HEPES buffer (pH 7.4) was injected by sterile syringe into the abdominal cavity, to collect peritoneal cells. Cell suspension was centrifuged at 1000 rpm for 10 min, the precipitated cells were suspended in DMEM (liquid medium (1X) with Na_2CO_3, without glutamine), cultured at 37 °C for 24 h, and centrifuged at 1000 rpm for 10 min. Supernatant was discarded, cells in the pellet were washed twice with 20 mM HEPES buffer (pH 7.4) and used to isolate resident peritoneal leukocytes.

Ehrlich ascites carcinoma was maintained in 3-month-old white mice in ascitic form under a week passage. Ascitic fluid from the mice was collected by *ip* puncture using a sterile syringe and the volume was measured to evaluate tumor growth. The ascitic fluid was centrifuged at 1000 rpm for 10 min, and the precipitated cells were washed twice with 20 mM HEPES buffer (pH 7.4) and used to isolate peritoneal leukocytes of EAC-bearing mice.

Isolation of peritoneal and blood leukocytes. Peripheral blood was drawn into 3.8% sodium citrate anticoagulant, mixed with 6 % dextran (prepared on 0.9 % NaCl) and incubated at 37 ºC for 60 min to remove erythrocytes from the fresh blood by gravity sedimentation. The decanted layer was centrifuged at 4 °C (6000 rpm, 10 min) and blood plasma was obtained in supernatant.

The blood decanted layer, resident peritoneal cells and ascitic fluid were admixed with 20 мM HEPES buffer (pH 7.4) at a ratio of 1:1 (v/v) and applied to ficoll-verografin gradient centrifugation at 3000 rpm for 20 min. Mononuclear cells and granulocyte were recovered in the density fractions of 1.087 and 1.129 g • ml^{-1} respectively, collected, washed twice, suspended in 20 мM HEPES buffer (pH 7.4) containing 0.25 M sucrose and combined in one leukocyte fraction.

Leukocyte subsets were identified in fixed smears stained by the Romanovsky-Giemsa method.[20] All cell preparations consisted of about 90 to 95 % viable cells as determined with the trypan blue exclusion test.

Preparation of cytoplasmic and mitochondrial fractions was performed by differential centrifugation.[21] Leukocytes suspended in 20 мM HEPES buffer containing 0.25 M sucrose (pH 7.4) were homogenized (1500 rpm, 3 min), centrifuged at 4 ºC (1200 rpm, 10 min) to remove nuclear fraction and cell debris. Pellet was discarded and the supernatant was further centrifuged at 4 ºC (11000 rpm, 20 min) to yield the crude mitochondrial preparation which was washed, suspended and homogenized in 20 mM Hepes buffer containing of 0.1 M NaCl, 10 % glycerol, 0.1 % Triton X-100-PC, and cocktail of protease inhibitors (Roche, Basel, Switzerland). The supernatant was used as the cytoplasm.

Measurement of L-arginine. Samples were deproteinized with 0.5 N NaOH and 10 % $ZnSO_4$. Following a centrifugation (15000 rpm, 3 min), the protein-free supernatants were sampled and analyzed for L-arginine according to Akamatsy & Watanabe with our modification.[24] Briefly: a sample of supernatant diluted with distilled water (1:1, v/v) was added in a ratio 3:1 (v/v) to a reagent (mixture of equal amounts of 0.4 % 8-oxychinoline in 96 % ethanol, 5 % sulfosalicylic acid in 0.01 M glycine buffer, 2.5 % NaOH), stirred with 1 % solution of sodium hypobromite and the absorbance was measured at 525 nm wavelength against reagent blank containing all the reagents minus the sample.

Arginase assay. The samples were added to the reaction mixture: 20 mM HEPES buffer containing 2 mM dithiothreitol (pH 7.4), 1.5 mM $MnCl_2 \cdot 4H_2O$, 4.75 mM L-arginine·HCl and incubated at 37 °C for 60 min, followed by the addition of 10 % TCA to stop the reaction.[22] Parallel control experiments were conducted in the presence of 60 mM L-valine, a non-selective inhibitor of the arginase isoforms. Following a centrifugation (15000 rpm, 3 min) the supernatants were sampled and analyzed for L-ornithine content. The arginase activity expressed as produced in an hour L-ornithine per mg of total protein.

Measurement of L-ornithine. Samples were mixed with 4.5 % ninhydrin (1:1,v/v), heated (90 ^oC, 20 min), cooled to the room temperature and the absorbance was measured at 505 nm wavelength against reagent blank containing all the reagents minus the sample.[22]

Nitric oxide synthase assay. A total NOS activity was assessed by measuring stable intermediate of NO, nitrite (NO_2^-) accumulated during a long-term incubation of samples (37 °C for 22 h) in 20 mM HEPES buffer (pH 7.4), containing 2 mM dithiothreitol and 3 mM $MgCl_2 \cdot 6H_2O$, in the presence of NOS substrate, 5.5 mM L-arginine·HCl, and cofactors: 0.2 mM NADPH, 6 μM FAD, 5.5 μM FMN, 20 μM ((6R)-5,6,7,8-tetrahydro-L-biopterin dihydro- chloride) and 1.7 mM $CaCl_2$. Parallel control experiments were conducted in the presence of 5 mM N^G–monomethyl-L-arginine hydrochloride, non-selective inhibitor of all the NOS isoforms. Reaction was initiated by addition of samples to the incubation medium and terminated by subsequent addition of 0.5 N NaOH and 10 % $ZnSO_4$. Following a centrifugation (15000 rpm, 3 min) the supernatants were sampled and analyzed for nitrite content. The NOS activity expressed as produced in 22 h nitrite per mg of total protein.

Measurement of nitrite. Samples were deproteinized with 0.5 N NaOH and 10 % $ZnSO_4$. Following a centrifugation (15000 rpm, 3 min), the protein-free supernatants were sampled and analyzed for nitrite using colorimetric technique based on diazotization.[23] Samples were mixed in equal parts with Griess-Ilosvay reagent (1:1 mixture of 0.17 % sulfanilic acid and 0.05 % α-naphthylamine in 12.5 % acetic acid), and the absorbance was measured at 546 nm wavelength against reagent blank containing all the reagents minus the sample.

Measurement of L-citrulline. Samples were deproteinized with 10 % TCA, centrifuged (15000 rpm, 3min), then protein-free supernatants were mixed with 9.6 % H_2SO_4 and reagent (5 mÌ diacetylmonoxime, 0.9 mM thiosemicarbazide, and 0.025 mÌ $FeCl_3$) at a ratio of 1:1:1 (v/v), heated in a boiling water bath for 10 min, cooled to the room temperature and the absorbance was measured at 490 nm wavelength against reagent blank containing all the reagents minus the sample.[25]

Indices of oxidative stress referring to lipid peroxidation processes were established by measuring malondialdehyde (MDA) using thiobarbituric acid.[26] Samples were deproteinized with 10 % TCA and the precipitates were removed by centrifugation at 15000 rpm for 3 min, supernatants obtained were mixed with 0.72 % TBA and 0.6 N HCl in proportion 1: 0.8 : 0.2 (v/v), heated for 15 min in boiling water bath that resulted in the formation of pink-colored secondary product of MDA and the absorbance was measured at 535 nm wavelength against reagent blank containing all the reagents minus the sample.

Protei*n* was determined using crystalline bovine serum albumin as standard.[27]

Statistical analysis. All data were analyzed using a one-way analysis of variance (ANOVA) followed by post hoc Holm-Sidak test (SigmaStat 3.5 for Windows). Relationships between biochemical parameters studied were determined calculating the Pearson linear correlation coefficient (r). Data are expressed as the mean ± S.E.M. Differences are considered significant at $P < 0.05$.

RESULTS AND DISCUSSION

Before presenting the major experimental results, we would like to briefly discuss cell separation procedures that were used to facilitate the analysis of the functional capacities of leukocyte and neoplastic cells from malignant effusions. Current evidence suggests a complex alteration of immune cell differentiation and function in cancerous conditions that involves polymorphonuclear and monocytic cells, including MDSC, immunosuppressive tumor-associated macrophages and regulatory T cells.[28,29] We have studied an overall picture of immune response using the joined fraction of granulocyte and mononuclear cells (macrophage/monocyte and lymphocyte) recovered in the density fractions 1.129 and 1.087 g • ml^{-1} respectively, including the low density granulocyte recovered with

mononuclears in EAC-bearing mice. Notably, there are the findings of other authors that activated granulocytes in advanced cancer patients and healthy donor with N-formyl-L-methionyl-L-leucyl-L-phenylalanine (both may inhibit cytokine production by T cells) exhibit low density and co-purified with low density peripheral blood mononuclears.[30] At the same time, conventional mast cells have a greater density than granulocytes up to 1.2g • ml^{-1}, while the mast cells from tumor are recovered with malignant EAC cells in the lowest density fractions (up to 1.06 g • ml^{-1}), because of high content of lipid and mucopolysaccharide laden vacuoles.[31] It should be noted that mast cells were not studied in the present work.

Antitumor and antioxidant effects of E. coli following Ehrlich ascites carcinoma

E coli strain EM0 isolated from the feces of a healthy human volunteer was used for treatment of EAC-bearing mice. It is described as a non-pathogenic strain that had no adverse effect in germfree mice after colonization, despite the fact that EM0 may express hemolysin and cytotoxic necrotizing factor in vitro.[32] Two days after EAC transplantation, a single non-invasive treatment of eyes and mouth of two-month-old white male mice with live *E. coli* isolate prolonged a life span by 75 %. On 11th day of EAC, *E. coli* caused a decrease of approximately thrice in the volume of ascitic fluid that accompanied by appropriate changes in the body weight of animals. Previously, we have demonstrated that after administration, *E. coli* is mainly concentrated in the ascitic fluid of EAC-bearing mice, and a much less its number was detected at sites remote from tumor, particularly in blood.[33] Concomitantly, *E. coli* induced inflammatory response which interfered with induction and maintenance of the oncogenic phenotype of cancer cells appearing as a diminished anaplasia, in contrast to non-treated animals.

Both macrophages and neutrophils are activated in tumor-bearing patients and experimental animals and produce the elevated levels of reactive oxygen species (ROS) and down-regulate the ROS scavengers and antioxidant enzymes thus contributing to the oxidative stress associated with immunosuppression and carcinogenesis.[34,35] Carcinoma cells also produce ROS and other free radicals at elevated rates in vitro, and, many tumors have developed resistance то oxidative stress in vivo.[36] High activity of antioxidant enzymes may contribute to resistance of tumor cells to overproduction of ROS. Notably, a significant up-regulation of superoxide dismutase (SOD) is observed on the stationary phase of EAC cells.[37] At the same time, impaired functioning of the antioxidant system is demonstrated in the leukocytes isolated from area of tumor growth and blood.[38] Neutrophils from the blood of patients with larynx carcinoma exhibit low level of SOD prior to surgery, especially in the patients with advanced tumor stages.[34]

Our data also suggests the prevalence of oxidative stress in the leukocyte over that of tumor cells on the 11th day of EAC development, viz. the level of a marker of oxidative stress, MDA (a measure of lipid peroxidation) was two-fold higher in the homogenates of peritoneal leukocytes (PL) than in EAC cells (165.3 ± 26.4 vs. 82.0 ± 11.2 pmol MDA • mg^{-1} protein respectively). Lipid peroxidation processes were significantly stimulated in PL and blood in EAC, and inhibited following *E. coli* treatment (Fig. 1). The MDA levels were increased to 41-, and 11-fold in the cytoplasm and mitochondria of PL, and to 7-, and 5-fold in those of blood leukocyte (BL), as well as to 4.6- fold in blood plasma of EAC-bearing mice compared respectively to the basal levels.

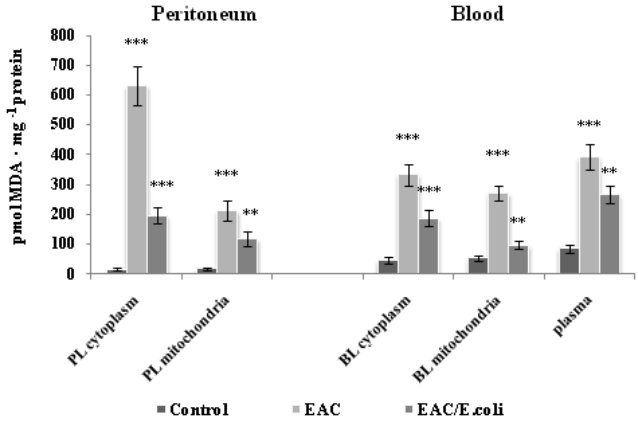

Figure 1. Lipid peroxidation in the peritoneum and blood following Ehrlich ascites carcinoma (EAC) and *E. coli* treatment. Data are expressed as $M \pm SEM$, n=18. The confidence probability (p) of parameters evaluated for EAC-bearing mice compared to the control, and p for *E. coli*-treated mice compared to untreated EAC-bearing mice. Peritoneal leukocytes (PL): cytoplasm - F=59.3, p<0.001; mitochondria - F=16.1, p<0.001. Blood leukocytes (BL): cytoplasm - F=30.2, p<0.001; mitochondria - F=40.9, p<0.001; plasma - F=24.4, p<0.001. # p >0.05, * p <0.05, ** p <0.01, *** p<0.001.

After *E. coli* treatment, the MDA amounts decreased by 3.2 and 1.8 times in the cytoplasm and mitochondria of PL, and by 1.8 and 2.8 times in those of BL compared respectively to EAC-bearing mice. Simultaneously, the MDA level in plasma dropped lower than control values. Hence, *E. coli* may counteract the oxidative stress, particularly EAC-induced redox imbalance in leukocytes preventing their oxidative damage and impairment in antitumor activity. The inhibition of ROS production by immune cells could cancel their suppressive effects in mice and patients with cancer.[28,39] Antioxidant activity of E. coli appears to be due to its polyamines, which are effective scavengers of ROS, and could also trigger a transcription of protective proteins under conditions of strong oxidative stress.[40] Capability of *E. coli* to rapidly adapt to the oxidative environment was demonstrated on the *E. coli* strain MG1655 which metabolite profile was normalized in 40-60 min after exposure to a sub-lethal concentration of hypochlorite.[41]

One interesting observation is a profound increase in the L-arginine level in leukocytes following EAC (Fig. 2). The L-arginine content was approximately the same and distributed equally in the cytoplasm and mitochondria of both PL and BL under physiological circumstances. On the 11th day of EAC transplantation, the L-arginine content was elevated by 4.4 and 2.3 times in the cytoplasm and mitochondria of PL, and by 4.2 and 3.8 in the cytoplasm and mitochondria of BL compared respectively to control. The most significant increase in the L-arginine level was observed in plasma (about 11-fold) in which it was higher than that in leukocyte.

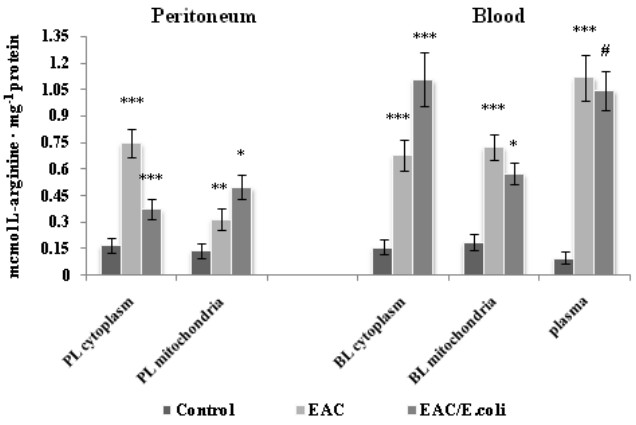

Figure 2. L-arginine level in the peritoneum and blood following Ehrlich ascites carcinoma (EAC) and *E. coli* treatment. Data are expressed as $M \pm$ SEM, n=18. The confidence probability (p) of parameters evaluated for EAC-bearing mice compared to control, and p for *E. coli*-treated mice compared to untreated EAC-bearing mice. Peritoneal leukocytes (PL): cytoplasm - F=22.4, p<0.001; mitochondria - F=9.6, p<0.001. Blood leukocytes (BL): cytoplasm - F=21.6, p<0.001; mitochondria - F=21.5, p<0.01; plasma - 32.2, p<0.001. # p >0.05, * p <0.05, ** p <0.01, *** p<0.001.

An elevation of the arginine content might be a consequence of EAC-induced exacerbation of free radical oxidation that apparently may intensify intracellular protein degradation. In turn, the tRNA mediated, posttranslational, N-terminal arginylation of proteins (occurred in all eukaryotic cells) may lead to rapid ubiquitination of arginylated proteins degraded by cytosolic proteases by the N-end rule pathway.[42] High amounts of L-arginine may affect the ion balance causing resistant hyperkalemia, a typical and the most life-threatening of tumor lysis syndrome.[43,44] Hence, negative consequences at this stage of EAC appear to be caused not by arginine deficiency, but rather of its increase.

Despite of a decrease in the arginase activity (vide infra), the L-arginine level dropped twice in the cytoplasm of PL following *E. coli* treatment. Simultaneously, L-arginine content was elevated by 1.6 times in the mitochondria of PL, possibly, due to *E. coli*-mediated normalization of the mitochondrial arginase activity (vide infra) and/or penetration of amino-acid from the cytoplasm. *E. coli*-induced decrease in oxidative stress might interfere with protein breakdown served as a source of L-arginine and diminish the L-arginine level. Notably, the cytoplasmic L-arginine high pool in contrast to other creatine analogues and related compounds can inhibit creatine transporters localized on inner and outer mitochondrial membrane fractions and interfere with the creatine transport from cytoplasm into mitochondria.[45] Thus, *E. coli* mediated modulation of the L-arginine level in the cytoplasm of PL could facilitate their energy production.

L-arginine may be converted to agmatine by the cytosolic arginine decarboxylase of *E. coli* in which it exists in constitutive and inducible isoforms.[46] Agmatine in turn may serve as a free radical scavenger by protecting against the oxidation of sulfhydryl groups and decreasing hydrogen peroxide content, preserving from mitochondrial damage and apoptosis.[47] At the same time, agmatine released into ascitic fluid may exert cytostatic activity in proliferating cancer cells, because of its preferable uptake by transformed cell with short cycling times lines (H-ras- and Src-transformed murine NIH/3T3 cells, Ras/3T3 and Src/3T3, respectively) accompanied by a suppression of cell growth via agmatine-mediated induction of the antizyme synthesis, which inhibits ornithine decarboxylase activity attenuating polyamine formation.[48,49] Further, *E. coli* lacks endogenous arginase and NO-synthase, enzymes that can compete with arginine decarboxylase.[50,51]

E. coli caused a 1.6-fold increase in the L-arginine level in the cytoplasm of BL and a slight decrease in the mitochondria of BL compared to non-treated EAC-bearing mice, whereas no changes were detected in blood plasma. As noted, after treatment a much less number of *E. coli* was observed in blood, compared to ascitic fluid, and signaling mechanisms appear to be involved, particularly *E. coli's* LPS among other pro-inflammatory stimuli can upregulate the L-arginine cationic amino acid transporter 2 (CAT2).[52] This may contribute to *E. coli*-induced elevation of the arginine level in BL. Presumably, L-arginine would be utilized by such arginine-metabolizing enzymes as ARG1 and NOS that are also activated in the cytoplasm of BL following *E. coli* administration (vide infra). Early concomitant induction of iNOS, ARG2, argininosuccinate synthase and ornithine decarboxylase, and CAT2 and late induction of ARG1 are demonstrated in LPS-activated peritoneal macrophages.[53]

Arginase activity in peritoneal and blood leukocytes following EAC and *E. coli* treatment.

Oxidative stress and elevated intracellular levels of L-arginine appear to contribute to the stimulation of both arginase and NOS in the peritoneal and blood leukocytes on the 11th day of EAC inoculation. Arginase hydrolizes L-arginine to L-ornithine and urea and is presented in mammalian tissues with two isoforms: cytoplasmic (ARG1) and mitochondrial (ARG2) constitutively expressed in murine granulocytes and monocyte/macrophages.[54,55] ROS, superoxide anion and hydrogen peroxide can induce the LPS-mediated increase in the activity of ARG1 and ARG1 mRNA level in alveolar macrophages, and to the less extent the nitrite accumulation and iNOS mRNA expression.[56] ARG1 expression is also potently induced by oxidized low-density lipoproteins in macrophages.[57] Fig. 3 shows the intracellular changes in the arginase activity in the peritoneum and blood of EAC-bearing and *E. coli*-treated mice. The activities of ARG1 and ARG2 were distributed equally in the cytoplasm and mitochondria of both PL and BL from testing native mice, and the ARG1 and ARG2 activities in PL were of a 3.4 and 2.5-fold higher than those respectively in BL. Malignancy was accompanied by a 5 and 3-fold increase in the ARG1 and ARG2 activity in PL, and by a 7.7 and 12-fold in those of BL respectively. EAC shifted the intracellular arginase activity balance in PL towards the ARG1, which activity was by 1.8 times higher than that ARG2, conversely, in BL the ARG2 activity dominated and was 1.6 times higher than that of ARG1.

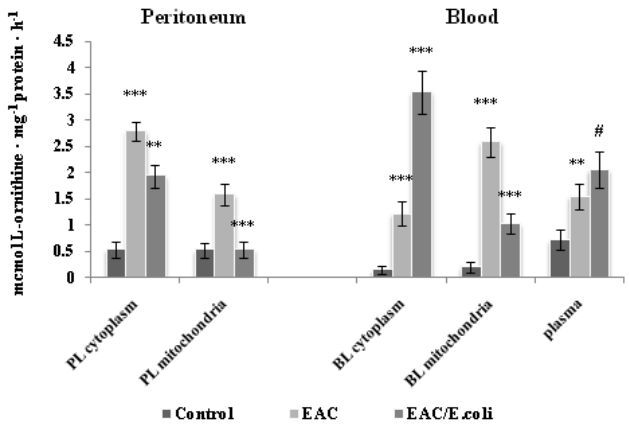

Figure 3. Arginase activity in the peritoneum and blood following Ehrlich ascites carcinoma (EAC) and *E. coli* treatment. Data are expressed as $M \pm SEM$, n=18. The confidence probability (p) of parameters evaluated for EAC-bearing mice compared to control, and p for *E. coli*-treated mice compared to untreated EAC-bearing mice. Peritoneal leukocytes (PL): cytoplasm - F=37.7, p<0.001; mitochondria - F=13.5, p<0.001. Blood leukocytes (BL): cytoplasm - F=59.6, p<0.001; mitochondria - F=35.4, p<0.001; plasma - F=7.1, p=0.002. # p >0.05, * p <0.05, ** p <0.01, *** p<0.001.

E. coli-treatment decreased the ARG1 activity by 1.44 times and normalized ARG2 in PL of EAC-bearing mice, while in BL a 3-fold increase in the ARG1 activity was detected and a 2.5-fold decrease in that of ARG2 respectively compared to non-treated mice. Inhibition of arginase isoforms in PL and ARG2 in BL indicated to ameliorating effect of bacterial treatment interfering with imminosuppresive effects of arginases. Besides, ARG2 plays a critical role in macrophage proinflammatory responses promoting mitochondrial ROS production.[58] At the same time in blood *E. coli*/LPS-mediated non-specific immune response is, presumably, associated with the activation of both ARG1 and iNOS (vide infra). Interestingly, iNOS/NO could exclusively affect ARG1 activity (not ARG2) via S-nitrosylation of 2 cysteine residues (C168 and C303), and through S-nitrosylation of C303 stabilized ARG1 trimer and reduced its Km value 6-fold, both in vitro and ex vivo.[59] In contrast to ARG1, ARG2 is not significantly modulated by Th1 or Th2 cytokines.[60] Although, recent data suggests that IFNã interferes with arginase activity in the three murine renal cell carcinoma cell lines, perhaps by inhibiting transcription of the ARG2 gene there through inhibiting proliferation of cells.[61] Whether IFN-γ is implicated in *E. coli* impact on the ARG2 activity in leukocytes must be elucidated. It can be speculated that *E. coli* via stimulation of the ARG1 activity and subsequent urea overproduction in the cytoplasm of BL is metabolically aimed to down-regulate the iNOS activity. Urea inhibits the iNOS/NO in a dose-dependent manner facilitating proliferation of LPS-stimulated mouse macrophages (RAW 264.7).[62] Interestingly, the same distribution of the intracellular arginase activities was observed both in PL and BL after *E. coli* treatment (ARG1 : ARG2 = 3.6 : 1).

One of the major products of arginase is L-ornithine, a precursor in the production of polyamines, whose elevated levels are associated with neoplastic growth.[63] Ornithine levels are significantly dropped in blood plasma and other tissues in the double knockout ARG1 and ARG2-deficient mice, indicating that arginase is critical to the maintenance of ornithine homeostasis.[64] Fig. 4 shows the alterations in the L-ornithine content in the peritoneum and blood following EAC and *E. coli* treatment. Positive correlation between arginase activity and L-ornithine level was determined in the PL cytoplasm (r=0.63, p=0.0053) and mitochondria (r=0.99, p<0.0001), and in the BL cytoplasm (r = 0.97, p <0.0001) and mitochondria (r = 0.96, p <0.0001), as well as in plasma (r = 0.55, p = 0.02). Although, L-ornithine may inhibit the two isoforms of arginase *in vivo* by a feedback mechanism, no inhibitory effect was observed in the studied leukocytes over L-ornithine concentration range determined *in vitro*.

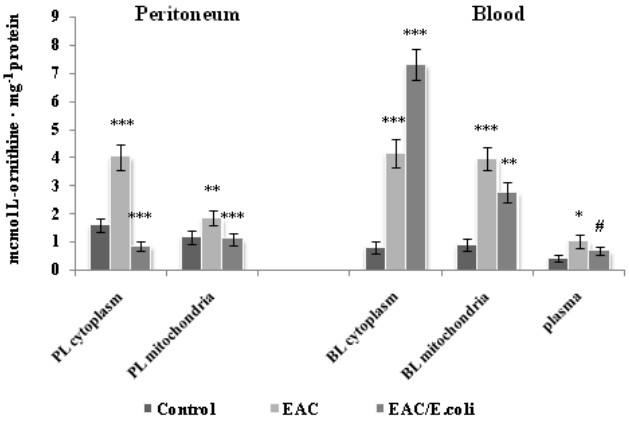

Figure 4. L-ornithine level in the peritoneum and blood following Ehrlich ascites carcinoma (EAC) and *E. coli* treatment. Data are expressed as $M \pm SEM$, n=18. The confidence probability (p) of parameters evaluated for EAC-bearing mice compared to control; and p for *E. coli*-treated mice compared to untreated EAC-bearing mice. Peritoneal leukocytes (PL): cytoplasm - F=28.6, p<0.001; mitochondria - F=8.27, p<0.001. Blood leukocytes (BL): cytoplasm - F=42.6, p<0.001; mitochondria - F=24.3, p<0.001; plasma - F=2.7, p=0.078. # p >0.05, * p <0.05, ** p <0.01, *** p<0.001.

Despite EAC-induced stimulation of the arginase activity, the level of arginine was markedly high in the studied cellular compartments of both PL and BL. Hence, arginase-induced arginine deficiency that may lead to inhibition of natural killer cell activity, T-cell dysfunction, including decreased proliferation and loss of the z-chain peptide during cancer was not observed.[65] No clear association with ARG1 expression and T-cell dysfunction (altered ability to produce cytokines in response to stimulation and inhibition of proliferation) was observed in myeloid cells from peripheral blood of patients with early-stage breast cancer.[66] Findings of other authors indicate that the ARG2 activity does not induce immunosuppression through CD3 æ down-regulation in both peripheral blood lymphocytes, and CD8+ T lymphocytes infiltrating tumor in patients with prostate carcinoma.[67] Notably, even during dramatically increased arginase activity, the concentrations of l-arginine in endothelial cells remained sufficiently high to provide NOS-dependent NO synthesis.[68] This has led authors to the conclusion that there is subcellular compartmentalization of l-arginine into poorly interchangeable intracellular pools. Nevertheless, arginase induction in leukocyte can enhance

tumor cell growth and not only through depletion of L-arginine, but also by providing them with polyamines, because the progression of a malignancy correlates with an elevated expression of both or specific isoform of arginase (depending on the type of tumor), while an inhibition of tumor growth is accompanied by a decrease in the expression and activity levels of arginase.[61,66]

Nitric oxide synthase activity in peritoneal and blood leucocytes following EAC and *E. coli* treatment.

There are three main isoforms of NOS, namely, constitutive (cNOS), including neuronal and endothelial NOSs and iNOS, which are highly induced by LPS, lipoteichoic acid, and proinflammatory cytokines.[69] A total NOS activity was assessed in the leukocyte cytolasmic and mitochondrial compartments, in which all the NOS isoforms are presented (Chen, K., 2010). S.S. Greenberg et al., 1998; T. Wallerath et al., 1997).[70.71.72] As shown in Fig. 5, on the 11th day of EAC transplantation a total NOS activity increased by 2.4 and 2.3 times in the cytoplasm and mitochondria of PL, and 8.5 and 6.3 times in those of BL respectively compared to control. It should be noted, that enhanced mitochondrial NO production and increased free radical generation, disrupt the electron transport system and mitochondrial permeability transition.[73] NO may potentially de-energise mitochondria via inhibition of creatine kinase, aconitase, cytochrome c oxidase.[69,74] Interestingly, in some cases involving proteins with N-terminal Cys, arginylation can happen only after nitric oxide-dependent Cys oxidation and such oxidation-dependent arginylation are likely to target proteins for degradation.[75] *E. coli* decreased the NOS activity in cytoplasm up to basal values, whereas no changes in the NO production were detected in mitochondria of PL.

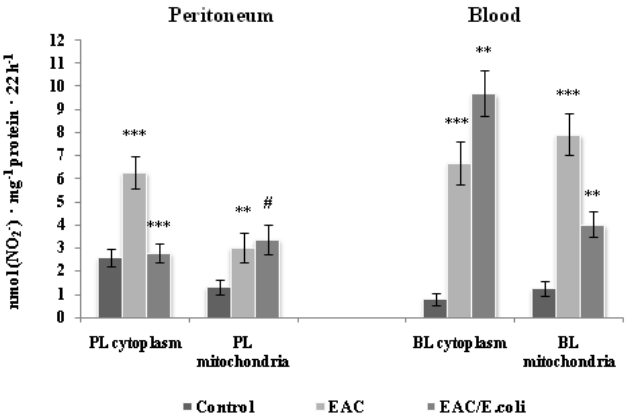

Figure 5. Nitric oxide synthase activity in the peritoneum and blood following Ehrlich ascites carcinoma (EAC) and *E. coli* treatment. Data are expressed as M ± SEM, *n*=18. The confidence probability (*p*) of parameters evaluated for EAC-bearing mice compared to control; and *p* for *E. coli*-treated mice compared to untreated EAC-bearing mice. Peritoneal leukocytes (PL): cytoplasm - F=16.4, $p<0.001$; mitochondria - F=12.6, $p<0.001$. Blood leukocytes (BL): cytoplasm - F=32.5, $p<0.001$; mitochondria - F=28.3, $p<0.001$. Note: NOS activity was not determined in plasma. # $p>0.05$, * $p<0.05$, ** $p<0.01$, *** $p<0.001$.

EAC-enhanced arginine level in the leukocytes appear to up-regulate a total NOS activity, particularly the iNOS, which in contrast with the cNOS is a high-output form strongly dependent on the presence of intracellular L-arginine that is a rate-limiting factor in NO synthesis.[76] As noted, peritoneal macrophages in ascites tumor-bearing animals express high levels of iNOS accompanied by overproduction of NO.[17] The iNOS can produce NO for prolonged periods and contribute to excessive NO, which is the only biomolecule produced in high enough concentrations to out-compete SOD for superoxide and forming peroxynitite ($ONOO^-$, PN), a potent oxidizing and nitrating agent that modifies tyrosine in proteins and creates nitrotyrosines leaving a footprint detectable in vivo.[77] NO released from PL may interact with superoxide generated by extracellular NADPH oxidase, the activity of which was revealed in ascitic fluid and was about 28 % higher than that in serum of healthy mice, and 8-10 times higher than in the EAC cells on terminal stage of EAC.[78] MnSOD and CuZnSOD are inactivated when exposed to simultaneous fluxes of superoxide and NO, and PN may inactivate the MnSOD via the direct reaction with the Mn center and a metal-catalyzed nitration of Tyr-34 in MnSOD.[79] PN could be involved in the inactivation of T-cell receptor complex via nitration and subsequent inhibition of the protein tyrosine phosphorylation in purified lymphocytes and priming them to undergo apoptotic cell death after phytohemagglutinin or CD3-mediated activation.[80] The presence of high levels of nitrotyrosine in T lymphocytes infiltrating human prostate carcinoma, suggests production of PN.[67]

Interestingly, population of circulating $CD11b^+$IL-4 receptor α^+ ($CD11b^+$ IL-$4R\alpha^{++}$), inflammatory-type monocytes elicited by growing tumors and producing IL-13 and IFN-γ contributing to stimulation of both ARG1 and iNOS that in turn are involved in the suppression of antigen-activated $CD8^+$ T lymphocytes.[81] Notably, cNOS-derived NO could block the nuclear factor kappaB (NF-kB) activation and proinflammatory mediators release, vice versa iNOS/NO could stimulate these processes.[82] This becomes even more important, since inhibition of NF-kB signaling in ARG1-expressing tumor-associated macrophages transformed them into tumor-cytotoxic effector cells.[83] In addition, iNOS-derived NO may inhibit cNOS by a feedback mechanism through the formation of stable inhibitory ferrous nitrosyl complexes, whereas in case of the iNOS it appears weak.[84]

E coli decreased the NOS activity in the cytoplasm up to basal values in PL, but no changes in the mitochondrial NOS activity were detected. It is not excluded that agmatine produced by *E. coli* may competitively inhibit in a dose-dependent manner the activity of the three NOSs, and most potently the iNOS as it was demonstrated in macrophages.[85] Moreover, agmatine could be converted to putrescine and urea by agmatinase, and urea in turn may also contribute to the iNOS inhibition (vide supra). It should be further investigated, how the contribution of *E. coli* to nitrergic response of PL is related to the iNOS and/or the cNOS in EAC. At the same time, *E coli* stimulated a total NOS activity by 1.5 times in the cytoplasm of BL, and decreased it approximately twice in the mitochondria, in which, possibly, dominating cNOS was inhibited by iNOS/NO.

Thus, contrary to PL, *E. coli* may up-regulate both ARG1 and cytoplasmic NOS activity in BL of EAC-bearing mice that might be mediated by LPS. It is documented that LPS as well as various inflammatory stimuli may increase the NO production and the expression and activity of iNOS and arginase in rodents.[86,87]

Subcellular changes in the NOS activity were associated with appropriate alterations in the levels of its products, stable metabolite of NO, nitrite and L-citrulline in the peritoneum and blood following EAC and *E. coli* treatment (Fig. 6 and 7, respectively).

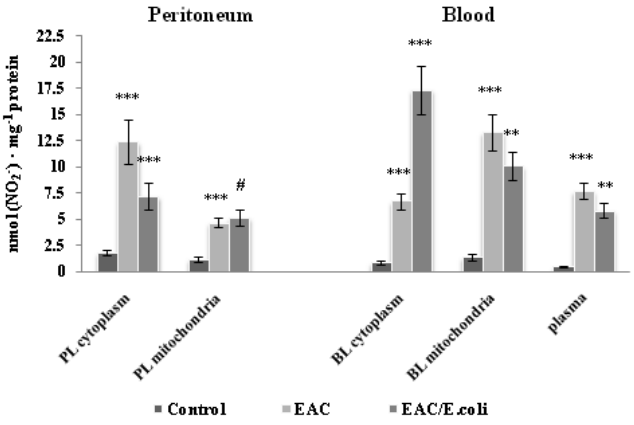

Figure 6. L-citrulline level in the peritoneum and blood following Ehrlich ascites carcinoma (EAC) and *E. coli* treatment. Data are expressed as $M \pm$ SEM, n=18. The confidence probability (p) of parameters evaluated for EAC-bearing mice compared to control, and p for *E. coli*-treated mice compared to untreated EAC-bearing mice. Peritoneal leukocytes (PL): cytoplasm - F=18.2, p<0.001; mitochondria - F=9.1, p<0.001; Blood leukocytes (BL): cytoplasm - F=27.8, p<0.001, mitochondria - F=12.7, p<0.001, plasma - F=58.8, p<0.001. # p >0.05, * p <0.05, ** p <0.01, *** p<0.001.

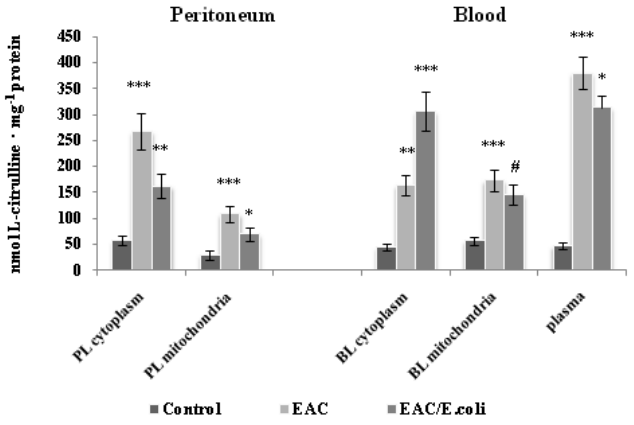

Figure 7. Nitrite level in the peritoneum and blood following Ehrlich ascites carcinoma (EAC) and *E. coli* treatment. Data are expressed as $M \pm$ SEM, n=18. The confidence probability (p) of parameters evaluated for EAC-bearing mice compared to control, and p for *E. coli*-treated mice compared to untreated EAC-bearing mice. Peritoneal leukocytes (PL): cytoplasm - F=13.6, p<0.001; mitochondria - F=15.3, p<0.001; Blood leukocytes (BL): cytoplasm - F=26.4, p<0.001; mitochondria - F=24.5, p<0.001; plasma - F=37.4, p<0.001. # p >0.05, * p <0.05, ** p <0.01, *** p<0.001.

Positive correlations between total NOS activity and L-citrulline levels were determined in the cytoplasm (r=0.89, p<0.0001) and mitochondria (r = 0.78, p=0.0002) of PL, and in the cytoplasm (r = 0.97, p <0.0001) and mitochondria (r = 0.92, p<0.0001) of BL, as well as between total NOS activity and nitrite levels in the cytoplasm (r=0.88, p<0.0001) and mitochondria (r=0.99, p<0.0001) of PL, and in the cytoplasm (r = 0.89, p<0.0001) and mitochondria (r = 0.78, p=0.0002) of BL.

It has been recently demonstrated that only modulating both enzymes arginase and NOS *in vivo* may reduce tyrosine nitration and restore responsiveness of tumor infiltrating T lymphocytes to human prostatic adenocarcinoma that was confirmed also on a transgenic mouse prostate model.[67] We believe that the beneficial effect of the non-pathogenic *E. coli* strain is in part due to its antioxidant activity and associated impact on the mentioned enzymes in the PL. Our findings highlight also the importance of the subcellular location of arginine and arginine metabolizing enzymes as well as their substrate and products during EAC and bacterial treatment and should be further investigated.

CONCLUSION

In summary, we suggest that in the stationary to terminal phases of EAC an overproduction of ROS and an enhancement of L-arginine levels occurred and accompanied by stimulation of the ARG1 and ARG2 and total NOS activity in the cytoplasm and mitochondria of both peritoneal and blood leukocytes. The most important novel finding of this study is that antitumor activity of non-pathogenic *E. coli* EM0 strain appear to be associated with its inhibition of lipid peroxidation and differential modulation of L-arginine metabolic pattern depending on whether leukocytes are localized in the ascitic fluid or in the peripheral blood. After administration, *E. coli* was generally concentrated in the ascitic fluid and directly affected the surrounding cells including peritoneal leukocytes, in which the EAC-induced high activity of ARG1 decreased and a total cytoplasmic NOS and ARG2 were normalized. Negligible number of *E coli* were observed at sites remote of tumor which suggests its indirect effects, presumably via stimulation of LPS-mediated non-specific immune response associated with activation of both ARG1 and NOS in the cytoplasm of blood leukocytes in which they might contribute to inhibition of ARG2 and mitochondrial NOS, implicated in the reciprocal regulation of host antitumor response, and interfered with *E. coli* dissemination, as well. The data obtained should be taken into account in the further study aimed to use non-pathogenic *E. coli* strains in the therapy of ascites tumors. Overall, a precise understanding of indigenous bacteria impact on the arginine pathways in cancer may contribute to the development of more adequate therapy.

ACKNOWLEDGMENTS

The authors greatly thank Dr. Hrach M. Stepanyan (Science & Technology Center of Pharmaceutical organic chemistry NAS RA) who kindly provided us with Ehrlich ascites tumor cells, Dr. Isabella S. Hakobyan (Medical

Center "Armenikum") who provided us non-pathogenic *E. coli* EM0 strain, and for her help in establishing the methodological procedures necessary for this study, Ms. Ani Hakobyan (Master of English language and literature) for editing the manuscript.

REFERENCES

[1]Jemal, A., Siegel, R., Xu, J., Ward, E., *CA Cancer J. Clin.,* **2010**, *60(5),* 277.

[2]Lewis, C. E. and Pollard, J. W., *Cancer Res.*, **2006**, *66(2)*, 605.

[3]Wang, T., Liu, G. and Wang, R., *Front. Immunol.*, **2014**, *5*, 358.

[4]Raber, P., Ochoa, A. C. and Rodríguez, P. C., *Immunol. Invest.* **2012**, *41(6-7)*, 614.

[5]Greten, T. F., Manns, M. P. and Korangy, F., *Int. Immunopharmacol.*, **2011**, *11(7)*, 802.

[6]Munder, M., *British J. Pharmacol.*, 2009, *158(3)*, 638.

[7]Lim, H. X., Hong, H. J., Cho, D. and Kim, T. S., *J. Immunol.*, **2014**, *193(11),* 5453.

[8]Serafini, P., Meckel, K., Kelso, M., Noonan, K., Califano, J. and Koch, W., *J. Exp. Med.*, **2006**, *203(12)*, 2691.

[9]Das, P., Lahiri, Am., Lahiri, Ay. and Chakravortty, D., *PLOSpathogens*, **2010**, *6(6)*,1-7.

[10]Chen, M., Bao, W., Aizman, R., Huang, P., Aspevall, O., Gustafsson, L.E., Ceccatelli, S. and Celsi, G., *J Infect Dis.*, **2004**, *190(1)*, 127.

[11]Hoption Cànn, S. A., van Netten, J. P. and van Netten, C., *Postgrad. Med. J.,* **2003**, *79(938)*, 672.

[12]Patyar, S., Joshi, R., Byrav, P., Prakash, A., Medhi, B. and Das, B. K., *J. Biomed. Sci.,* **2010**, *17(1)*, 21.

[13]Wong, C. K., Fung, K. P., Lee, C. Y. and Choy, Y. M., *Cancer Lett.*, **1992**, *63(1)*, 7.

[14]Fiore, N., Green, S., Williamson, B., Carswell, E., Old, L. J. and Hlinka, J., Proc. Am. Assoc. *Cancer Res.*, **1975**, *16(1)*, 125.

[15]Gambashidze, K., Khorava, P., Azaladze, T., Kalandarishvili, K., Jaiani, E., Lasareishvil, B., Azaladze, A. and Tediashvili, M., *Exp. Oncol.*, **2012**, *34 (2)*, 107.

[16]Chakravortty, D. and Hensel, M., *Microb. Infect.*, **2003**, *5(7)*, 621.

[17]Nishikawa, M., Sato, E., Kashiba, M., Kuroki, T., Utsumi, K. and Inoue, M., *Hepatology*, **1998**, *28(6)*, 1474.

[18]Lodinová-Zádníková, R., Cukrowska, B. and Tlaskalova-Hogenova, H., *Inter. Arch. Allerg. Immunol.*, **2003**, *131(3)*, 209.

[19]Mazumder, U. K., Gupta, M., Maiti, S. and Mukherjee, M., *Indian J. Exp. Biol.*, **1997**, *35(5)*, 473.

[20]Putintceva, O. V., Artukhov, V. G. and Koltakov, I. A., *Immunology. PartII*. Voronezh. **2008**, 45.

[21]Dizhe, G. P., Eshchenko, N. D., Dizhe, A. A. and Krasouskaya, I. E. *Introduction to the techniques of biochemical experiments.* SPb. **2003**, 86.

[22]Iyamu, E. W., Asakura, T. and Woods, G. W., *Anal. Biochem.*, **2008**, *383(2)*, 332.

[23]Schmidt, H.H.H.W. and Kelm, M. (Feelisch M. and Stamler J. S., eds.) *Methods in Nitric Oxide Research.* Wiley, Chichester. **1996**, 491.

[24]Akamatsy S., Watanabe T.J., *J. Biochem.,* **1961**, *77(3)*, 484.

[25]Moore, R. B. and Kauffman, N. J., *Anal. Biochem.*, **1970**, *33(2)*, 263.

[26]Buge, J. A. and Aust, S. D., *Method enzymol.*, **1978**, *52*, 302.

[27]Lowry, O. H., Rosebrough, N. J., Farr, A. L. and Randall, R. J., *J. Biol. Chem.*, **1951**, *193(1)*, 265.

[28]Diaz-Montero, C. M., Finke, J. and Montero, A. J., *Semin. Oncol.,* **2014**, *41(2)*,174.

[29]Gratchev, A., Kzhyshkowska, J., Kothe, K., Muller-Molinet, I., Kannookadan, S., Utikal, J. and Goerdt, S., *Immunobiology*, **2006**, *211(6-8)*, 473.

[30]Schmielau, J., Finn, O.J., *Cancer Res.*, **2001**, *61(12)*, 4756.

[31]Hamburger, A. W., Dunn, F. E. and White, C. P., *Br. J. Cancer*, **1985**, *51(2)*, 253.

[32]Hudault, S., Guignot, J. and Servin, A.L., *Gut,* **2001**, *49(1)*, 47.

[33]Aghababova, A. A., Movsesyan, N. H., Hakopyan, A. M. and Avagyan, H. Kh., *Reports of NAS of Armenia*, **2013**, *113(3)*, 303.

[34]Szuster-Ciesielska, A., Hryciuk-Umer, E., Stepulak, A., Kupisz, K. and Kandefer-Szerszen, M., *Acta Oncol.*, **2004**, *43(3)*, 252-258.

[35]Corzo, C. A., Cotter, M. J., Cheng, P., Cheng, F., Kumartsev, S., Sotomayor, E., Padhya, T., McCaffrey, T. V., McCaffrey, J. C. and Gabrilovich D. I., *J. Immunol.*, **2009**, *182(9)*, 5693.

[36]Storz, P., *Front. Biosci.*, **2005**, *10*, 1881-1896.

[37]Smirnova, L. P, Kondakov, I. V., *Biomed. Chem.*, **2004**, *50(6)*, 566-575.

[38]Potselueva, M. M, Naumov, A. A., Sukhomlin, T. K., Zinatullina, G. G. and Shatalin, Iu. V., [Article in Russian]. *Tsitologia*, **2013**, *55(5)*, 307.

[39]Kusmartsev, S., Nefedova, Y., Yoder, D. and Gabrilovich, D. I., *J. Immunol.*, **2004**, *172(2)*, 989.

[40]Tkachenko, A. G. and Fedotova, M. V., *Biochemistry (Mosc)*, **2007**, *72(1)*, 109.

[41]Drazic, A., Kutzner, E., Winter, J. and Eisenreich, W., *PLoS One*, **2015**, *10(5),* e0125823.

[42]Yu, M., Chakraborty, G., Grabow, M. and Ingoglia, N. A., *Neurochem. Res.*, **1994**, *19(1)*, 105.

[43]Krichevskaya, A. A., Lukash, A. I., Shugalei, V. S. and Bondarenko, T. I., *Aminoacids, its derivartives and regulation of metabolic pathways.* Rostov, **1983**, 112.

[44]Semenova, A. I., *Practical oncology*, **2006**, *7(2)*, 101.

[45]Dolder, M., Walzel, B., Speer, O., Schlattner, U., Wallimann, T., *J. Biol. Chem.*, **2003**, *278(20)*, 17760.

[46]Wu, W.H. and Morris, D.R., *J. Biol. Chem.*, **1973**, *248(5),*1687.

[47]Arndt, M. A., Battaglia, V., Parisi, E., Lortie, M. J., Isome, M., Baskerville, C. and Pizzo, D. P., *Am. J. Physiol. Cell Physiol.*, **2009**, *296(6)*, C1411.

[48]Isome, M., Lortie, M.J., Murakami, Y., Parisi, E., Matsufuji, S., Satriano, J., *Am. J. Physiol. Cell Physiol.*, **2007**, *293(2)*, C705.

[49]Satriano, J., Matsufuji, S., Murakami, Y., Lortie, M. J., Schwartz, D., Kelly, C. J., Hayashi, S. and Blantz, R. C., *J. Biol. Chem.*, **1998**, *273(25)*, 15313.

[50]Philippovich, S.Y., Biochemistry (Mosc), **2010**, *75(10)*, 1367.

[51]Gabrilovich, D. I., Ostrand-Rosenberg, S. and Bronte, V., Coordinated regulation of myeloid cells by tumors. *Nat. Rev. Immunol.,* **2012**, *12(4)*, 253.

[52]Thompson, R. W., Pesce, J. T., Ramalingam, T., Wilson, M. S. and White, S., *PLoS Pathog.*, **2008**, *4 (3)*, 1.

[53]Salimuddin, Nagasaki, A., Gotoh, T., Isobe, H. and Mori, M., *Am J Physiol.* **1999**, *277(1 Pt 1)*, E110.

[54]Khallou-Laschet, J., Varthaman, A., Fornasa, G., Compain, C., Gaston, A. T., Clement, M., Dussiot, M., Levillain, O., Graff-Dubois, S., Nicoletti, A. and Caligiuri, G., *PLoS One,* **2010**, *5*, e8852.

[55]Munder, M., Mollinedo, F., Calafat, J., Canchado, J., Gil-Lamaignere, C., Fuentes, J.M, Luckner, C., Doschko, G., Soler, G., Eichmann, K., Muller, F.M., Ho, A.D., Goerner, M. and Modolell, M., *Blood*, **2005**, *105(6)*, 2549.

[56]Matthiesen, S., Lindemann, D., Warnken, M., Juergens, U. R. and Racké, K., *Eur. J. Pharmacol.*, **2008**, *579(1-3)*, 403.

[57]Gallardo-Soler, A., Gómez-Nieto, C., Campo, M. L., Marathe, C., Tontonoz, P., Castrillo, A. and Corraliza, I., *Mol. Endocrinol.*, **2008**, *22 (6)*, 1394.

[58]Ming, X-F., Rajapakse, A.G., Yepuri, G., Xiong, Y., Carvas, J.M., Ruffieux, J., Scerri, I., Wu, Z., Popp, K., *J. Am. Heart Assoc.,* **2012**, *1*, e000992 doi: 10.1161/JAHA.112.000992.

[59]Santhanam, L., Lim, H. K., Lim, H. K., Miriel, V., Brown, T., Patel, M., Balanson, S., Ryoo, S., Anderson, M., Irani, K., Khanday, F., Di Costanzo, L., Nyhan, D., Hare, J. M., Christianson, D. W., Rivers, R., Shoukas, A. and Berkowitz, D. E., *Circ. Res.*, **2007**, *101(7)*, 692.

[60]Rodriguez, P. C., Zea, A. H., DeSalvo, J., Culotta, K. S., Zabaleta, J., Quiceno, D. G., Ochoa, J. B. and Ochoa A.C., *J. Immunol.*, **2003**, *171(3)*, 1232.

[61]Tate D. J. Jr., Patterson J. R., Velasco-Gonzalez C., Carrol E. N. and Trinh J., *Int. J. Biol. Sci.*, **2012**, *8(8)*, 1109.

[62]Moeslinger, T., Friedl, R., Volf, I., Brunner, M., Baran, H., Koller, E. and Spieckermann, P. G. *Kidney Int.*, **1999**, *56(2)*, 581.

[63]Casero R. A. and Pegg A. E., Polyamine catabolism and disease. *Biochem J.,* **2009**, *421(3)*, 323.

[64]Deignan, J. L., Livesay, J. C., Yoo, P. K., Goodman, S. I., Pegg, A. E., O'Brien, W. E., Iyer, R. K., Cederbaum, S. D. and Grody, W. W., *Mol. Genet. Metab*., **2006**, *89(1-2)*, 87.

[65]Popovic, P.J., Zeh III, H.J., Ochoa, J.B., *J. Nutr.*, **2007**, *137 (6 Suppl 2)*, 1681S.

[66]De Boniface, J., Mao, Y., Schmidt-Mende, J., Kiessling, R. and Poschke, I., *Oncoimmunol.*, **2012**, *1(8)*, 1305.

[67]Bronte, V., Kasic, T., Gri, G., Gallana, K., Borsellino, G., Marigo, I., Battistini, L., Iafrate, M., Prayer-Galetti, T., Pagano, F. and Viola, A., *J. Exp.l Med*., **2005**, *201(8)*, 1257.

[68]Chen, F., Lucas, R. and Fulton, D., *Front. Immunol.*, **2013**, *4*, 184.

[69]Alderton, W. K., Cooper, C. E. and Knowles, R. G., *Biochem. J.*, **2001**, *357(Pt 3)*, 593.

[70]Wallerath, T., Gath, I., Aulitzky, W. E., Pollock, J. S., Kleinert, H. and Forstermann, U., *Thromb. Haemost.,* **1997**, *77(1)*, 163.

[71]Greenberg, S. S., Ouyang, J., Zhao, X. and Giles, T. D., *Nitric Oxide*, **1998**, *2(3)*, 203.

[72]Chen, K., Northington, F. J. and Martin, L. J., *Brain Struct. Funct.*, **2010**, *214 (2-3)*, 219.

[73]Jacobson, J., Duchen, M. R., Hothersall, J., Clark, J. B. and Heales, S. J. *J. Neurochem.*, **2005**, *95(2)*, 388.

[74]Delwing, D., Cornelio, A. R., Wajner, M., Wannmacher C. M. and Wyse A. T., *Metab. Brain Dis.*, **2007**, *22(1)*, 13.

[75]Hu, R. G., Sheng, J., Qi, X., Xu, Z., Takahashi, T. T. and Varshavsky, A., *Nature*, **2005**, *437(7061)*, 981.

[76]Lowenstein, C. J. and Padalko, E., *J. Cell Sci.,* **2004***, 117(Pt 14)*, 2865.

[77]Beckman, J. S. and Koppenol, W. H., *Am. J. Physiol.*, **1996**, *271(5 PT 1)*, C1424.

[78]Alexanyan, Ì. Ê., Simonyan, R. M., Simonyan, G. M., Babayan, M. A., Alexanyan, S. S. and Simonyan, Ì.À., *Med. Sci. Arm.*, **2011**, *51(4)*, 47.

[79]Demicheli, V., Quijano, C., Alvarez, B. and Radi, R., *Free Radic. Biol. Med.*, **2007**, *42(9)*, 1359.

[80]Brito, C., Naviliat, M., Tiscornia, A. C., Vuillier, F., Gualco, G., Dighiero, G., Radi, R. and Cayota, A. M., *J. Immunol.*, **1999**, *162(6)*, 3356.

[81]Gallina, G., Dolcetti, L., Serafini, P., De Santo, C., Marigo, I., Colombo, M. P., Basso, G., Brombacher, F. and Borrello, I., *J. Clin. Invest.*, **2006**, *116(10)*, 2777.

[82]Stefano, G. B., Coumon, Y., Bilfinger, T. V., Welters, I. D. and Cadet, P., *Prog. Neurobiol.*, **2000**, *60(6)*, 513.

[83]Hagemann, T., Lawrence, T., McNeish, I., Charles, K. A., Kulbe, H., Thompson. R. G., Robinson, S. C. and Balkwill, F. R., *J. Exp. Med.*, **2008**, *205(6)*, 1261-1268.

[84]Abu-Soud, H. M., Wang, J., Rousseeau, D. L., Fukuto, J. M., Ignarro, L. J. and Stuehr, D. J., *J. Biol. Chem.*, **1995**, *270(39)*, 22997.

[85]Galea, E., Regunathan, S., Eliopoulos, V., Feinstein, D. L. and Reis, D. J., *Biochem. J.*, **1996**, *316(Pt 1)*, 247.

[86]Corraliza, I. M., Soler, G., Eichmann, K. and Modolell, M., *Biochem. Biophys. Res. Commun.*, **1995**, *206(2)*, 667.

[87]Hrabak, A., Bajor, T. and Csuka, I. *Inflamm. Res.*, **2006**, *55(1)*, 23.

Received: 25.06.2015.
Accepted: 25.07.2015.

STRUCTURE OF (2*E*,2'*E*)-3,3'-(1,3-PHENYLENE)BIS(1-(ANTHRACENE-9-YL)PROP-2-*EN*-1-ONE): A CHALCONE DERIVATIVE

Rajni Kant[a]*, Ratika Sharma[a], Vinutha V. Salian[b], B. K. Sarojini[c] and B. Narayana[b]

Keywords: anthracene, single crystal XRD, direct method, intermolecular interactions, hydrogen bonding.

The title compound $C_{40}H_{26}O_2$ [(2*E*, 2'*E*)-3, 3'-(1,3-Phenylene)-bis(1-(anthracene-9-yl)prop-2-en-1-one)] was prepared from the reaction of isophthalaldehyde and 9-acetylanthracene treated with solution of ethanol and sodium hydroxide. It has been crystallized from DMF using slow evaporation method in the triclinic space group P-1 with Z=2 and unit cell parameters, *a* = 9.8276(8) *b* = 10.7470(8), *c* = 14.5606(10) Å, α= 99.833(6), β=104.495(6), γ= 97.371(6)°. The architecture of the crystal structure is determined mainly by three intermolecular interactions [C23-H10…O1, C25-H15…O1, C16-H17…O1], here O1 acts as an acceptor to three different carbon atoms, resulting into the formation of a trifurcated hydrogen bond, forming a graph set motif $R^2_2(8)$ through a pair of C25-H15...O1 interactions. These motifs are further extended through another intermolecular hydrogen bond [C3-H6...O2] forming a ladder like network, extending along the c-axis.

* Corresponding Authors
Fax: +91 191 243 2051
E-Mail: rkant.ju@gmail.com
[a] X-ray Crystallography Laboratory, Department of Physics and Electronics, University of Jammu, Jammu Tawi-180 006, India.
[b] Department of Studies in Chemistry, Mangalagangothri, Mangalore University, Mangalagangothri-574 199, India.
[c] Department of Industrial Chemistry, Mangalore University, Mangalagangothri-574 199, India

Introduction

Chalcones are an interesting class of compounds which have been reported to posses various useful properties. They have been studied for non-linear optical properties[1], biological activities including anti-inflammatory, antileishmanial, antimicrobial, antioxidant[2-4] and HIV-1 protease inhibitor[5] as well as fluorescence properties[6,7]. Chalcones are important intermediates in organic synthesis of variety of pharmacologically important heterocyclic compounds. Due to the presence of enone functionality, chalcones are an interesting target class of compounds which are extensively studied for their broad spectrum of biological activities such as, antileishmanial[8], anti-invasive[9,10], antitubercular[11], antifungal[12], antimalarial[13], anticancer[14,15] and anti-inflammatory properties[16].

In this paper we report precise synthesis and a detailed X-ray structure of a chalcone derivative containing anthracene moiety and possessing interesting biological properties.

Experimental

Synthesis

The reaction scheme for the synthesis of the tiltle compound is presented in Figure 1. To a mixture of isophthalaldehyde (0.67 g, 0.005 mol) and 9-acetyl-anthracene (2.20 g, 0.01 mol) in ethanol (50 mL), 15 mL of 10 % sodium hydroxide solution was added and stirred at 0–5 °C for 3 h. The precipitate formed was collected by filtration and purified by recrystallization from ethanol. Single crystal was grown from DMF by slow evaporation method (M. P.: 523-525 K).

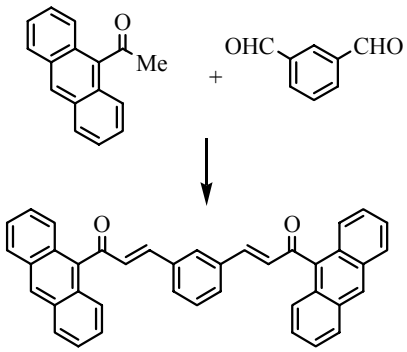

Figure 1. Synthesis of the chalcone derivative

X-Ray Intensity Data Collection

Structure Solution

X-ray intensity data of a crystal having well-defined crystal morphology (0.30 x 0.20 x 0.10 mm) were collected at 293(2)K on *X'calibur* CCD area-detector diffractometer equipped with graphite monochromated Mo*Kα* radiation (λ = 0.71073Å). The intensities were measured by employing *ω* scan mode for the diffraction angle ranging from 3.58 to 26.00°. A total number of 10030 reflections were measured of which 5641 were found to be unique. The criterion *(I > 2σ(I))* was employed to the unique data set and hence 2418 reflections were treated as observed. Data were corrected for Lorentz and Polarization factors. The structure was solved by direct methods using SHELXS97.[17]

Table 1. Crystal data and other experimental details.

CCDC Number	**1407267**
Crystal description	Block
Crystal size	*0.30 x 0.20 x 0.10* mm
Empirical formula	$C_{40}H_{26}O_2$
Formula weight	538.61
Radiation, Wavelength	Mo *Kα*, 0.71073 Å
Unit cell dimensions	*a* = 9.8276(8) Å ,
	b = 10.7470(8) Å
	c = 14.5606(10) Å
	α= 99.833(6)°
	β=104.495(6)º
	γ = 97.371(6)°
Crystal system, Space group	Triclinic, *P-1*
Unit cell volume	14443.25(19) Å^3
No. of molecules per unit cell, *Z*	2
Absorption coefficient	0.075 mm^{-1}
F(000)	564
θ range for entire data collection	3.58< *θ* < 29.12º
Reflections collected / unique	10030 / 5641
Reflections observed *(I > 2σ(I))*	2418
Range of indices	*h*= -12 to 12,
	k= -13 to 12,
	l= -17 to 17
No. of parameters refined	467
Final *R*-factor	0.0643
wR(F^2)	0.1989
R_{int}	0.0298
R_σ	0.0839
Goodness-of-fit	0.989
(Δ/σ)max	0.001
Final residual electron density	-0.199< *Δρ* >0.036 eÅ^{-3}

Table 2. Some important bond lengths (Å) and bond angles (º)

S.	Bond lengths(Å)		Bond angles(º)	
1.	O1-C15	1.220	O1-C15-C10	119.70
2.	O2-C15	1.225	O2-C15-C16	119.86
3.	C5 -C10	1.413	C16 -C15-C10	120.42
4.	C9-C10	1.396	C16-C17-C18	126.46
5.	C10-C15	1.496	C15-C16-C17	125.46
6.	C15-C16	1.462	C26-C25-C24	124.78
7.	C17-C18	1.467	C22-C24-C25	127.00
8.	C27-C28	1.398	C25-C26-O2	120.03
9.	C27-C40	1.404	C27-C26-C27	120.30
10	C32-C24	1.454	C25-C26-C27	119.66
.				

Structure Refinement

Full-matrix least-squares refinement was carried out using SHELXL97[17]. The final refinement cycles converged to *R* = 0.0643 and w*R*(F^2) = 0.1989 for the 2418 observed reflections. Residual electron density ranges from -0.199 to 0.036 eÅ^{-3}. Atomic scattering factors were taken from International Tables for X-ray Crystallography (1992, Vol. C, Tables 4.2.6.8 and 6.1.1.4). The crystallographic data are summarized in Table 1. Some selected bond angles which plays an important role in collating the structural properties of this molecule with the related structures are presented in Table 2. An ORTEP[18] view of the molecule with atomic labelling is shown in Figure 2. The geometry of the molecule was calculated using the PLATON[19] and PARST[20] software. The Cambridge Crystal Data Centre Number assigned to this structure is CCDC-1407267.

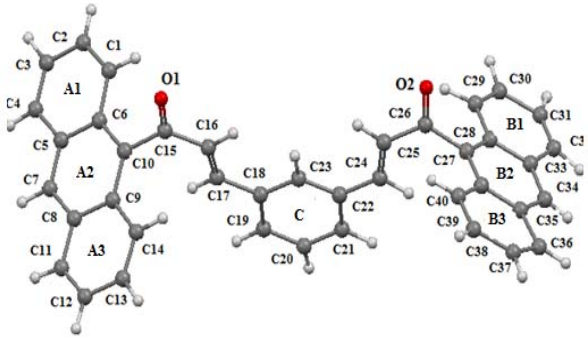

Figure 2. ORTEP view of the molecule showing the atom-labelling scheme

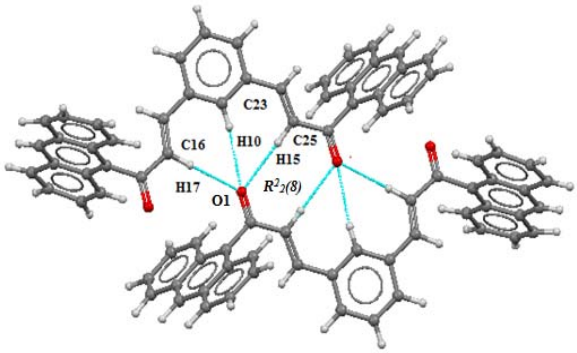

Figure 3. A plot of two molecules of the title compound showing trifurcated intermolecular C-H…O hydrogen bonds (dashed lines) forming $R^2_2(8)$ motif

Result and Discussion

The molecule comprises of two anthracene moieties separated by the chalcone chain system including a phenyl ring labelled as C. The two anthracene moieties are labelled as A (consisting of ring A1, A2 and A3) and B (consisting of ring B1, B2 and B3), respectively (**Figure 2**). All bond lengths and angles are normal and correspond to those observed in related structures[21, 22]. The endocyclic bond angles in moiety A and B are very close to 120°, indicating perfect aromatic character in them.[23]. C15=O1 and C26=O2 keto distances are confirmed by respective distances of [1.220(3) and 1.220(4) Å] and are slightly longer than the standard value for carbonyl bonds[23] (1.210 Å) probably because atoms O1 and O2 both are involved in C-H…O intermolecular hydrogen bonds. These keto distances are in well agreement with the values observed for related structures.[24,25] The plane of moiety A forms a dihedral angle of 70.95(6)° with the plane of the moiety B. The ring C is twisted from the plane formed by the ring atoms C1/C6/C10/C9/C14 (in moiety A) and C29/C28/C27/C40/C39 (in moiety B), through the dihedral angles of 69.19(1)° and 76.82(2)°, respectively. The co-planar geometry of ring C with both the carbonyl groups [C15=O1 and C26=O2], confirmed the torsion angles values being close to zero.

Table 3. Geometry of intra and inter molecular hydrogen bonds

D-H…A	D-H (Å)	H…A(Å)	D…A(Å)	θ[DH…A(º)]
C14-H1…O1	0.98(2)	2.53(3)	3.110(4)	118
C3- H6…O2^{i}	0.98(3)	2.58(3)	3.773(5)	139
C23-H10…O1^{ii}	0.94(3)	2.53(2)	3.455(4)	169
C25-H15…O1^{ii}	1.00(3)	2.51(3)	3.473(4)	161
C16-H17…O1^{ii}	1.02(3)	2.37(3)	3.392(4)	174

Symmetry codes: (i) x-1, y, z-1 (ii) –x+1,-y, -z+1

The atom O1 is playing a key role in the stabilization of crystal structure as it participates in three inter and one intra molecular hydrogen bonds out of total five hydrogen bond interactions present in the molecule. The architecture of the crystal structure is determined mainly by three intermolecular interactions in which O1 acts as a hydrogen bond acceptor via hydrogen atoms H6, H15 and H17 to the carbon atoms C23, C25 and C16 respectively, resulting into the formation of a trifurcated hydrogen bonded structure. This generates a graph set motif R22(8)26 through the pair of C25-H15...O1 interactions (Figure 3). The geometry of hydrogen bonding is presented in Table 3.

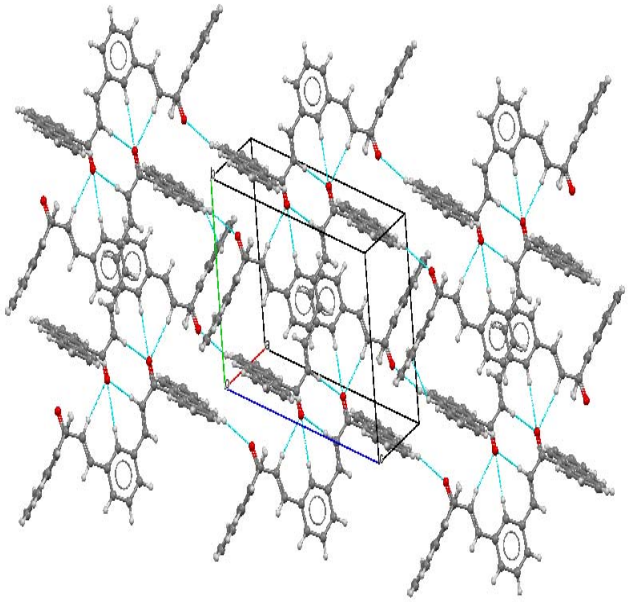

Figure 4. Packing view of the molecule projected alone the bc plane

The supramolecular structure formed by the trifurcated hydrogen bonding is further connected by the C3-H6...O2 hydrogen bonds, extending along the c-axis forming a ladder like network as shown in Figure 4.

Acknowledgements

One of the authors (Rajni Kant) acknowledges the Department of Science & Technology for single crystal X-ray Diffractometer as a National Facility under Project No. SR/S2/CMP-47/2003 and DST Project No: EMR/2014/000467. RS acknowledges University Grant Commission (UGC) for the award of NET-JRF scholarship under ref. No. 23/12/2012 (ii) EU-V. BN thanks UGC for financial assistance through BSR one time grant for the purchase of chemicals. VVS thanks Mangalore University for research facilities.

References

[1]Patil, P. S., Dharmaprakash, S. M., *Mater. Lett.,* **2008**, *62*, 451–453.

[2]Nowakowska, Z., *Eur. J. Med. Chem.*, **2007**, *42*, 125–137.

[3]Oliveira, E., Vicente, M., Valencia, L., Macı´as, A., Bertolo, E., Bastida, R., Lodeiro, C., *Inorg. Chim. Acta*, **2007**, *360*, 2734–2743.

[4]Saydam, G., Aydin, H. H., Sahin, F., Kucukoglu, O., Erciyas, E., Terzioglu, E., Buyukkececi, F., Omay, S. B., *Leuk. Res.,* **2003**, *27*, 57–64.

[5]Tewtrakul, S., Subhadhirasakul, S., Puripattanavong, J., Panphadung, T., *Leuk. Res., Songklanakarin J. Sci. Technol.*, **2003**, *25*, 503–508.

[6]Kobkeatthawin, T., Chantrapromma, S., Fun, H.K., *Acta Cryst.,* **2010**, *E66*, o254–o255.

[7]Svetlichny, V. Y., Merola, F., Dobretsov, G. E., Gularyan, S. K., Syrejshchikova, T. I., *Chem. Phys. Lipids,***2007**, *145*, 13–26.

[8]Suwunwong, T., Chantrapromma, S., Karalai, C., Pakdeevanich, P., Fun, H.-K., *Acta Cryst.*, **2009**, *E65*, o420–o421.

[9]Chantrapromma, S., Horkaew, J., Suwunwong, T., Fun, H. K., *Acta Cryst.* **2009**, *E65*, o2673–o2674.

[10]Chantrapromma, S., Suwunwong, T., Boonnak, N., Fun, H.-K., *Acta Cryst.,* **2010**, *E66,* o312–o313.

[11]Nielsen, S. F., Christensen, S. B., Cruciani, G., Kharazmi, A., Liljefors T., *J. Med. Chem.,***1998**, *41,* 4819–4832.

[12]Mukherjee, S., Kumar, V., Prasad, A. K., Raj, H. G., Bracke, M. E., Olsen, C. E., Jain, S. C., Parmar, V. S., *Bioorg. Med. Chem*., **2001**, *9,* 337–345.

[13]Wang, L., Chen, G., Lu, X., Wang, S., Han, S., Li, Y., Ping, G., Jiang, X., Li, H., Yang, J., Wu, C., *Eur. J. Med. Chem*., **2015**, *89,* 88-97.

[14]Dimmock, J. R., Elias, D. W., Beazely, M. A., Kandepu, N. M., *Curr. Med. Chem.,* **1999**, *6*, 1125-1149.

[15]Lopez, S. N., Castelli, M. V., Zacchino, S. A., Dominguez, J. N., Lobo, G., Jaime, C. C., Cortes, J. C. G., Ribas, J. C., Devia, C., Ana, M. R., Ricardo, D. E., *Bioorg. Med. Chem*., **2001**, *9***,** 1999–2013.

[16]Agarwal, A., Srivastava, K., Puri, S. K., Chauhan, P. M. S., *Bioorg. Med. Chem*., **2005**, *13***,** 4645–4650.

[17]Sheldrick, G. M., *Acta Cryst*., **2008**, *A64*, 112.

[18]Farrugia, L. J., *J. Appl. Cryst*., **1999**, *32*, 837.

[19]Spek, A. L. *Acta Cryst*., **2009,** *D65*, 148.

[20]Nardelli, M., *J. Appl. Cryst.*, **1995,** *28*, 659.

[21]Jaruwan, J., Suchada, C.,Thawanrat, K., Hoong, K., *Acta Cryst.*, **2010**, *E66*, o2669–o2670.

[22]Jirapa, H., Thitipone, S., Suchada, C., Chatchanok, K., Hoong, K., *Acta Cryst.,* **2010**, *E66*, o800–o801.

[23]Allen, F. H., Kennard, O., Watson, D. G., Brammer, L., Orpen, A. G., *Taylor, R., J. Chem. Soc., Perkin Trans-II,* **1987**, S1.

[24]Thitipone, S., Suchada, C., Chatchanok, K., Paradorn, P., Hoong, K., *Acta Cryst.,* **2009**, *E65*, o420–o421.

[25]Hoong, K., Thawanrat, K., Jaruwan , J., Suchada, C., *Acta Cryst.,* **2010**, *E66*, o3312–o3313.

[26]Bernstein J, Davis RE, Shimoni L, Chang NL, *Angew. Chem. Int. Ed. Engl*., **1995**, *34*, 1555-1573.

Received: 20.06.2015.
Accepted: 25.07.2015.

TOTAL LIPIDS, PROTEINS, MINERALS AND ESSENTIAL OILS OF *PINUS NIGRA* ARNOLD AND *PINUS SYLVESTRIS* GROWING WILD IN KOSOVO

Fatmir Faiku[a]*, Arben Haziri[a], Fatbardh Gashi[a], Naser Troni[a] and Haxhere Faiku[b]*

Keywords: *Pinus nigra* Arnold, *Pinus sylvestris*, proteins, lipids, minerals, essential oils.

The soil and climatic conditions are conducive for the growth of a lot of medical herbs in Kosovo. Lipids, proteins, minerals and essential oils were quantitatively determined from the *Pinus nigra* Arnold and *Pinus sylvestris* growing wild in Germia Park (located in the north-east of Pristina). Total proteins were analyzed, by Kjeldahl method. The total amount of proteins in *Pinus nigra* Arnold is 7.714 % and in *Pinus sylvestris* is 4.375 %. Lipids are analyzed by Soxhlet extraction. The total amount of lipids in *Pinus nigra* Arnold are 7.185 % and in *Pinus sylvestris* 6.670 %. Essential oils were isolated using steam distillation. The total amount of essential oils in *Pinus nigra* Arnold are 0.35 % and in *Pinus sylvestris* 0.32 %. The mineral content was studied and analyzed by flame atomic absorption spectrometry. Six elements, sodium, potassium, calcium, zinc, iron and copper were determined in *Pinus nigra* Arnold and *Pinus sylvestris*. The mean levels of sodium, potassium, calcium, zinc, iron and copper are 246 mg kg^{-1}, 1280 mg kg^{-1}, 4260 mg kg^{-1}, 17.2 mg kg^{-1}, 173 mg kg^{-1}, 3.83 mg kg^{-1} in *Pinus nigra* Arnold, respectively. The mean levels of sodium, potassium, calcium, zinc, iron and copper are 6.9 mg kg^{-1}, 420 mg kg^{-1}, 1180 mg kg^{-1}, 95 mg kg^{-1}, 840 mg kg^{-1}, 19 mg kg^{-1} in *Pinus sylvestris*, respectively. Calcium and potassium are present in large amounts in *Pinus nigra* Arnold while calcium and iron are present in large amounts in *Pinus sylvestris*.

*Corresponding Authors
E-Mail: f_faiku@hotmail.com; haxhere_f@hotmail.com
[a] Department of Chemistry, Faculty of Natural Sciences, University of Prishtina, Kosovo
[b] Association Loyola-Gymnasium, Prizren, Kosovo

Introduction

The cultivation and use of medicinal herbs dates from Roman times. Until the nineteenth century and beginning of the twentieth century, medicinal herbs were the raw material for making medicines. Today, even though the active medicinal materials are obtained from synthesised chemicals the use of medicinal herbs in medicine is widespread and is important.[1] There is an increasing demand for natural products as curative agent. The medicinal plants are the primary sources for natural products and are used not only in the poorer countries but also in developing countries as alternate source of medicines to treat different diseases.[2-4]

The genus *Pinus* of the family *Pinaceae* (division *Pinophyta*) is comprised of more than 100 species and is spread worldwide.[5]

Pinus nigra Arnold is a large coniferous evergreen tree, growing to 20–55 meters tall at maturity. The bark is grey to yellow-brown, and is widely split by flaking fissures into scaly plates, becoming increasingly fissured with age. The leaves ("needles") are thinner and more flexible in western populations.[6]

Pinus sylvestris is an evergreen tree of 20-45 m height living up to 500 years. Pine is a source of wood, it is also used to protect the erosion of soil and its buds, needles and bark are used in phototherapy. Pine needles are rich in vitamin C, tannins, alkaloids and essential oils. Moreover, pines as all coniferous are very sensitive to air pollution, and the analysis of secondary metabolites allow evaluating both the physiological state of a plant and the environmental conditions under which it is growing.[5]

Our research group is interested to analyze the chemical profile of different medicinal plants which are growing wild in the region of Kosova and Albania.[7-13] The aim of this research was to determine the quantity of proteins, lipids, minerals and essential oil in the *Pinus nigra* Arnold and *Pinus sylvestris* in growing in Germia Park. Germia is a regional Park located in the north-east of Pristina, capital city of Kosovo, and it covers an area of 62 km^2.

Materials and methods

The needles of *Pinus nigra* Arnold and *Pinus sylvestris*, growing wild in Germia Park (located in the north-east of Pristina), was collected in July 2013. We took three samples from *Pinus sylvestris* and three from *Pinus nigra* Arnold. Voucher specimens were deposited in the Herbarium of the Department of Veterinary, University of Prishtina. The plants were dried at room temperature (22 °C). Proteins were determined according to the Kjeldahl method,[14] whereas lipids were determined according to the Soxhlet method.[15,16] As solvent was used diethyl ether. The essential oil was extracted with steam distillation for 4 h of 100 g of air dried needles.

The analysis, of the dry needles samples collected, resulted in the finding of minerals as sodium, potassium, calcium, zinc, iron and copper by using the method described by Taleisnik et al.[17] Therefore, the needles were

washed with destillated water to remove any dust and were dried in an oven at 105 °C for 48 h. The dried samples were pounded in a porcelain mortar until they formed a powder. Then, a 2 g sample, was calcified in an oven at 300-400 °C. The ashes were placed into 100 cm^3 of normal flask. Next, 10 cm^3 of 1 mol dm^{-3} nitric acid (HNO_3) was added to each flask, homogenized, and then shaken for 20 minutes in a shaker. The homogenized samples were filtered and filled till 100 cm^3 with 1 mol dm^{-3} HNO_3. Minerals like sodium, potassium, calcium, zinc, iron and copper were analyzed Atomic Absorption Spectrometry (Buc Scientific Model 200A).

Results and Discussion

Pinus nigra Arnold and *Pinus sylvestris* are analyzed in chemical aspect with the goal to research the chemical nature. We have analyzed the primary and secondary metabolites in quantitative manner. The amount of lipids, proteins and essential oil of *Pinus nigra* Arnold and *Pinus sylvestris* is given in Tables 1 and 2.

From experimental data (Table 1) we can see that the amounts of lipids were 7.185 %, proteins 7.714 % and essential oil 0.35 % in the *Pinus nigra* Arnold. From experimental data (Table 2) we can see that the amounts of lipids were 6.670 %, proteins 4.375 % and essential oil 0.32 % in the *Pinus sylvestris*.

Figures 1 and 2 shows the diagrams for the lipids, proteins and essential oil amounts to the *Pinus nigra* Arnold and *Pinus sylvestris* giving in percentage.

On Figures 1 and 2 we can see that the amounts of proteins, lipids and essential oils in *Pinus nigra* Arnold and in *Pinus sylvestris* are as follows: proteins > lipids > essential oil. The amount of essential oil is same in both the plants, but if we compare the amounts of proteins and lipids we can see that *Pinus nigra* Arnold contains higher amount of proteins and lipids (7.714 %, 7.185 % respectively) compared with the amounts of proteins and lipids in *Pinus sylvestris* (4.375 %, 6.670 % respectively).

The amount of essential oil in *Pinus nigra* Arnold (0.35 %) is almost same if we compare it with the amount of essential oil from different cities of Turkey[6] (Bursa 0.33-0.65 %, Antalya 0.38-0.55 %, Içel 0.38-0.65 %). The amount of essential oil of *Pinus sylvestris* (0.32 %) is same with the amount of essential oil of *Pinus sylvestris* growing wild in Lithuania (0.25-0.47 %).[5]

The amount of proteins in *Pinus nigra* Arnold (7.714 %) is lower than the amount of proteins from Turkey[18] (25.75 %). The amount of proteins in *Pinus sylvestris* (4.375 %) is lower than the amount of proteins from Mongolia[19] (45.1 %). The amount of lipids from *Pinus nigra* Arnold (7.185 %) are greater than to the *Pinus sylvestris* (6.670 %) growing wild in Kosovo. Also we did the research in the quantity of the minerals sodium, potassium, calcium, zinc, iron and copper. The amount of minerals of *Pinus nigra* Arnold and *Pinus sylvestris* are given in Tables 3 and 4

Table 1. The amounts of lipids, proteins and essential oil of the *Pinus nigra* Arnold

Components (%)	Mean	Standard deviation
Lipids	7.185	0.313
Proteins	7.714	0.169
Essential oil	0.35	0.112

Table 3 shows that the average values in mg kg^{-1} of sodium, potassium, calcium, zinc, iron and copper from *Pinus nigra* Arnold are 246 mg kg^{-1}, 1280 mg kg^{-1}, 4260 mg kg^{-1}, 17.2 mg kg^{-1}, 173 mg kg^{-1} and 3.83 mg kg^{-1}. From Table 4 we can see that the average values in mg kg^{-1} of sodium, potassium, calcium, zinc, iron and copper from *Pinus sylvestris* are 6.9 mg kg^{-1}, 420 mg kg^{-1}, 1180 mg kg^{-1}, 95 mg kg^{-1}, 840 mg kg^{-1} and 19 mg kg^{-1}.

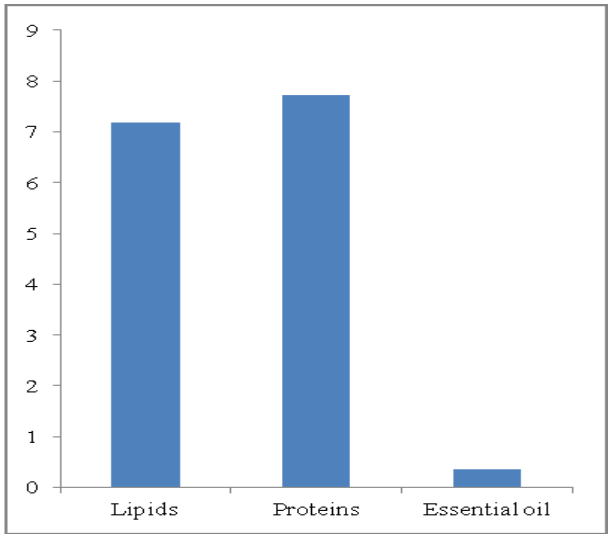

Figure 1. The diagram of the quantity of the lipids proteins and essential oil of the *Pinus nigra* Arnold

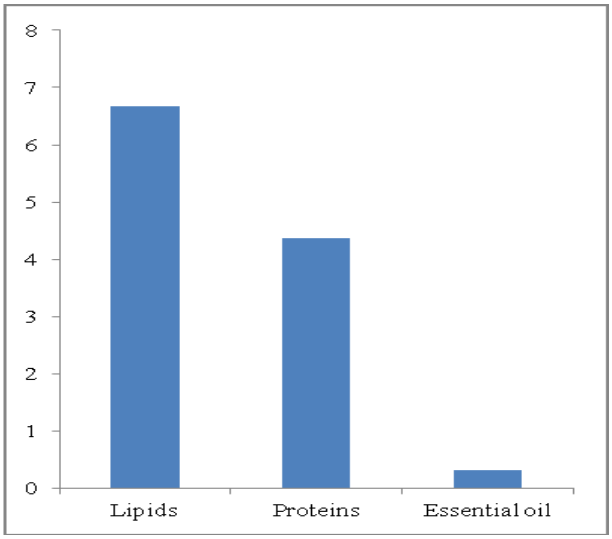

Figure 2. The diagram of the quantity of the lipids, proteins and essential oil of the *Pinus sylvestris*

Figures 3 and 4 shows the average values of elements in mg kg^{-1} from *Pinus nigra* Arnold and *Pinus sylvestris*.

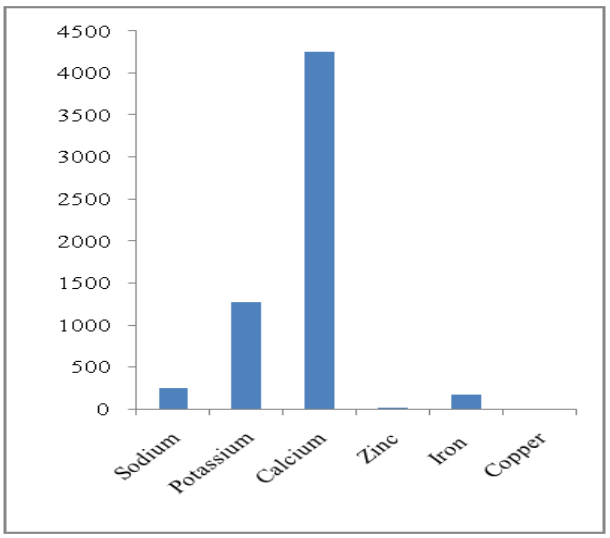

Figure 3. Diagram of the quantities of the minerals in the *Pinus nigra* Arnold

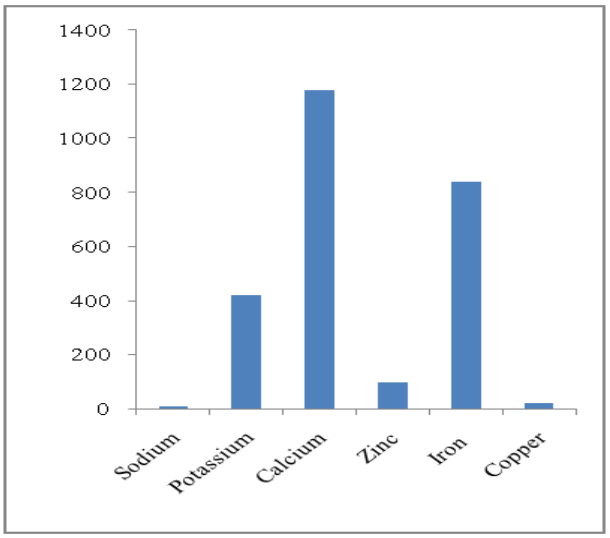

Figure 4. Diagram of the quantities of the minerals in the *Pinus sylvestris*

Pinus nigra Arnold contains large amounts of calcium (4260 mg kg^{-1}) and potassium (1280 mg kg^{-1}) (Figure 3), while *Pinus sylvestris* contains large amounts of calcium (1180 mg kg^{-1}) and iron (840 mg kg^{-1}) (Figure 4). The amount of sodium, potassium calcium from *Pinus nigra* Arnold are greater than that present in the *Pinus sylvestris*, while the amount of zinc, iron and copper in *Pinus sylvestris* are greater than to the *Pinus nigra* Arnold (Table 3 and 4).

The amounts of zinc (95 mg kg^{-1}), iron (840 mg kg^{-1}) and copper (19 mg kg^{-1}) of *Pinus sylvestris* growing wild in Kosovo are lower than to the *Pinus sylvestris* growing wild in Mongolia[19] (zinc 300 mg kg^{-1}, iron 2000 mg kg^{-1} and copper 500 mg kg^{-1}).

Pinus sylvestris contains large amounts of calcium (1180 mg kg^{-1}) compared to the amounts of calcium (500 mg kg^{-1}) in *Pinus sylvestris* growing wild in Mongolia.[19]

Table 2. The amounts of lipids, proteins and essential oil of the *Pinus sylvestris*

Components (%)	Mean	Standard deviation
Lipids	6.670	0.52638
Proteins	4.375	0.35865
Essential oil	0.320	0.05292

Table 3. Quantity of minerals of the *Pinus nigra* Arnold giving in mg kg^{-1}

Elements	Mean	Standard deviation
Sodium	246.0	30.000
Potassium	1283	20.167
Calcium	4260	16.252
Zinc	17.20	2.843
Iron	173.0	25.658
Copper	3.830	1.756

Table 4. Quantity of minerals in the *Pinus sylvestris* giving in mg kg^{-1}

Elements	Mean	Standard deviation
Sodium	6.90	0.56862
Potassium	420	88.88194
Calcium	1180	75.05553
Zinc	95.0	4.50925
Iron	840	87.17798
Copper	19.0	2.08167

Conclusion

The aim of this research was to determine the quantity of primary metabolites (lipids and proteins) and to analyze minerals as sodium, potassium, calcium, zinc, iron and copper.

From the results we can conclude that needles of *Pinus nigra* Arnold contain more proteins 7.714 % than *Pinus sylvestris* 4.375 %. Also, lipids in *Pinus nigra* Arnold are 7.185 % and in *Pinus sylvestris* 6.670 %, which means that they contain equal amounts of them. The total amount of essential oils in *Pinus nigra* Arnold are 0.35 % and in *Pinus sylvestris* 0.32 %.

In this research we have analyzed the amounts of minerals and from them we can order these elements in terms of their quantity. In *Pinus nigra* Arnold they are ordered as follows: Ca > K > Na > Fe > Zn > Cu. Order of the elements of *Pinus sylvestris* given mg kg^{-1} is as follows: Ca> Fe> K> Zn> Cu > Na. *Pinus nigra* Arnold contains large amounts of calcium and potassium, while *Pinus sylvestris* contains large amounts of calcium and iron.

As conclusion these two trees contain large amounts of essential oil and proteins. In the future our country should has attention to grow them in terms to get essential oil for different purposes. Let's hope that in the future programs of agricultural policies of our country, through developmental programmers in different private enterprises and municipalities, this field will get the attention it deserves.

References

[1]Sujata, B., Bhimsen, A., Meenakshi, S., *Chemistry of Natural Products*, First Edition, Springer, **2005**.

[2]Soomro, T., Zahir, E., Mohiuddin, S., Khan, N., Naqvi, Ll., *Pak. J. Biol. Sci.,* **2008**, *11(2)*, 285-289.

[3]Karak, T., Bhagat, R., *Food Res. Int.*, **2010**, *43(9)*, 2234-2252.

[4]Diacony, D., Diacony, R., Navrotescu, T., *Ovidius Univ. Ann. Chem.,* **2012**, *23(1)*, 115-120.

[5]Asta, J., Šližytė, J., Stiklienė, A., Kupèinskienė, E., *Chemija*, **2006**, *17(4)*, 67–73.

[6]Sezik, E., Ustun, O., Demirci, B., *Turk J. Chem*., **2010**, *34*, 313 – 325.

[7]Faiku, F., Haziri, A., Domozeti, B., Mehmeti, A., *Eur. J. Exp. Biol.,* **2012**, *2(4)*, 1273-1277.

[8]Faiku, F., Haziri, A., *Int. J. Pharm. Phytopharmacol. R*, **2013**, *3(3*), 254-257.

[9]Haziri, A., Aliaga, N., Ismaili, M., Govori, S., Leci, O., Faiku, F., Arapi, V., Haziri, I., *Am. J. Biochem. Biotechnol.,* **2010**, *6(1)*, 32-34.

[10]Haziri, A., Faiku, F., Mehmeti, A., Govori, S., Abazi, S., Daci, M., Haziri, I., Bytyqi-Damoni, A., Mele, A., *Am. J. Pharmacol. Toxicol.,* **2013**, *8(3)*, 128-133.

[11]Haziri, A., Govori, S., Ismaili, M., Faiku, F., Haziri, I., *Am. J. Biochem. Biotechnol.,* **2009**, *5(4)*, 226-228.

[12]Hajdari, A., Novak, J., Mustafa, B., Franz, C., *Nat. Prod. Res.,* **2012**, *26(18)*, 1676-1681.

[13]Hajdari, A., Mustafa, B., Franz, C., Novak, J., *Nat. Prod. Commun.,* **2011**, *6(9)*, 1343-1346.

[14]Kjeldahl, J., *Z. Anal. Chem.,* **1883**, *22(1),*366-383.

[15]Soxhlet, F., *Dingler's Polytechn. J.* (in German), **1879**, *232*, 461–465.

[16]Jensen, B., *J. Chem. Educ.,* (ACS), **2007**, *84(12)*, 1913–1914.

[17]Taleisnik, E., Peyrano, G., Arias, C., *Trop. Grasslands*, **1997**, *31*, 232-240.

[18]Ozler, H., Pehlivan, S., Bayrak, F., *Asian J. Plant Sci.,* **2009**, *8(4)*, 308-312.

[19]Dogan, M., *Ekoloji*, **2013**, *22(89)*, 40-48.

Received: 08.05.2015.
Accepted: 25.07.2015.

SOLVATION EFFECT ON SELF-ORGANIZATION OF COBALT COMPLEXES WITH SUBSTITUTED PHTHALOCYANINES

Alena Voronina[a], Anna Filippova[a], Mikhail Razumov[b], Ilya Kuzmin[b], Maxim Shepelev[c], Artur Vashurin[b]* and Oleg Golubchikov[d]

Keywords: phthalocyanine, cobalt complexes, aggregates, solvation effect.

The influence of solvating power of medium on self-organization of metallophthalocyanines in solution has been studied. It is shown that phthalocyanine macrocycles form *H*-associates in universal solvation medium. In case of specific solvation the nature of peripheral substitution of phthalocyanine macrocycle plays important role in the formation of ordered structure.

*Corresponding Authors
E-Mail: asvashurin@mail.ru
[a] Faculty of Fundamental and Applied Chemistry of Ivanovo State University of Chemistry and Technology, 153000, Russia, Ivanovo, Sheremetevsky ave., 7
[b] Department of Inorganic Chemistry of Ivanovo State University of Chemistry and Technology, 153000, Russia, Ivanovo, Sheremetevsky ave., 7
[c] Department Physical and Colloid Chemistry of Ivanovo State University of Chemistry and Technology, 153000, Russia, Ivanovo, Sheremetevsky ave., 7
[d] Department of Organic Chemistry of Ivanovo State University of Chemistry and Technology, 153000, Russia, Ivanovo, Sheremetevsky ave., 7

Introduction

Liquid-phase materials based on porphyrin and phthalocyanine complexes with d- and f-metals are widely used as photosensitizers,[1,2,3] as catalysts,[4,5,6,7] photovoltaics,[8,9] and in analytical chemistry.[10,11] The formation of supramolecular assemblies based on metallophthalocyanines is possible due to existence of molecular complexation processes. Central metal cation of macrocycle forms ordered phthalocyanine structures[12] by taking polidentate axial ligands into fifth and sixth coordination positions. Besides, phthalocyanine structures are able to form self-associates in solutions due to π-stacking and intermolecular interaction on macrocycle periphery.[13,14] Coordination centers on the periphery of phthalocyanine molecule are crucial for creation of materials with desired properties.

Nature of solvent has great influence on self-association of metallophthalocyanines in solution.[15,16] Obviously, solvents, having donor atoms such as nitrogen, oxygen or sulfur, act as not only universal solvating agents but as molecular ligands too. It is also known that molecular complexes formed between metallophthalocynine and solvent could be moved from a solution to crystal solvates.[17,18]

Present work assesses the impact of solvating power of a solvent on formation of self-ordered phthalocyanine structures.

Experimental

Solvents used viz., acetonitrile (An), pyridine (Py), N,N-dimethylformamide (DMF), dimethylsulfoxide (DMSO), ethanol (EtOH), were purified using known methods.[19] The water was double-distilled before the experiment. All solvents were stored in vacuo.

Sulfonated derivatives of cobalt phthalocyanine with peripheral substituents of regularly changing nature are investigated (Figure 1).

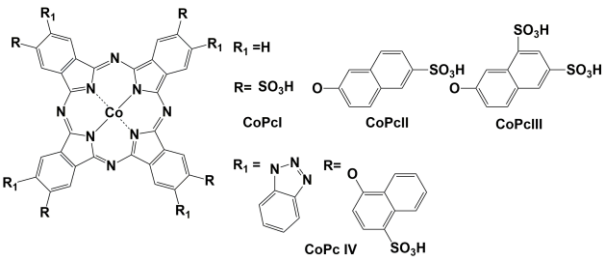

Figure 1. Structure of phthalocyanines.

Cobalt(II) tetrasulfophthalocyaninate (CoPcI) is synthesized and purified by "Weber-Busch" method.[20]

3,10,17,24-Tetrakis(6-sulfonaphthalen-2-yloxy)phthalocyaninato]cobalt(II) (CoPcII)[21,22] was synthesized by heating a mixture of 0.78 g of potassium 6-(1,3-dioxo-2,3-dihydro-1H-isoindol-2-yloxy)-naphthalene-2-sulfonic acid and 0.065 g of anhydrous cobalt(II) chloride for 60 min at 190-195 °C with stirring. The resulting cobalt phthalocyanine was extracted into DMSO and precipitated from the extract with anhydrous ethanol. The precipitate was filtered off and washed with ethanol in a Soxhlet extractor. The product was further purified by chromatography on silica gel M 60 using aqueous DMF (1:1 by volume) as eluent. The product was a blue–green powder, readily soluble in water, aqueous DMF, DMSO, and aqueous alkali and the yield = 0.39 g (54 %). IR spectrum, ν, cm^{-1}: 1045 ($S{=}O_s$), 1103 ($S{=}O_{as}$), 1205 (C–O–C). Found, %: C 58.42; H 2.70; N 7.62; S 8.80. $C_{72}H_{40}CoN_8O_{16}S_4$. Calculated, %: C 59.22; N 2.74; N 7.68; S 8.80.

3,10,17,24-Tetrakis(6,8-disulfonaphthalen-2-yloxy)phthalocyaninato]cobalt(II) (CoPcIII)[21,22] was synthesized in a similar way from 1.01 g of dipotassium 7-(1,3-dioxo-2,3-dihydro-1H-isoindol-2-yloxy)naphthalene-1,3-disulfonate. Yield: 0.53 g (59 %); blue–green powder, readily soluble in water, aqueous DMF, DMSO, and aqueous alkali. IR spectrum, ν, cm^{-1}: 1039 ($S=O_s$), 1103 ($S=O_{as}$), 1210 (C–O–C). Found, %: C 48.32; H 2.20; N 6.23; S 14.43. $C_{72}H_{40}CoN_8O_{28}S_8$. Calculated, %: C 48.57; H 2.25; N 6.30; S 14.39.

Synthesis of 2,9,16,23-tetrakis(1-benzotriazolyl)-3,10,17,24-tetrakis(4-sulfo-1-naphthoxy)phthalocyaninato-cobalt(II) (CoPcIV) was carried out by directed sulfonation of initial phthalocyanine.[23] There are characteristic vibrational bands (cm^{-1}) for CoPcIV in FT-IR spectra (KBr): 745 (C-N), 1045 (N=N), 1230 (Ar-O-Ar), 1060 (C-S), 1150-1190 (S=O in SO_3H). MS (MALDI-TOF) *m/z* 1932.71 $[M+4H]^+$. In ^1H NMR (500 MHz, DMSO-d_6): δ (ppm) 7.45 (Ar-5H), 7.94 (Ar-4H), 8.07 (Ar-6H), 8.29 (Ar-3H) – triazole groups, 7.64 (Ar-8H), 7.73 (Ar-7H), 7.85 (Ar-11H), 8.18 (Ar-10H), 8.53 (Ar-9H), 8.85 (Ar-12H) – naphthoxy groups, 8.97 (SO_3H).

FT-IR spectra were recorded using IR-Fourier spectrophotometer Avatar 360 (USA) in 400-4000 cm^{-1} frequency range. NMR spectra of the solutions were recorded on Bruker AVANCE-500 NMR spectrometer at 500 MHz (^1H) operating frequency. Measurements were performed under the Fourier transformation conditions in 5 mm cells at various temperatures. Chemical shifts were measured with reference to TMS as the internal standard. The accuracy of measurements was ± 0.005 ppm. Electron adsorption spectra (UV-VIS) were registered on Unico 2800 spectrophotometer in a spectral range of 200 – 1000 nm. Quartz optical cell were used for the measurements. UV-Vis spectra were recorded at 298.15 ± 0.03 K. Mass spectra were measured on an Axima MALDI-TOF mass-spectrometer (Shimadzu).

Contributions of monomeric and dimeric components in UV-VIS spectra were found using the method of statistical expansions on the Gaussian function.[24, 25] Further, extinction coefficients for monomeric (ε_M) and dimeric (ε_D) forms of the phtalocyanine were calculated based on these data using Beer-Lambert-Bouguer law.

Results and Discussion

Sulfonated derivatives of cobalt phthalocyanine form self-assembled structures in solvent mediums with high universal solvation toward macrocycle. Solvent does not affect conjugated *π*-electronic system when universally solvate the periphery of macrocycle molecule, so it does not prevent formation of *H*- and *J*-aggregates (Figure 2). The following equilibrium (Eqn. 1) is observed in the system.

$$2CoPc{\cdot}nSolv \rightleftharpoons (CoPc)_2{\cdot}nSolv \quad (1)$$

Obviously, it is possible to regulate π-π-repulsion and π-σ-contraction processes, due to which *H*-aggregates are formed, by changing of specific solvation ability of the solvent. Hence it affects the reaction (1). Simultaneously the solvent becomes a competing agent in *J*-aggregates formation due to donor-acceptor interaction with central metal cation.

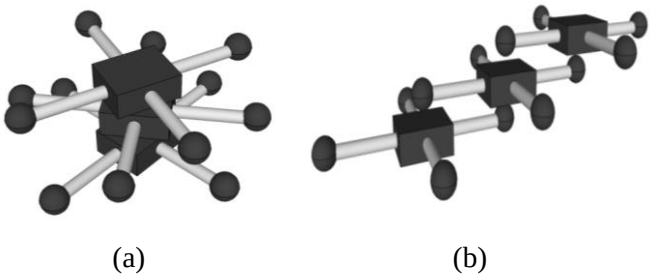

(a) (b)

Figure 2. Scheme of CoPc self-associates in solutions: (a) H-aggregates, (b) J- aggregates.

If the solvent acts as axial ligand, the following reactions are likely to be present.

$$(CoPc)_2 + L \rightleftharpoons CoPc{\cdot}L + CoPc \quad (2)$$

$$CoPc + L \rightleftharpoons CoPc{\cdot}L \quad (3)$$

$$CoPc{\cdot}L + L \rightleftharpoons L{\cdot}CoPc{\cdot}L \quad (4)$$

Investigation of concentration dependence of UV-VIS spectra for CoPc(I-III) shows that these macrocycles are associated in water. Figure 3 presents typical changes in UV-VIS spectra of aqueous solutions of CoPc.

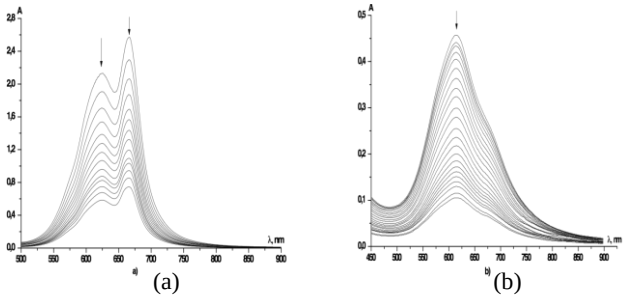

(a) (b)

Figure 3. Typical changes in UV-VIS spectra during dilution of aqueous solutions of phthalocyanines (a) CoPcI, (b) CoPcII in concentration range of 2 $x10^{-4}$ – 2 x 10^{-7} mol L^{-1}.

The presence of absorption maximum in range of 600-650 nm suggests high degree of self-association of phthalocyanine structures in solution. Previously[22,26,27] extinction coefficients of dimers of CoPcI, CoPcII and CoPcIII in aqueous solutions were determined by us. It was also shown that these macrocycles form dimers due to π-π-interaction.[22,28] Obviously, the water in the system acts as universal solvent for phthalocyanine. It is known that water is a self-assembled system and forms assemblies due to hydrogen bond lattices.[28,29] That is why detachment of water molecule from the general system for coordination

interaction with phthalocyanine leads to disturbance of energy balance of the system. However, formation of ordered phthalocyanine structure with twenty molecules of water has been reported.[30] Evidently, the water in this case acts as not only agent promoting dimerization but as direct participant of the process. Thus, the reactions (3) and (2) should be observed in reverse sequence instead of reaction (1) in the system. Besides the role of hydration of CoPcI monomeric molecule in associate formation is not clear.

Introduction of naphthalene fragment into peripheral substituent (CoPcII and CoPcIII) leads to decreasing of influence of electron acceptor group (-SO_3H) on conjugated macrocycle system. It promotes stabilization of partially uncompensated charge on central metal cation of phthalocyanine, amplification of π-π-contraction processes and diminution of association. The data of Table 1 shows that stability of dimeric structures decreased in the series CoPcI– CoPcII – CoPcIV – CoPcIII. Exceptional position of CoPcIII is likely due to stabilization of associates caused by coordination interaction of sulfonic groups with π-π-dimer. It leads to stable coordinated associates (*J*-aggregates) formed by introduction of fragment of phthalocyanine peripheral substituent into centre of π-π-dimer. Addition of triazole fragment in annelated benzene ring as second peripheral substituent (CoPcIV) leads to redistribution of electronic effects of the periphery on conjugated macrocycle π-system and as consequence to formation of self-assembled structures in solutions. Presence of the second organic fragment causes decreasing of the solvating power of the water toward the phthalocyanine and increasing association.

Table 1. Extinction coefficients and dissociation constants of *H*-dimers in aqueous solutions of metallophthalocyanines.

Macrocycles	ε_M, L mol cm^{-1}	ε_D, L mol cm^{-1}	$K_{diss}\times10^{-4}$ mol L^{-1}
CoPcI	-	15200±50	1.17
CoPcII	-	4800±50	1.54
CoPcIII	-	800±20	2.23
CoPcIV	32700 ± 80	8930 ± 50	1.91

The influence of temperature on dimerization was investigated to confirm the type of associates fromation. On one side increasing of temperature should decrease the dielectric constant of the medium which in turn should decrease the solvating power of the solvent and amplify association. However, in the case of fromation *H*-aggregates increasing of kinetic energy of the system promotes dissociation of dimers.

The changes of UV-VIS spectra of aqueous solution of phthalocyanine as a function of temperature are presented in Figure 4. The figure shows that every investigated system exhibits different spectral changes on heating. An increase of intensity of *Q*-band absorption and transition to monomeric state of macrocycle conjugated π-system are observed for CoPcI. Probably, significant increasing of molecules mobility occurs in solution in case of this phthalocyanine, which compensates for the decrease in the solvating power of the water. Presence of isosbestic points in UV-Vis spectra suggests several forms of phthalocyanine chromophore system (obviously monomeric and associated).

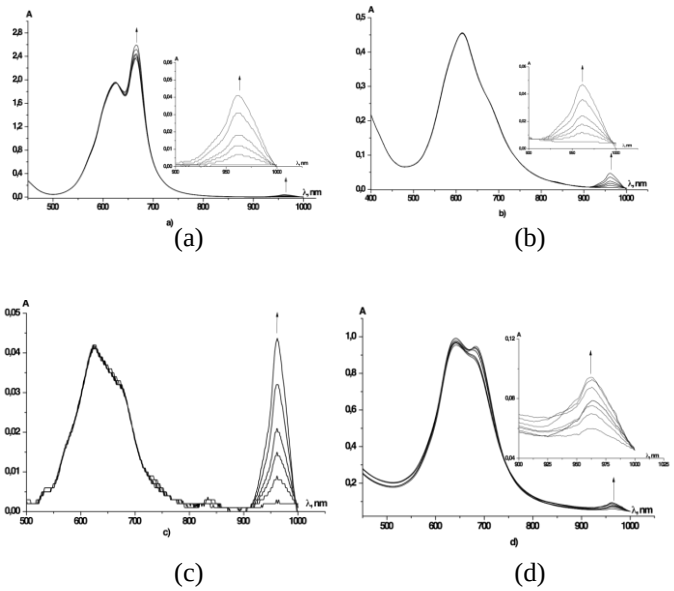

Figure 4. UV-Vis spectra of aqueous solutions of (a) CoPcI (12.75×10^{-5} mol L^{-1}), (b) CoPcII (9.49×10^{-5} mol L^{-1}), (c) CoPcIII (5.63×10^{-5} mol L^{-1}), (d) CoPcIV (7.64×10^{-5} mol L^{-1}) varying the temperature from 298.15 K to 333.15 K.

There are no significant changes in range of *Q*-band absorption for macrocycles CoPcII and CoPcIII. There are interesting changes for CoPcIV. The increasing of temperature from 298.15 K to 318.15 K leads to shifting of associative balance toward monomerization. Further, increase in temperature leads to abrupt aggregation of CoPcIV. This may be explained by loss of solvating power of water toward peripheral substituents of CoPcIV containing functional groups. Along with this, it is likely that significant amplification of hydrophobic influence of triazole fragment on association has occurred.

Increase of temperature in all systems causes appearance of new absorption band in range of 950-970 nm. In our view, this effect is caused by amplification of association due to reduction of solvation and of interparticle interaction of phthalocyanine molecule in solution. Besides, this fact together with changes in visible part of spectrum (500 – 800 nm) suggests formation of thread-like assemblies based on CoPc *H*-dimers. In case of CoPcIII this type of associates becomes predominant.

It is possible to control the monomer-dimer equilibrium and hence to carry out the directed formation of supramolecular phthalocyanine systems by amplification /reduction of solvating power of the medium. UV-VIS spectra for the investigated phthalocyanines in DMF are presented on Figure 5.

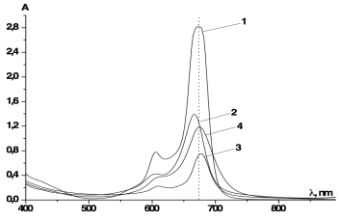

Figure 5. UV-Vis spectra of solutions under the temperature of 298.15 K in DMF: (1) CoPcI (6.25×10^{-5} mol L^{-1}), (2) CoPcII (5.49×10^{-5} mol L^{-1}), (3) CoPcIII (6.3×10^{-5} mol L^{-1}) and (4) CoPcIV (5.3×10^{-5} mol L^{-1}).

The presented data show that all investigated macrocycles are monomeric in DMF. DMF is a solvent having electron donor atoms. Hence it interacts by coordination with central metal cation of phthalocyanine macrocycle. Besides, DMF has specific solvation ability toward peripheral substituents of phthalocyanine due to its donor-acceptor properties (DN 26.6[31,32] and AN 16[31,32]). CoPcI has the highest solvation. Introduction of naphthalene fragment into peripheral substituent promotes reduction of phthalocyanine solvation which is reflected in hypsochromic effect and hypsochromic shift up to 10 nm for absorption *Q*-band of CoPcII compared to CoPcI. It may be explained, based on suggestion, that the main centre of specific solvation is central metal cation. In this case the dissociation of *H*-aggregates will occur, but ordered structures will be formed due to weak hydrogen bonds, that are reflected in observed spectral changes. Introduction of second functional group on periphery of macromolecule promotes additional electrostatic repulsion of phthalocyanines that leads to amplification of monomerization and bathochromic shift. It is observed for CoPcIII. Relatively small intensity of absorption for *Q*-band is caused by weakening of chromophore solvation. Probably, coordination and electrostatic interaction of the solvent with two macrocycles at the same time is possible due to presence of resonance structure of DMF.[33] Similar changes are observed for DMSO. Molar extinction coefficients CoPcI – CoPcIV are shown in Table 2.

There is significant shifting of associative equilibrium toward monomeric form under the condition of 10-fold molar excess of coordinating solvent when DMF is added to CoPc solutions (Figure 6). There is small relaxation maximum of absorption in range of 590-610 nm for compounds CoPcI – CoPcIII. It is characteristic of residual associated structures formed due to hydrogen bonds on periphery of the molecule. UV-VIS spectra of CoPcIV is staying wide enough when DMF is added, wherein there is small shoulder observed in range of dimers absorption. In our opinion it is connected with the fact that the solvent solvates primarily triazole fragment of peripheral substituent and the system reaches equilibrium state with a large number of associated forms compared to CoPcI-CoPcIII.

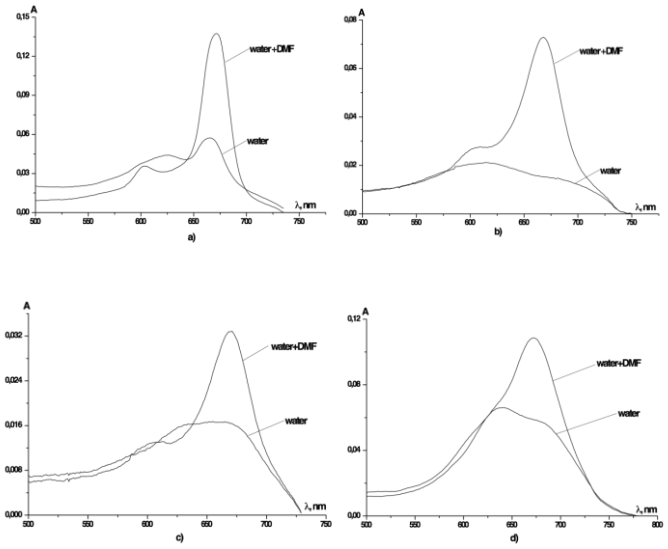

Figure 5. UV-Vis spectra of solutions under 298.15 K, n_{DMF}/n_{CoPcI} 10:1, S 1.99 mm.(a) CoPcI (2.89×10^{-6} mol L^{-1}), (b) CoPcII (4.12×10^{-6} mol L^{-1}), (c) CoPcIII (1.48×10^{-5} mol L^{-1}), (d) CoPcIV (7.39×10^{-6} mol L^{-1}).

Table 2. Extinction coefficients (L mol^{-1} cm^{-1}) of metallophthalocyanines monomeric forms.

Solvent	CoPcI	CoPcII	CoPcIII	CoPcIV
DMF	58400± 90	24200 ± 90	10400 ± 50	22350 ± 40
DMSO	45000 ± 70	18850 ± 60	2320 ± 20	24420 ± 40

Thus, the present work shows that specific solvation of the solvent plays great role in formation of ordered structures of phthalocyanines in solution. If the solvent universally solvate the phthalocyanine, *H*-associates are formed predominantly. Shifting of associative equilibrium toward monomeric structures is possible in binary systems when one of solvents is coordinating. Thus, the solvating power of the medium is key for self-assembling of Co(II)-phthalocyanines sulfo-derivatives.

Acknowledgments

The work is carried out within the public tasks of the Ministry of Education and Science of the Russian Federation and partially financially supported by grant of the President of the Russian Federation (project No MK-2776.2015.3).

References

[1]Jiang, Z., Shao, J., Yang, T., Wang, J., Jia, L., *J. Pharm. Biomed. Anal.*, **2014**, *87*, 98.

[2]Ağırtaşa, M. S., Karataşa, C., Özdemir, S., *Spectrochim. Acta*, **2015**, *A135*, 20.

[3]Zhao, P., Woo, J., Park, Y.-S., *Macromol. Res*., **2010**, 18, 496.

[4]Sorokin, A. B., *Chem. Rev*., **2013**, *113*, 8152.

[5]Vashurin, A., Maizlish, V., Pukhovskaya, S., Voronina, A., Kuzmin, I., Futerman, N., Golubchikov, O., Koifman, O., *J. Porphyrins Phthalocyanines*, **2015**, *19*, 573.

[6]Vashurin, A. S., Pukhovskaya, S. G., Semeikin, A. S., Golubchikov, O. A., *Macroheterocycles.***2012,** *5*, 72.

[7]Basu, B., Satapathy, S., Bhatnagar, A. K.,*Catal. Rev. Sci. Eng*., **1993**, *35(4)*, 571.

[8]Stuzhin, P. A., Mikhailov, M. S., Travkin, V. V., Gudkov, E. Yu., Pakhomov, G. L., *Macroheterocycles*,**2012,** *5*, 162.

[9]Wahab, F., Sayyad, M. H., Tahir, M., Khan, D. N., Aziz, F., Shahid, M., Munawar, M. A., Chaudry, J. A., Khan, G., *Synth. Metals*, **2014**, *198*, 175.

[10]Vashurin, A., Pukhovskaya, S., Kuzmicheva, L., Titova, Yu., Golubchikov, O., *Nat. Sci.*, **2012**, *4*, 461.

[11]Biesaga, M., Pyrzyn´ska, K., Trojanowicz, M., *Talanta*, **2000**, *51*, 209.

[12]Thordarson, P., Nolte, R. J. M., Rowan, A. E., *The Porphyrin Handbook.*, *Elsevier Science*, **2003**, *18*, 281.

[13]Tonga, S.-L., Zhang, J., Yana, Y., Hua, Sh, Yua, J., Yu, L., *Solid State Sci.*, **2011**, *13*, 1967

[14]Palewska, K., Sworakowski, J., Lipinski, J., *Optic. Mater*, **2012,** *34*, 1717.

[15]Lukyanets, E. A., Nemykin, V. N., *J. Porphyrins Phthalocyanines*, **2010**, *14*, 1

[16]Ji, L., Jing, L., Lin, Sh., Deng, X., Zhu, P., Zhang, X., *Dyes and Pigments*, **2014**, *106*, 176.

[17]Vashurin, A. S., Tikhomirova, T. V., Maizlish, V. E., *Russ. J. Inorg. Chem.*, **2015,** *60*, 431.

[18]Antina, E. V., V'yugin, A. I., *Russ. J. Gen. Chem*, **2012**, *82*, 298.

[19]Weissberger, A., Proskauer, E. S., Riddick, J. A., Toops, E. E., *Organic solvent: physical properties and methods of purification., New York: Inter. Science Publishers Inc*, **1955**.

[20]Weber, J. H., Busch, D. H., *Inorg. Chem*., **1965,** *4*, 469.

[21]Kulinich, V. P., Shaposhnikov, G. P., Badaukaite, R. A., *Macroheterocycles*, **2010**, *3*, 23.

[22]Voronina, A. A., Kuzmin, I. A., Vashurin, A. S., Shaposhnikov, G. P., Pukhovskaya, S. G., Golubchikov, O. A., *Russ. J. Gen. Chem*., **2014**, *84*, 1777.

[23]Znoiko, S. A., Kambolova, A. S., Maizlish, V. E., Shaposhnikov, G. P., Abramov IG, Filimonov, S. I., *Russ. J. Gen. Chem*., **2009**, *79*, 1735.

[24]Martyanov, T., Ushakov, E. N., Klimenko, L. S., *Macroheterocycles*, **2013**, *6*, 240.

[25]Mood, A. M, Graybill, F. A., Boes, D. C., *Introduction to the Theory of Statistics. 3rd ed., New York: McGraw-Hill*, **1974**.

[26]Voronina, A. A., Vashurin, A. S., Litova, N. A., Shepelev, M. V., Pukhovskaya, S. G., *Izv. Vysh. Uchebn. Zaved. Khim. Khim. Technol.*,**2014**, *57*, 51. (*in Russ*.)

[27]Filippova, A., Voronina, A., Litova, N., Razumov. M., Vashurin, A., Pukhovskaya, S., *Eur. Chem. Bull*., **2014**, *3(11)*, 1055.

[28]Teixeira, J., *Mol. Phys.* **2012**, *110*, 249.

[29]Malenkov, G., *J. Phys.: Condens. Matter*, **2009**, *21*, 3101.

[30]Abel, E. W., Pratt, J. M., Whelan, R., *J. Chem. Soc. Dalton Trans*, **1976**, 509.

[31]Gutman, V., Schmid, R., *Coord. Chem. Rev.*, **1974**(3), 263.

[32]Mayer, U., *A semiempirical model for the description of solvent effects on chemical reactions, Pure & Appl. Chem*. **1979**, *51*, 1697.

[33]Vasudevan, V., Mushrif S. H., *J. Mol. Liq*, **2015**, *206*, 338.

Received: 13.06.2015.
Accepted: 26.07.2015

AN ADDITIONAL POSSIBILITY OF USING THE HILL COEFFICENTS

V. I. Krupyanko[a]

Keywords: Hill coefficients, active centers of enzymes.

The possibility of using the Hill coefficients to estimate the first $K^0_{0.5(A1)}$ and the second $K^0_{0.5(B1)}$ constant for the active center of two-subunits of enzymes is considered. The method to calculate $K^0_{0.5(A1)}$ and $K^0_{0.5(B1)}$ constants is discussed.

*Corresponding Authors
Fax: 8 -495- 956-33-70
E-Mail: krupyanko@ibpm.pushchino.ru; pH76@mail.ru
[a] G.K. Skryabin Institute of Biochemistry and Physiology of Microorganisms, Russian Academy of Sciences, prospect Nauki, 5, Pushchino, Moscow region 142290 Russia

Introduction

A considerable number of papers have been published in enzymology dealing with the properties of allosteric (associated as subunits) enzymes. These studies suggested positive or negative cooperativity on the basis of the mechanism of the their action on a substrate. The kinetics of the studies invariably showed the presence of the Michaelis-Menten kinetics.[1-9], in which a saturation curve is obtained when the initial velocity v_0 of the reaction is plotted against the substrate concentration as is shown in curve *a*, Figure 1.

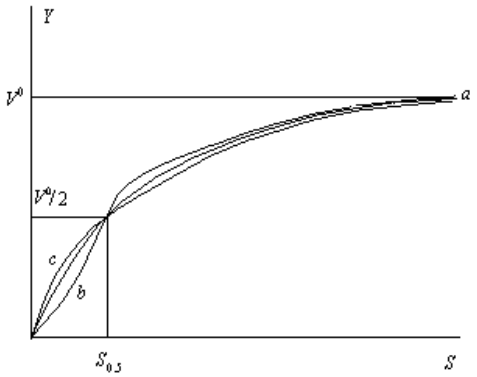

Figure 1. The reaction progress curve showing the dependence on progress curve of velocity changes v_0 on the concentration of substrate S when the Hill coefficient $h = 1$ (curve *a*, bold line), curve *b* if $h > 1$, and curve *c* when $h < 1$. Y – the parameter of enzyme saturation; $V^0 \rightarrow Y$ (by $S >> K^0_m$).

The aim of this investigation was to obtain the information not only on the catalytic activity (V^0), but also on the strength of binding (K^0_m) between the enzyme and the substrate.[3, 7-9, 11, 14-16] The (Eq. 3) is obtained when the Hill coefficient h is equal to 1.

The dependence of the initial velocity of the reactions, catalyzed by cooperative enzymes, is given by the Hill equation (1), whereas the Michaelis-Menten equation is expressed in Equation (2).

$$v_0 = V^0 \frac{S_0^h}{S_0^h + S_{0.5}^h}, \quad (1)$$

$$v_0 = V^0 \frac{S}{S + K^0_m} = V^0 \frac{S}{S + S_{0.5}}, \quad (2)$$

where V^0 is the maximum reaction velocity reached at the maximum substrate concentration S as given in equation (2) wherein K^0_m is the Michaelis constant which is equal to the substrate concentration at which the reaction rate is half of V_{max}.

The comparison of the equation (1) with the equation (2) suggests that at $h = 1$ $S^h_0 = S$ and $S^h_{0.5} = K^0_m$.

In enzymology the value of the Michaelis constant K^0_m is characteristic of the enzyme signifying the strength of binding between the enzyme and the substrate; the lower is the value of the K^0_m constant, the greater is the binding strength between the enzyme and the substrate i.e. the substrate conversion is more effective (V^0 increases). The Hill coefficient h in equation (1) determines the number of substrate-binding centers on the molecule of the allosteric enzyme and the strength of the binding between the active centers and the substrate. The Hill coefficient h is dimensionless.[17] As a general rule, when $h > 1$, indicates the positive cooperativity in a process of substrate conversion; the binding of the second molecule on the second active center of the enzyme increases the initial velocity v_0 of conversion of the first substrate on the first active center of the enzyme (Fig. 1, curve *b*); if the Hill coefficient is $h < 1$, the binding of the second substrate (on the second active center of the enzyme) makes the binding of the first substrate on the first active center weaker, hence the velocity v_0 of the conversion of the first substrate slows down pointing to the negative cooperativity in the mechanism of enzyme action (Fig. 1, curve *c*).

The equation (2) is used to test the data for the strength of the binding of an enzyme to a substrate (an inhibitor or activator), assuming that $h = 1$).[1, 6, 18-20]

$$V^0 \frac{S_0^h}{S_o^h + S_{0.5}^h} \rightarrow V^0 \frac{S}{S + K_m^0} \quad (3)$$

It can be useful if $h = 1$ or it is not larger than the error interval:

$$S_{0.5}^h \rightarrow S_{0.5}^1 = K_m^0. \quad (4)$$

Let us consider one of the most common "parallel-subsequent" schemes of the catalytic conversion of the substrate by the enzymes consisting of two E_A and E_B subunits:

$$NS + \left(\frac{E_A}{E_B}\right) \rightarrow \left(\frac{E_A S_3}{E_B^*} \rightarrow \frac{E_A^*}{E_B S_2}\right) + Pr(s_1) \rightarrow \left(\frac{E_A^*}{E_B S_2} + \frac{E_A S_1}{E_B^*}\right) + Pr(s_2) + \ldots \quad (5)$$

where E_A is a subunit located on the "upper" part of the enzyme and E_B is on the lower part, (Eq. 5) is associated with noncovalent powers of interaction i.e. hydrogen, hydrophobic etc.

There exists an additional possibility of using the Hill coefficients when $h > 1$ or $h < 1$.

Positive cooperativity ($h > 1$). Let us consider that the value for the Hill coefficient $h = 1.75$ (dimensionless units). If this coefficient is written as a sum of two numbers: $h = (1.0 + 0.75)$, Eq. (4) can be rewritten as:

$$S_{0.5}^{1.75} \rightarrow S_{0.5}^1 S_{0.5}^{0.75} = K_m^0 S_{0.5}^{0.75}, \quad (6)$$

where $S^1{}_{0.5}$ is the concentration of first substrate bound to the "upper" subunit E_A of the enzyme.

The relationship $h = 1$ is necessary and sufficient condition (according to Michaelis-Menten theory) for the conversion of the first substrate on subunit E_A into reaction product $Pr(s_1)$, and the remaining value 0.75 characterizes the strength of binding of the second substrate on the second subunit E_B.

It follows that at half value of the substrate concentration, $v_0 = V^0/2$. Taking $S_{0.5} = 4.4 \times 10^{-4}$ M (for ease of analysis), the value of $S_{0.5(A)}$ for the binding of the first substrate on the active center of subunit E_A is given by the equation (7):

$$S_{0.5(A)} = K^0{}_{mA} = \frac{4.4 \times 10^{-4}\ \text{M}}{(1 + 0.75)} = 2.514 \times 10^{-4}\ \text{M}. \quad (7)$$

Similarly the value of $S_{0.5(B)}$ (for the binding of the second substrate on the active center of subunit E_B) is expressed by the equation (8):

$$S_{0.5(B)} = K^0{}_{mB} = \frac{2.514 \times 10^{-4}\ \text{M}}{0.75} = 3.35 \times 10^{-4}\ \text{M}. \quad (8)$$

The values of the parameters h and $S^1{}_{0.5}$ are reported very often.[1-7,12,18-22]

Negative cooperativity ($h < 1$). Assuming $h = 0.85$, an analysis similar to that described in equations (1 – 8) can be made. Thus it implies that the binding strength of the second molecule of the substrate (S) on the second subunit E_B of the enzyme, expressed by the equation (10), is more efficient than the binding strength of the molecule of the first substrate S on subunit E_A, which is expressed by the equation (9)

$$S_{0.5(A)} = K^0{}_{mA} = 4.4 \times 0.85 \times 10^{-4}\ \text{M} = 3.74 \times 10^{-4}\ \text{M}, \quad (9)$$

and molecule of the second substrate S on subunit E_B:

$$S_{0.5(B)} = S_{0.5(A)} \times 0.85 = 3.74 \times 0.85 \times 10^{-4}\ \text{M} = 3.179 \times 10^{-4}\ \text{M}. \quad (10)$$

Symmetrically-opposite position of the Hill coefficient (h) in (Eqs. 9 – 10) with regard to (Eqs. 7 and 8) is in agreement both with the symmetry of the position of curves b and c (Fig. 1) and with the ratio of the values of the relevant coefficients ($h < 1$) and ($h > 1$).

Eqs. (7, 8 and 9, 10) can be useful for the calculation of the values of $K^0{}_{mA}$ and $K^0{}_{mB}$ constants in order to gain the insight into the strength of the binding of the enzyme to a substrate not only on the first $K^0{}_{mA}$ but also on the second $K^0{}_{mB}$ active center of two-subunit enzymes.

The above could probably be applied to the analysis of data of not only bi- (E_A/E_B) and tetra-($E_{A1}E_{A2}/(E_{B1}E_{B2})$) but two-subunit enzymatic complexes of more higher order ($E_{A1}E_{A2}E_{A3}/(E_{B1}E_{B2}E_{B3})$ as well.

Table 1. An additional possibility of using the Hill coefficients.

Sources of enzyme	pH	$S_{0.5}$, mM	n_H	K_m, mM	K_{mA}, mM	K_{mA}, mM	K_{mB}, mM
L, plant.	5.5	0.65[21]	1.1	0.77		*0.59**	*5.91**
	7.8	0.22[21]	1.0	0.23	0.23 [21]	*0.22*	
	8.5	0.36[21]	1.1	0.39		*0.327*	*3.273*
L. acido.	6.0	0.27[21]	1.1			*0.245*	*2.45*
	7.6	0.37[21]	1.8			*0.206*	*0.257*
	8.3	0.36[21]	2.5			*0.144*	*0.096*
Mtb FolB		0.48 μM[22]	2.0			*0.00024*	*0.00024*
G360P		75 mM[16]	0.68			*51.0*	*34.7*
ATPase		63 μM[23]	0.6			*0.038*	*0.023*

*Iitalicized figures have been obtained using Eqs. 7 – 10. *L. plant* – phosphofructokinase from *L. plantarum*; *L. acido* - phosphofructokinase from *L. acidophilus*; *G360P* – mutant CTP synthase from *Lactococcus lactis*; *Mtb FolB* – 7,8-dehydroneopterin aldolase from *M. tuberculosis*; *ATPase* – Na/K-ATPase from Pig Kidney

References

[1]Kazerounian S., Pitari G. M., Ruitz-Stewart I., Schulz S., Waldman S. A., *Biochemistry,* **2002***, 41(10)*, 3396.

[2]Chan M., Sim T-S., *Biochem. Biophys. Res. Comm*., **2005,** *326(1)*, 188.

[3]Mercante J., Suzuki K., Cheng X., Babitzke P., Romeo T., *J. Biol. Chem*., **2008**, *281(42)*, 31832.

[4]Saito J., Yamada M., Watanabe T., Iida M., *Protein Sci.*, **2008**, *17(4)*, 691.

[5]Diaz A., Munoz-Clares R. A., Rangel P., Valdes V-J., Hansberg W., *Biochemie*, **2005**, *87(1)*, 205.

[6]Choudhary M. I., Punckar N. S., *FEBS Letters*, **2007,** *581(3)*, 2733.

[7]Rao D. N., Rao N. A., *Biochem. Biophys. Res. Comm*., **1980,** *92(4)*, 1166.

[8]Ureta T., *J. Biol. Chem*., **1976**, *251(16)*, 5035.

[9]Andersen J. F., Ribeiro J. M. C., *Biochemistry*, **2006**, *45(17)*, 5450.

[10]Gopal E., Fel Y-J., Miyauchi S., Zhuang L, Prasad P. D., Ganpathy V., *Biochem. J*., **2005,** *388(2)*, 309.

[11]Fassy F., Krabs G., Lowinsky M., Ferrari P., Winter J., Collard-Dutilleul; V., Salahbey H. V., Salahbey H. K., *Biochem. J*., **2004**, *384(3)*, 619.

[12]Zemlyanukhin A. A., Popova T. N., Kurichenko V. A., *Biochemistry* (Moscow), **1987**, *52(7)*, 1201.

[13]Valle P., Arriaga D., Busto F., Soler J., *Biochim. Biophys. Acta*, **1986**, *874(1)*, 193.

[14]Murkin A. S., Chou W. K., Wakarchuk W. W., Tanner M. E., *Biochemistry*, **2004**, *44 (44)*, 14290.

[15]Zaitseva J., Jenewein S., Wiedenmann A., Benabdelhak H., Holland J. B., Schmitt L., *Biochemistry*, **2005**, *44(28)*, 9680.

[16]Willemoes M., Molgaard A., Johannson E., Martinussen J. Lid L., *FEBS J.*, **2005**, 272(*4*), 856.

[17]Kurganov B. I., *Allosteric Enzymes*. Moscow, Nauka. **1990**, pp. 3 – 248, (in Russian).

[18]Bheemanaik S., Chandrashekaran S., Nagaraja V., Rao D. N., *J. Biol. Chem*., **2003**, *277(35)*, 31499.

[19]Chen Q-X.,. Huang H., Kubo I., *J. Prot. Chem*., **2003**, *22(5)*, 481.

[20]Majumdar C., Abbotts J., Broder S., Wilson S. H., *J. Biol. Chem*., **1988**, *263(30)*, 15657.

[21]Simon W. A., Hoper H. W., *Biochim. et Biophys. Acta*, **1977**, *481(2)*, 450.

[22]Goulding C. W., Apostol M. I., Sawaya M. R., Phillips M., Parseghian A., Eisenberg D., *J. Mol. Biol*., **2005,** *349(1)*, 61.

[23]Tannoe K., Kaya S., Hayashi Y., Abe K., Imagawa T., Taniguchi K., Sakaguchi K., *J. Biochem*., **2006**, *140(1)*, 599.

Received: 04.04.2015.
Accepted: 29.07.2015.

EXTRACTION OF LEAD(II) AND CADMIUM(II) BY CROSS LINKED POLYSTYRENE THIOUREA

Omar Abderrahim[a], Benaïssa Esma[a] and Mohamed Amine Didi[a]*

Keywords: Pb(II), Cd(II), polystyrene thiourea, kinetics, thermodynamics, diffusion.

The aim of this study is to investigate Lewatit TP 214, which is a chelating ion-exchange polymer containing chemically bonded thiourea group, for the sorption of Pb(II) and Cd(II) ions from aqueous solutions. The effects of parameters such as the concentration, pH, contact time, ionic strength and temperature have been investigated. The results showed more affinity of resin towards cadmium than for lead cations. Lewatit TP 214 exhibited a good sorption potential at initial pH values for Pb(II) and Cd(II) at room temperature. The extraction kinetics, for both Pb(II) and Cd(II), is best described by the pseudo second order model. This study showed that the diffusion of moving boundary particles fits well the experimental data (r > 0.99) for the sorption of both Pb(II) and Cd(II) ions. The Langmuir isotherm fits better with the obtained equilibrium data as compared to that with the Freundlich isotherm. The thermodynamic data for the sorption of Pb(II) and Cd(II), on the resin, indicate that the process is endothermic for Pb(II) while it is exothermic for Cd(II). The process showed negative ΔG values, indicating that the sorption of both Pb(II) and Cd(II) ions is spontaneous.

* Corresponding Author
Fax: +21343213198
E-Mail: madidi13@yahoo.fr
[a] Laboratory of Separation and Purification Technology, Department of Chemistry, Tlemcen University, Box 119, Tlemcen 13000, Algeria.

Introduction

Heavy metals are significantly hazardous due to their toxicity even at very low concentration in water.[1] Exposure to lead and cadmium are old problems with modern prevalence, they are widely dispersed in the environment, and exposure to either element can give rise to a number of adverse health effects, due to their toxicity after accumulation in multiple body organs.[2] The main sources of these elements are metal plating industries, abandoned disposal sites, and mining industries.[3] The removal of heavy metals from waste waters can be carried out by a number of separation technologies, such as chemical precipitation,[4] membrane processes,[5,6] ion exchange,[7,8] adsorption,[9,10] and solvent extraction.[11-13] Nonetheless, many conventional technologies are inadequate, expensive or produce large amounts of sludge, which create disposal problems.[14] Moreover, they are not economical to reduce metal toxicity to extremely low levels, as required by the environmental regulations, which limits the usage of these technologies to drinking water purification.[14] Solid-phase extraction (SPE) is the most common technique used for metal pre-concentration in aqueous phase because of the advantages it offers, i.e. high enrichment factor, high recovery, rapid phase separation, low cost, reversible process and low consumption of organic solvents.[15,16] In SPE, the choice of an appropriate chelating agent is critical to obtain a full recovery and a high enrichment factor. For this reason, modification of resins with thiourea has been extensively investigated.[17-20] Lewatit TP 214 is a monospherical, macroporous chelating resin with thiourea groups and has a high affinity for metal cations.

The objective of this research is to carry out a comparative study on the solid-phase extraction of both Pb(II) and Cd(II) ions from aqueous solutions, using resin Lewatit TP 214. The effects of analytical parameters, such as the metal concentration in aqueous phase, pH level, contact time, ionic strength and temperature on the degree of extraction have been investigated.

Experimental

Reagents and Apparatus

Lewatit TP 214 (Bayer) is a chelating ion-exchange resin having thiourea as functional group in a divinylbenzene cross linked polystyrene matrix (Figure 1). All chemicals products used in this work were of analytical grade. Cadmium nitrate, lead nitrate, hydrochloric acid (37 %), sodium hydroxide (80 %) and 4-(2-pyridylazo)-resorcinol (PAR) were from Merck. Absolute ethanol, sodium chloride, potassium chloride and sodium nitrate were provided by Fluka. Acetic acid (100 %) and nitric acid (60 %) were obtained from Riedel-de Haen.

Stock and standard solution of Pb(II) and Cd(II) ions were prepared by dissolving an appropriate amount of their salts in distilled water. Solutions of lower concentrations were prepared by the dilution of stock solution.

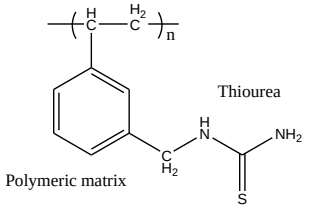

Figure 1. Structure of Lewatit TP 214 resin.

The sorption of Pb(II) and Cd(II) ions on Lewatit TP 214 resin was studied by the batch technique. A shaker (Haier model) was used for adsorption experiments except for temperature effect where a magnetic stirrer (RCT Basic IKAMAG Stirrer with ETS-D5 Temperature Controller) was used. All pH measurements were performed with a WTW 3310 Set 2 digital pH meter.

Sorption Studies

The sorption of lead and cadmium ions onto Lewatit TP 214 beads was investigated in solid-phase extraction from aqueous media in a batch system. Lewatit resin (0.050 g) was added to 5 mL of a solution containing metal cations, in a glass flask (25 mL) and the mixture was shaken for a suitable time. Then, the aqueous phases were separated from the chelating resin by filtration. The concentration of Pb(II) and Cd(II) ions, in aqueous phase, were determined , before and after sorption, at pH = 10 and 5.5 at λ_{max} = 525 nm and λ_{max} = 510 nm, respectively using a spectrophotometer (Analytik Jena Specord 210Plus) with PAR as complexant.[21,22]

Kinetic studies on the removal of Pb(II) and Cd(II) ions were carried out, with an initial ion concentration of 1.0 x 10^{-3} mol L^{-1} at room temperature. The effect of contact time on the sorption was studied up to 120 minutes, while other parameters, like the sorbent dosage, shaking speed (Ø) and pH were kept constant. The effect of the initial pH on the removal of Pb(II) and Cd(II) ions, was studied at pH 1.4 to 5.5 and 2.0 to 6.1, respectively. The pH was adjusted by adding appropriate quantities of HCl or NaOH solutions (0.01 mol L^{-1}). The percentage removal (φ) of Pb(II) and Cd(II) ions was determined by using Eqn. (1).

$$\varphi = \frac{C_0 - C_t}{C_0} 100, \% \qquad (1)$$

The amount of Pb(II) and Cd(II) ions uptakes at time *t*, q_t (mg g^{-1}), was calculated by Eqn. (2).

$$q_t = \frac{C0 - Ct}{W} V \qquad (2)$$

where C_0 and C_t are the metal ion concentration in the beginning and at time *t*, respectively. *V* (L) is the volume of the solution, *M* (g mol^{-1}) is the molar mass of metal ion and *W* is the mass of the chelating resin used (g).

Results and Discussion

Effect of pH

The effect of the pH on the recovery of Pb(II) and Cd(II) ions was investigated in the pH range of 1.4 to 5.5 and 2.0 to 6.1, respectively, using 5 mL of each one of the solution of Pb(II) and Cd(II), and 0.050 g of Lewatit TP 214 resin. The results (Figure 2) indicated that the extraction yield for Cd(II) continuously increased reaching a value of 60.4 % at pH 6.1, whereas that of Pb(II) was 52 % at pH 4.1 and thereafter it decreased. However, when the pH is lowered, the extraction yield decreases, and this may be attributed to the hydrogen ions which compete with the metal ions for the sorption sites in the chelating resin Lewatit TP 214.[23]

Effect of Contact Time

The effect of contact time is shown in Figure 3. The sorption of both Pb(II) and Cd(II) ions was rapid in the initial 15 min, and then the extraction yield increased slowly. The sorption process reached equilibrium at nearly 15 and 30 min, respectively, for the removal of Pb(II) and Cd(II) ions by Lewatit TP 214 resin. The % extraction yield, almost in equal proportions, was rapid in the beginning of the contact time. It is related to the availability of a larger number of active sites on the resin surface, which improved diffusion of metal ions to the surface.[24]

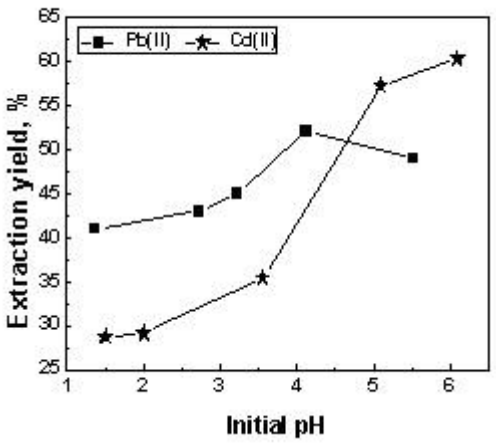

Figure 2. Effect of initial pH of solution on Pb(II) and Cd(II) ions extraction yield. $[Pb(II)]_0$ = 1.0 mM, $[Cd(II)]_0$ = 1.0 mM, *W* = 0.050 g, *V* = 5 mL and Ø = 250 rpm.

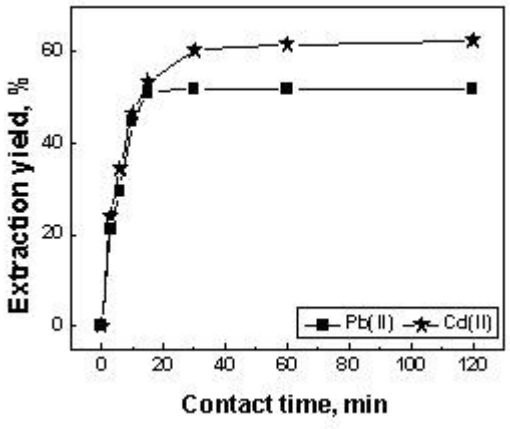

Figure 3. Effect of contact time on extraction yield of both Pb(II) and Cd(II) ions removal. $[Pb(II)]_0$ = 1.0 mM, $[Cd(II)]_0$ = 1.0 mM, *W* = 0.050 g, *V* = 5 mL, pH = 5.0 and Ø = 250 rpm.

Effect of the Initial Concentration of Metal Ions

The retention capacity of the chelating resin Lewatit TP 214 was determined by equilibrating 0.050 g of resin with 5 mL of the solution containing different concentrations (1.0 x 10^{-4} to 1.0 x 10^{-1} mol L^{-1}) of metal ions. For the removal of Pb(II), by Lewatit TP 214, the uptake (q_t) increased with the initial concentration of Pb(II) up to the maximum value q_{max} = 55.59 mg g^{-1} (Figure 4). The observed sorption capacity is higher than that of some of the other sorbent materials reported in literature, like phosphatic clay (35.83 mg g^{-1}),[25] chars from co-pyrolysis (1.87 mg g^{-1}),[26] Jordanian kaolinite (54.35 mg g^{-1}),[27] and carbon nanotubes coated with crystalline manganese dioxide nanoparticles (20.0 mg g^{-1}).[28] Figure 4 also shows that the sorption capacity for Cd(II) (81.75 mg g^{-1}) is much better than that for Pb(II) (55.59 mg g^{-1}), which means that resin Lewatit TP 214 can more efficiently remove Cd(II) present in aqueous solutions compared to other sorbent materials, for instance the adsorption of cadmium(II) on MnO_2-loaded resin (21.45 mg g^{-1}),[29] MnO_2 loaded D301 resin (77.88 mg g^{-1}),[30] and by the Amberlite XAD-7/Cyanex 921(13.0 mg g^{-1}).[31]

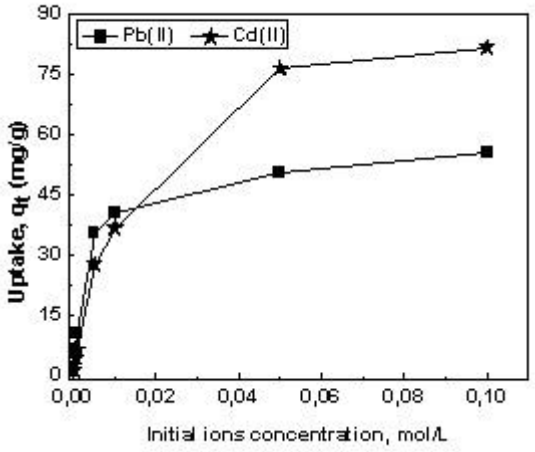

Figure 4. Effect of initial Pb(II) and Cd(II) ions concentration on their sorption capacities by Lewatit TP 214 resin: $[Pb(II)]_0$ = 1.0 mM, $[Cd(II)]_0$ = 1.0 mM, W = 0.050 g, V_{sol} = 5 mL, Ø = 250 rpm and pH ≅ 5.0.

Sorption Kinetics

In order to study the sorption mechanism of Pb(II) and Cd(II) ions onto Lewatit TP 214 resin, the pseudo first-order, pseudo second-order and second-order kinetic models were applied to the experimental data.[32] The linear form of the pseudo-first-order rate equation, given by Lagergren, is expressed as Eqn. (3),

$$\ln(q_e - q_t) = \ln q_e - k_1 t \qquad (3)$$

where q_e and q_t are the respective amounts of metal ions (mg g^{-1}) sorbed onto the resin, at equilibrium and at time t, and k_1 is the first-order sorption rate constant (min^{-1}). The linear form of the pseudo-second order rate equation is given by Eqn. (4),

$$\frac{t}{q_t} = \frac{1}{k_2 q_{es}^2} + \frac{1}{q_e} \qquad (4)$$

where q_{es} is the sorption capacity, calculated from the pseudo-second-order kinetic model (mg g^{-1}), and k_2 is the pseudo-second-order sorption rate constant (g mg^{-1} min^{-1}). The second order sorption kinetic rate equation is given by Eqn. (5).

$$\frac{1}{q_e - q_t} = \frac{1}{q_e} + k_3 t \qquad (5)$$

where k_3 (g mg^{-1} min^{-1}) is the second-order sorption rate constant.

The results of analysis in terms of the three equations are summarized in Table 1. The best correlation is obtained with the pseudo-second-order equation (r > 0.99). The plots of the sorption of Pb(II) and Cd(II) ions using the pseudo-second-order model are shown in Figure 5. From Table 2 and Figure 5, the equilibrium sorption capacity was calculated and was found to be close to the experimental value.

Table 1. Kinetic modelling of Pb(II) and Cd(II) ions sorption by Lewatit TP 214 resin

Models	Parameters	Pb(II)	Cd(II)
First-order rate model	q, calculated	15.01	6.69
	q, experimental	10.77	7.025
	k_1(min^{-1})	0.266	0.128
	r	0.971	0.998
Pseudo-second-order rate model	q, calculated	12.99	8.26
	q, experimental	10.77	7.025
	k_2(g mg^{-1} min^{-1})	0.015	0.027
	r	0.991	0.999
Second-order rate model	q, calculated	62.50	8.55
	q, experimental	10.77	7.025
	k_3(g mg^{-1} min^{-1})	0.056	0.041
	r	0.913	0.980

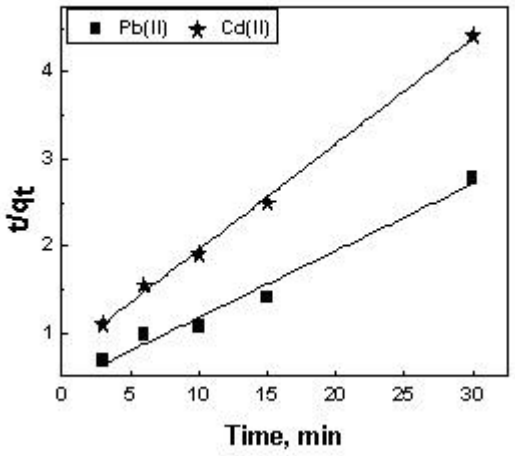

Figure 5. Pseudo second-order plots for the Pb(II) and Cd(II) ions sorption by Lewatit TP 214 resin: $[Pb(II)]_0$ = 1.0 x10^{-3} mol L^{-1}, $[Cd(II)]_0$= 1.0 x10^{-3} mol L^{-1}, W = 0.050 g, V_{sol} = 5 mL, pH = 5.0 and Ø = 250 rpm.

Diffusion Study

The sorption of Pb(II) and Cd(II) ions onto Lewatit TP 214 resin from their nitrate solutions may be considered as a liquid–solid phase reaction which includes several steps,[33-35] viz., (i) diffusion of ions from the solution to the resin surface, (ii) diffusion of ions within the solid resin, and (iii) chemical reaction between ions and the functional groups of resin. The transfer of ions can be described by means of Nernst–Planck equations which apply to the counter diffusion of two species in an almost homogeneous medium.[30] If the liquid film diffusion controls the exchange rate, the Eqn. (6) can be applied.

$$-\ln(1-F) = kt \qquad (6)$$

In case of diffusion of metal ions inside the resin, Dumwald-Wagner proposed a mathematical model,[35] which can be simplified into Eqn. (7).

$$-\ln(1-F2) = kt \qquad (7)$$

In both Eqns. (6) and (7), k is the kinetic coefficient or rate constant, which can be defined by Eqn. (8).

$$k = \frac{D_r \pi^2}{r_0^2} \qquad (8)$$

where F is is the fractional attainment of equilibrium at time t and is obtained by the ratio, $F = q_t/q_e$. D_r is the diffusion coefficient in resin phase and r_0 is the average radius of a resin particle.

When the adsorption of metal ions involves mass transfer accompanied by a chemical reaction, the process can be explained by the moving boundary model.[33] This model assumes a sharp boundary that separates a completely reacted shell from an unreacted core. This boundary advances from the surface toward the center of the solid with the progression of adsorption. In this case, the rate equation is given by Eqn. (9).

$$3-3(1-F)^{2/3}-2F = kt \qquad (9)$$

The correlation data of Figures 6, 7 and 8 are summarized in Table 2 and showed that the film diffusion fits well the experimental data (r = 0.999) in Cd(II) sorption while the moving boundary diffusion is more adequate in Pb(II) (r = 0.989) sorption.

Table 2. The regression constants and regression coefficients of diffusion study for Pb(II) and Cd(II) ions onto Lewatit TP 214**.**

Metal		Film Diffusion	Intraparticle diffusion	Moving boundary
Pb(II)	K (min^{-1})	0.0301	0.271	0.066
	r	0.978	0.967	0.989
Cd(II)	K (min^{-1})	0.123	0.099	0.034
	r	0.999	0.997	0.997

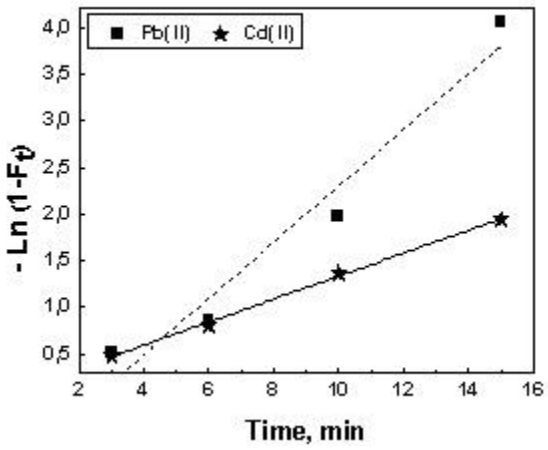

Figure 6. Plot of film diffusion (Eqn. 6) for Pb(II) and Cd(II) ions sorption onto Lewatit TP 214 resin: $[Pb(II)]_0$ = 1.0 mM, $[Cd(II)]_0$ = 1.0 mM, W= 0.050 g, V_{sol} = 5 mL, pH ≅ 5.0 and Ø = 250 rpm.

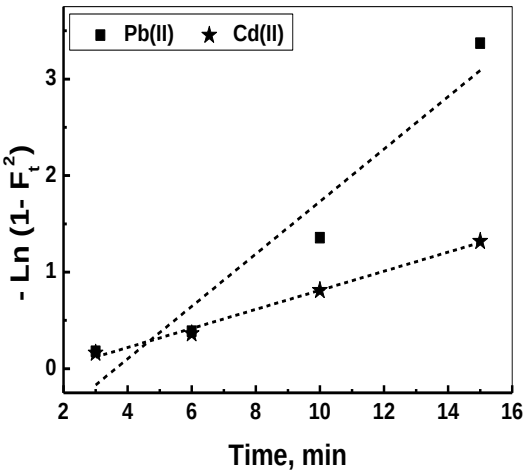

Figure 7. Plot of intraparticle diffusion (Eqn. 7) for Pb(II) and Cd(II) ions sorption onto Lewatit TP 214 resin. $[Pb(II)]_0$ = 1.0 mM, $[Cd(II)]_0$ = 1.0 mM, W = 0.050 g, V_{sol} = 5 mL, pH ≅ 5.0 and Ø = 250 rpm.

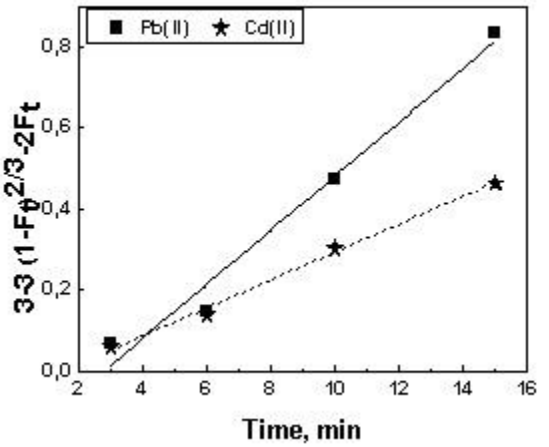

Figure 8. Plot of moving boundary model (Eqn. 9) for Pb(II) and Cd(II) ions sorption onto Lewatit TP 214 resin: $[Pb(II)]_0$ = 1.0 mM, $[Cd(II)]_0$ = 1.0 mM, W= 0.050 g, V_{sol} = 5 mL, pH ≅ 5.0 and Ø = 250 rpm.

 DOI: 10.17628/ecb.2015.4.343-349

Adsorption Isotherm

The equilibrium isotherm parameters often provide some insight into the sorption mechanism of the adsorbent. There are many equations for analyzing the experimental data for the adsorption equilibrium. In this work, the experimental results obtained were tested by the Langmuir and Freundlich isotherm models.[36,37] Their linear forms are expressed as Eqns. (10) and (11).

$$\frac{C_e}{q_e} = \frac{C_e}{q_m} + \frac{1}{q_m K_L} \quad (10)$$

$$\ln q_e = \ln K_F + \frac{1}{n} \ln C_e \quad (11)$$

where C_e the equilibrium concentration, q_m the maximum sorption capacity, K_L the Langmuir constant which is related to the heat of sorption, n the constant indicating the Freundlich isotherm curvature and K_F the Freundlich sorption coefficient. The Langmuir and Freundlich plots are shown in Figures 9 and 10. The higher regression coefficients obtained for Langmuir model (Table 3) as compared to that for the Freundlich model indicates that the Langmuir model is applicable to this system. Thus the sorption of Pb(II) and Cd(II) by Lewatit TP 214 is of a monolayer-type, which agrees with a previous report.[38]

Table 3. Sorption isotherm models for Pb(II) and Cd(II) ions adsorption onto Lewatit TP 214 resin.

Metal	Langmuir Isotherm			Freundlich Isotherm		
	K_L	Q_m, mg g^{-1}	r	K_F	n	r
Pb(II)	395.55	56.18	0.999	231.44	2.34	0.957
Cd(II)	187.09	86.21	0.998	311.45	2.15	0.981

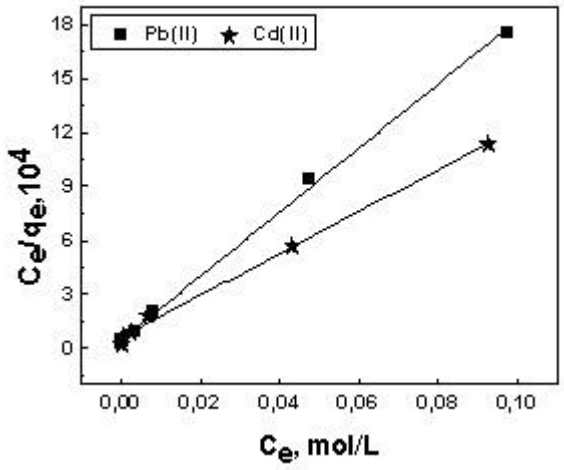

Figure 9. Langmuir isotherm for Pb(II) and Cd(II) ions sorption on Lewatit TP 214. W = 0.050 g, V_{sol} = 5 mL, pH ≅ 5.0 and Ø = 250 rpm.

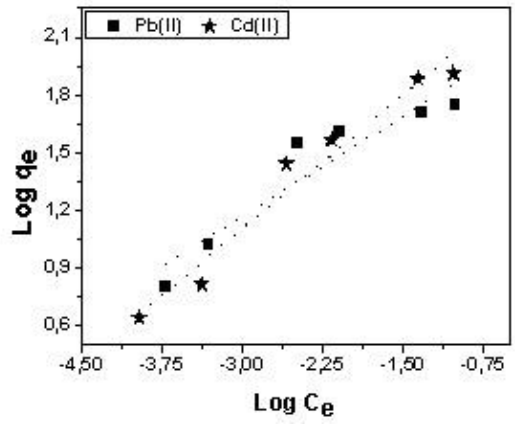

Figure 10. Freundlich isotherm for Pb(II) and Cd(II) ions sorption on Lewatit TP 214. W = 0.050 g, V_{sol} = 5 mL, pH ≅ 5.0 and Ø = 250 rpm.

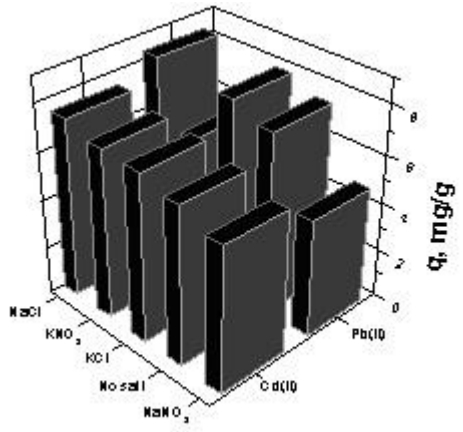

Figure 11. Effects of adding of an electrolyte on Pb(II) and Cd(II) ions sorption onto Lewatit TP 214 resin : $[Pb(II)]_0$ = 1.0 mM, $[Cd(II)]_0$ = 1.0 mM, [electrolyte] = 1.0 mol.L^{-1}, W = 0.050 g, V_{sol} = 5 mL and Ø = 250 rpm

Effects of Electrolytes

To study the effect of electrolytes on the sorption of Pb(II) and Cd(II) ions onto Lewatit TP 214 resin, 1 mol L^{-1} of each $NaNO_3$, NaCl, KNO_3 and KCl was added in separate experiments. The results are depicted in Figure 11. It was noted that the sorption of both Pb(II) and Cd(II) increased on the addition of KCl and NaCl. For Pb(II), the sorption increased from 7.50 to 8.06 and 8.36 mg g^{-1}, respectively. For Cd(II), it rose from 6.54 to 6.95 and 7.45 mg g^{-1} respectively. Addition of $NaNO_3$ (1 M) decreases the sorption of Pb(II) and Cd(II) to 4.84 and 5.96 mg g^{-1}, respectively, compared to the values obtained without electrolyte. It might be the consequence of difference in changes in hydration degree of cations take part in the sorption process. This is, however, depends on the concentration of the used electrolytes. Addition of KNO_3 increases Cd(II) sorption but reduces that of Pb(II) (see also section – *Effect of ionic strength*) .

Effects of Ionic Strength

To study the effect of ionic strength on Pb(II) and Cd(II) ions sorption onto Lewatit TP 214 resin, a series of batch experiments were carried using $NaNO_3$ at different concentrations (from 0.05 to 3 mol L^{-1}) as electrolyte. The solution ionic strength was set to have values ranged from 0.056 to 3.006 mol L^{-1}. The observed data are depicted in Figure 11. It was noted that both Pb(II) and Cd(II) ions sorption increased with increasing the solution ionic strength. For Pb(II) ions sorption the sorption capacity increases from 4.57 to 6.03 mg g^{-1} when $NaNO_3$ increased from 0.1 to 3 mol L^{-1} and for the Cd(II) ions sorption, the sorption capacity increases from 3.83 to 7.01 mg g^{-1} when $NaNO_3$ increased from 0.05 to 3 mol L^{-1} (Figure 12).

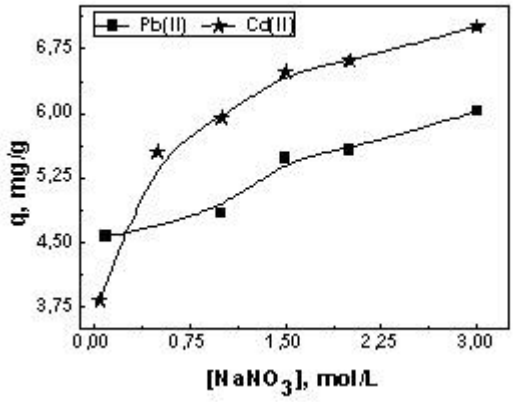

Figure 12. Effect of $NaNO_3$ concentration on Pb(II) and Cd(II) ions sorption onto Lewatit TP 214 resin: $[Pb(II)]_0$ = 1.0 mM, $[Cd(II)]_0$ = 1.0 mM, W = 0.050 g, V_{sol} = 5 mL and Ø = 250 rpm.

Effect of temperature

Few studies of effect of temperature changes have been carried out on chelating ion exchangers. Empirical studies show that temperature has a significant effect on retention in chelating exchange.[39] Thermodynamic parameters such as, the Gibbs free energy change (ΔG), enthalpy change (ΔH) and entropy change (ΔS) have been determined for the present system.

Table 4. Thermodynamics parameters for sorption process of Pb(II) and Cd(II) ions on Lewatit TP 214 resin

Parameter	***T*, K**	**Pb(II)**	**Cd(II)**
ΔH, kJ mol^{-1}		8.94	-51.65
ΔS, J mol^{-1} K^{-1}		32.51	-182.33
ΔG, kJ mol^{-}	*T*, K	Pb(II)	Cd(II)
	291	-	-1.41
	294	0.62	-
	298	-	-2.68
	308	-1.07	-4.51
	318	-	-6.33
	323	-1.56	-
	338	-2.05	-

A plot of ln *K* versus inverse of temperature is linear and the thermodynamic parameters were calculated by standard procedure (Table 4). A negative ΔG value indicates that the sorption of Pb(II) and Cd(II) ions with Lewatit TP 214 are spontaneous. These results show also that the sorption of Pb(II) ions onto Lewatit TP 214 is an endothermic process while that of Cd(II) ions is exothermic.

Conclusion

This work demonstrated the successful application of Lewatit TP 214 for an effective sorption and pre-concentration of lead and cadmium cations in batch mode. The experimental data showed that the sorption of Pb(II) and Cd(II) ions onto Lewatit TP 214 resin is highly affected by operational parameters, such as contact time, initial ion concentration, initial pH, ionic strength, and temperature. The maximum sorption of Pb(II) and Cd(II) ions was obtained at pH 4.1 and 6.1, respectively. The kinetic study showed an initial stage (the first 15 min) where the sorption reaction was fast for both cations (Pb(II) and Cd(II)), then the reaction rate decreased slightly until equilibrium was reached. The sorption capacity rose as the initial concentrations of lead and cadmium cations were increased. The sorption capacity of cadmium ions (81.75 mg g^{-1}) was better than that of lead ions (55.59 mg g^{-1}). The kinetic data were well described by the pseudo–second-order model (r > 0.99). The diffusion study showed that the moving boundary diffusion fits well the experimental data (r > 0.99). The observed equilibrium data showed a better fit with Langmuir isotherm model than with Freundlich model. This indicates that the sorption of Pb(II) and Cd(II) ions by Lewatit TP214 is of a monolayer-type. It was noted also that the sorption of Pb(II) and Cd(II) ions increased as the solution ionic strength went up. The thermodynamic study showed negative ΔG values, which indicates that the sorption of both Pb(II) and Cd(II) ions with Lewatit TP 214 is spontaneous. Moreover, this study showed that the sorption of Pb(II) ions onto Lewatit TP 214 is an endothermic process while that of Cd(II) is exothermic.

References

[1]Bentouami A., Ouali M. S., *J. Colloid Interfac Sci.*, **2006**, *293*, 270.

[2]Daher R. T., *Anal Chem*, **1995**, *67(12)*, 405.

[3]Corami A., Mignardi S., Ferrini V., *J. Colloid Interfac Sci.*, **2008**, *317*, 402.

[4]Hsien Lee I., Kuan Y. C., Chern J.M., *J. Hazard. Mater.*, **2006**, *B138*, 549.

[5]R. Banihashemi, *J. Hazard. Mater.*, **2009**, *165*, 630.

[6]Parhi P. K., Das N. N., Sarangi K., *J. Hazard. Mater.*, **2009**, *172*, 773.

[7]Wong C. W., Barford J. P., Chen G., *J Environ Chem Eng*, **2014**, *2*, 698.

[8]Srinivasa Rao K., Roy Chaudhury G., Mishra B. K., *Int J Miner Process*, **2010**, *97*, 68.

[9]Fan H T, Wu J B, Fan X. L., Zhang D., Su Z., Yan F., Ting S., *Chem Eng J*, **2012**, *198-199*, 355.

[10]Da Fonseca M G, de Oliveira M M, Arakaki L N H, *J. Hazard. Mater.*, **2006**, *B137*, 288.

[11]Sato K, Akama Y., Nakai T., *Anal Chim Acta*, **1988**, *207*, 367.

[12]Almela A, Elizalde M P, Gomez J. M., *Fluid Phase Equilibr*, **1998**, *145*, 301.

[13]Kumar V, Kumar M, Jha M K et al., 2009. *Hydrometallurgy*, **2009**, *96*, 230.

[14]Barreira L. D., Lito P. F., Antunes B. M., Otero M., Lin Z., Rocha J., Pereira E., Duarte A. C.,. Silva C. M., *Chem Eng J.*, **2009**, *155*, 728.

[15]Parham H, Pourreza N, Rahbar N., *J. Hazard. Mater.*, 2009, *163*, 588.

[16]Barciela-Alonso M. C., Plata-García V., Rouco-López A., A. Moreda-Piñeiro A., Bermejo-Barrera P., *Microchem J*, **2014**, *114*, 106.

[17]Fan L., Luo C., Lv Z., Lu F., Qiu H., *J. Hazard. Mater.*, **2011**, *194*, 193.

[18]Birinci E, Gülfen M, Aydın A.O., *Hydrometallurgy*, **2009**, *95*, 15.

[19]Zhou L., Liu J., Liu Z., *J. Hazard. Mater.*, **2009**, *172*, 439.

[20]Ghanei-Motlagh M., Fayazi M., Taher M. A., *Sensors Actuators*, **2014**, *B 199*, 133.

[21]Sekar M, Sakthi V, Rengaraj S., *J. Colloid Interfac Sci.*, **2004**, *279(2)*, 307.

[22]Hashem E. Y., *Spectrochim Acta A*, **2002**, *58*, 1401.

[23]Kazemipour M., Ansari M., Tajrobehkar S., Majdzadeh M., Kermani H. R., *J. Hazard. Mater.*, **2008**, *150*, 322.

[24]Luo C, Wei R, Guo D.,Zhang S., Yan S., *Chem Eng J*, **2013**, *225*, 406.

[25]Singh S P, Ma L Q, Hendry M J, 2006. *J. Hazard. Mater.*, **2006**, *B136*, 654.

[26]Bernardo M., Mendes S., Lapa N., Gonçalves M., Mendes B., Pinto F., Lopes H., Fonseca I., *J. Colloid Interfac Sci.*, **2013**, *409*, 158.

[27]Al-Harahsheh M., Shawabkeh R., Al-Harahsheh A., Tarawneh K., Batiha M. M., *Appl Surf Sci*, **2009**, *255*, 8098.

[28]Abdel Salam M., *Colloid Surface A*, **2013**, *419*, 69.

[29]Dong L, Zhu Z, Ma H., Qiu Y., Jianfu Zhao J., *J Environ Sci.*, **2010**, *22(2)*, 225.

[30]Zhu, Z., Ma, H., Zhang, R., Ge, Y., Zhao, J., *J Environ Sci*, **2007**, *19*, 652.

[31]Navarro R, Saucedo I, Núñez A., Ávila M., Guibal E., *React Funct Polym.*, **2008**, *68*, 557.

[32]Jing X. S., Liu F.Q., Yang X., Ling P. P. , Li L. J., Long C., Li A., *J. Hazard. Mater.*, **2009**, *167*, 589.

[33]Abderrahim O., Ferrah N., Didi M. A., Villemin D., *J Radioanal Nucl Chem*, **2011**, *290*, 267.

[34]Chunhua X, Yuan M, Caiping Y., *Iran. J. Chem. Chem. Eng*, **2011**, *30(1)*, 97.

[35]Raji F., Pakizeh M., *Appl Surf Sci*, **2014**, *301*, 568.

[36]Leyva-Ramos R., Rangel-Mendez J. R., Mendoza-Barron J., Fuentes-Rubio L., Guerrero-Coronado R.M., *Water Sci Technol*, **1997**, *35(7)*, 205.

[37]Çay S, Uyanık A, Özaşık A, *Sep Purif Technol*, **2004**, *38*, 273.

[38]Xiong C., Yao C., *Chem Eng J*, **2009**, *155*, 844.

[39]Gode F., Pehlivan E., *J. Hazard. Mater.*, **2003**, *B100*, 231.

Received: 24.06.2015.
Accepted: 29.07.2015.

SYNTHESIS OF 1H-1,2-DITHIOL-1-THIONES AND THIOAMIDES CONTAINING HYDROQUINOLINE GROUP

G. M. Manahelohe[a]*, K. S. Shikhaliev[a] and A. Y. Potapov[a]

Keywords: 1H-1,2-dithiol-1-thione, Willgerodt-Kindler reaction, thioamides, hydroquinolinecarbaldehyde.

This study is concerned with the synthesis and characterization of derivatives of 1H-1,2-dithiol-1-thiones and thioamides having the hydroquinoline moiety. 5-Alkyl-8-(carbonothioyl)-4,5-dihydro-4,4-dimethyl-1H-[1,2]dithiolo[3,4-*c*]quinoline-1-thiones were synthesized by reacting of N-alkyl-2,2,4-trimethyl-1,2-dihydroquinoline-6-carbaldehydes, cyclic secondary amines and excess elemental sulfur (7.33 equivalents) in refluxing DMF. A series of thioamides derivatives containing hydroquinoline fragment were obtained in 56-84% yields by the three-component reaction of N-alkylhydroquinoline-6-carbaldehydes, cyclic secondary amines and 1.33 equivalent of elemental sulfur by refluxing in DMF.

* Corresponding Authors
Mobile No. : +79601299727
E-Mail: gizachewm75@gmail.com
[a] Voronezh State University, Department of Organic Chemistry, Voronezh, Russian Federation. 394006 Voronezh Universitetskaya pl., 1.

Introduction

1H-1,2-dithiole-3-thiones are pseudo-aromatic heterocyclic compounds which are known for several years.[1-2] They have been synthesized from a wide range of starting materials. In most case sulfur or phosphorus pentasulfide is utilized to dehydrogenate and sulfurize an allylic methyl group[3-5] as shown in scheme 1 for propene. The 3,4-double bond and the 4-methyl group in N-alkyl-2,2,4-trimethyl-1,2-dihydroquinoline forms such a system. Thus, 1H-1,2-dithiol-1-thiones can be synthesized in the same way as 3H-1,2-dithiole-3-thiones.[6]

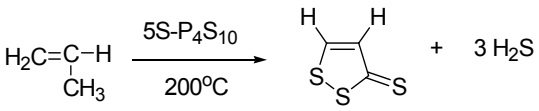

Scheme 1. Synthesis of 1,2-dithiole-3-thione.

Presently, there is an increased interest in the synthesis of 3H-1,2-dithiole-3-thiones due to their wide range of biological activities such as antischistosomal agent,[7] HIV-1 (AIDS) virus replication inhibitor,[8] chemoprotective agent,[9] fungicide[10] and insecticide.[11]

Thioamides are essential building blocks for the synthesis of heterocycles.[12] They have a wide range of biological properties, such as pesticidal,[13] fungicidal,[14] insecticidal,[15] antioxidant,[16] antitubercular,[17] and anthelmintic activity.[18] Furthermore, thioamides have a wide range of applications in the fields of peptide chemistry,[19] polymers[20] and organocatalysis.[21]

Numerous methods[22] are available in the literature for the synthesis of thioamides. Although the Willgerodt-Kindler method of preparation of thioamides using derivatives of benzaldehyde has been reported in the literature,[23] the use of hydroquinolinecarbaldehyde has so far received no attention.

Thus, in this work, we report the synthesis of 1H-1,2-dithiol-1-thiones via the reaction of N-alkyl-2,2,4-trimethyl-1,2-dihydroquinoline-6-carbaldehydes, amines and excess sulfur. We also describe the synthesis of thioamides containing the hydroquinoline moiety by the three-component reaction of N-alkylhydroquinoline-6-carbaldehydes, cyclic secondary amines and sulfur in DMF.

Experimental

General

DMF was purchased from Bekton company. Dry DMF was prepared by drying it overnight over calcium oxide, followed by filteration of the drying agent and vacuum distillation (~20 mmHg). All other commercial reagents were purchased from Bekton, Lancaster, Acros, Aldrich, and Sigma and were used as received. The course of the reactions and purities of the compounds were monitored by thin layer chromatography (TLC) on SILUFOL UV-254 plates, eluent: chloroform, methanol, hexane, ethyl acetate, petroleum ether in different proportions and spots were visualized by exposure to iodine vapors. The ^{1}H-NMR spectra were recorded on a Bruker DRX-500 spectrometer operating at 500.13 MHz, using DMSO-d_6 as solvent ($CDCl_3$ for compound **4d**) and TMS as internal standard. Elemental analyses were determined by using a Carlo Erba NA 1500 elemental analysis instrument. Melting points were recorded using *Stuart SMP30* melting point instrument.

General Procedure for the Synthesis of thioamides (3a-f, 3'a-h)

A mixture of the corresponding aldehyde **1** or **1'** (1 mmol), amine **2a-2g** (1.33 mmol), and elemental sulfur (1.33 mmol) in DMF (2 ml) was refluxed until the reaction is completed (monitored by TLC: hexane/ethyl acetate 7:3). On the

completion of the reaction the warm, dark syrup was poured in to 5 ml of vigorously stirred ice water containing 1 ml of 2N HCl. The resulting gum was solidified by triturating in the acid. The pH was maintained at about 4 by addition of more acid as needed. The solid obtained was filtered, washed with water and recrystallized in an appropriate solvent.[24] ^{1}H-NMR spectra of thiocarboxamides (**3a-f**, **3'a-g**) (δ) are given in ppm (J in Hz).

Piperidin-1-yl(1,2,2,4-tetramethyl-1,2-dihydroquinolin-6-yl)-methanethione (3a)

Yield = 67 %, m.p. 85-87 °C. ^{1}H NMR (DMSO-d_6): δ = 1.29 (s, 6H, $(CH_3)_2$-C2), 1.45-1.60 (bro. s., 6H, $3CH_2$-piperidin.), 1.89 (s, 3H, CH_3-C4), 2.76 (s, 3H, N-CH_3) 3.60-4.30 (bro. s., 4H, $2CH_2$-piperidin), 5.39 (s, 1H, CH-DHQ), 6.44 (d, J=8.54, 1H, ArH's), 6.95 (d, J=2.18, 1H, ArH's), 7.05 (dd, J=8.46, J=2.18, 1H, ArH's). Anal. Calcd. for $C_{19}H_{26}N_2S$: C, 72.56, H, 8.33, N, 8.91, S, 10.20 Found: C, 72.57, H, 8.39, N, 8.97, S, 10.22.

4-(1,2,2,4-Tetramethyl-1,2-dihydroquinoline-6-carbonothio-yl)piperazine-1-carbaldehyde (3b)

Yield = 65 %, m.p. >250 °C. ^{1}H NMR (DMSO-d_6): δ = 1.29 (s, 6H, $(CH_3)_2$-C2), 1.90 (s, 3H, CH_3-C4), 2.78 (s, 3H, N-CH_3), 3.50-4.30 (bro. s., 8H, $4CH_2$-piperazin.), 5.39 (s, 1H, CH), 6.45 (d, J=8.64, 1H, ArH's), 7.06 (s, 1H, ArH's), 7.17 (dd, J=8.54, J=1.97, 1H, ArH's), 8.10 (s, 1H, CHO). Anal. Calcd. for $C_{19}H_{25}N_3OS$: C, 66.44, H, 7.34, N, 12.23, S, 9.34 Found: C, 66.46, H, 7.40, N, 12.29, S, 9.35.

(1-Benzyl-2,2,4-trimethyl-1,2-dihydroquinolin-6-yl)(piperidin-1-yl)methanethione (3c)

Yield = 81 %, m.p. 80-82 °C. ^{1}H NMR (DMSO-d_6): δ = 1.35 (s, 6H, $(CH_3)_2$-C2), 1.45-1.70 (bro. s., 6H, $3CH_2$-piperidin.), 1.95 (s, 3H, CH_3-C4), 3.50-4.25 (bro. s., 4H, $2CH_2$-piperidin), 4.56 (s, 2H, CH_2-Bn), 5.48 (s, 1H, CH), 6.13 (d, J=8.61, 1H, ArH's), 6.85 (dd, J=8.53, J=2.17, 1H, arom.), 6.97 (d, J=2.19, 1H, ArH's), 7.15-7.35 (m, 5H, arom.).). Anal. Calcd. for $C_{25}H_{30}N_2S$: C, 76.88, H, 7.74, N, 7.17, S, 8.21 Found: C, 76.90, H, 7.75, N, 7.21, S, 8.24.

Pyrrolidin-1-yl(1,2,2,4-tetramethyl-1,2-dihydroquinolin-6-yl)methanethione (3d)

Yield = 58 %, m.p. 113-115°C. ^{1}H NMR (DMSO-d_6): δ = 1.28 (s, 6H, $(CH_3)_2$-C2), 1.87 (p, J=6.73, 2H, CH_2-pyrrolidin), 1.89 (s, 3H, CH_3-C4), 1.97 (p, J=6.94, 2H, CH_2-pyrrolidin), 2.77 (s, 3H, N-CH_3), 3.60 (t, J=6.62, 2H, CH_2-pyrrolidin), 3.77 (t, J=7.02, 2H, CH_2-pyrrolidin), 5.39 (s, 1H, CH), 6.43 (d, J=8.59, 1H, ArH's), 7.12 (d, J=2.20, 1H, arom.), 7.20 (dd, J=8.52, J=2.22, 1H, arom.). Anal. Calcd. for $C_{18}H_{24}N_2S$: C, 71.95, H, 8.05, N, 9.32, S, 10.67 Found: C, 71.97, H, 8.11, N, 9.38, S, 10.69.

(4-Methylpiperazin-1-yl)(1,2,2,4-tetramethyl-1,2-dihydroquinolin-6-yl)methanethione hydrochloride (3e)

Yield = 60 %, m.p. 160-162 °C. ^{1}H NMR (DMSO-d_6): δ = 1.30 (s, 6H, $(CH_3)_2$-C2), 1.92 (s, 3H, CH_3-C4), 2.75 (d, J=4.55, 3H, N-CH_3-piperazin), 2.78 (s, 3H, N-CH_3-DHQ), 4.10-4.85 (m, 8H, $4CH_2$-piperazin), 5.41 (s, 1H, CH), 6.51 (d, J=8.56, 1H, ArH's), 7.07 (d, J=2.05, 1H, ArH's), 7.20 (dd, J=8.48, J=2.16, 1H, ArH's), 11.40 (s, 1H, HCl). Anal. Calcd. for $C_{19}H_{28}ClN_3S$: C, 62.36, H, 7.71, N, 11.48, S, 8.76, Cl, 9.69 Found: C, 62.40, H, 7.75, N, 11.50, S, 8.81, Cl, 9.70.

(4-Phenylpiperazin-1-yl)(1,2,2,4-tetramethyl-1,2-dihydroquinolin-6-yl)methanethione (3f)

Yield = 72 %, m.p. 101-103°C. ^{1}H NMR (DMSO-d_6): δ = 1.29 (s, 6H, $(CH_3)_2$-C2), 1.91 (s, 3H, CH_3-C4), 2.78 (s, 3H, N-CH_3), 3.70-4.50 (bro. s., 8H, $4CH_2$-piperazin), 5.41 (s, 1H, CH), 6.46 (d, J=8.59, 1H, ArH's), 6.75-7.30 (m, 7H, ArH's). Anal. Calcd. for $C_{24}H_{29}N_3S$: C, 73.63, H, 7.46, N, 10.73, S, 8.19 Found: C, 73.66, H, 7.51, N, 10.79, S, 8.23.

(1-Benzyl-2,2,4-trimethyl-1,2,3,4-tetrahydroquinolin-6-yl)(piperidin-1-yl)methanethione (3'a)

Yield = 76 %, m.p. 115-117°C. ^{1}H NMR (DMSO-d_6): δ = 1.24 (s, 3H, $(CH_3)_{2A}$-C4), 1.25 (s, 3H, $(CH_3)_{2B}$-C4), 1.32 (d, J=6.59, 3H, CH_3-C4), 1.40-1.75 (m., 7H, CH_{2A}+$3CH_2$-piperidin), 1.90 (dd, J=13.03, J=4.67, 1H, CH_{2B}), 1.96 (m., 1H, CH), 3.50-4.15 (m, 4H, $2CH_2$-piperidin), 4.26 (d, J=18.06, 1H, CH_{2A}-Bn), 4.77 (d, J=18.09, 1H, CH_{2B}-Bn), 6.12 (d, J=8.65, 1H, ArH's), 6.85 (dd, J=8.60, J=2.13, 1H, ArH's), 7.10-7.35 (m, 6H, ArH's). Anal. Calcd. for $C_{25}H_{32}N_2S$: C, 76.48, H, 8.22, N, 7.14, S, 8.17 Found: C, 76.50, H, 8.25, N, 7.20, S, 8.21.

4-(1-Benzyl-2,2,4-trimethyl-1,2,3,4-tetrahydro-quinoline-6-carbonothioyl)piperazine-1-carbaldehyde (3'b)

Yield = 56 %, m.p. 160-162°C. ^{1}H NMR (DMSO-d_6): δ = 1.24 (s, 3H, $(CH_3)_{2A}$-C2), 1.26 (s, 3H, $(CH_3)_{2B}$-C2), 1.32 (d, J=6.36, 3H, CH_3-C4), 1.64 (t, J=12.77, 1H, CH_{2A}), 1.91 (dd, J=12.92, J=4.50, 1H, CH_{2B}), 2.96 (m, 1H, CH), 3.60-4.20 (m., 8H, $4CH_2$-piperazin), 4.27 (d, J=17.75, 1H, CH_{2A}-Bn), 4.78 (d, J=18.25, 1H, CH_{2B}-Bn), 6.14 (d, J=8.69, 1H, ArH's), 6.90-7.40 (m, 7H, ArH's), 8.07 (s, 1H, CHO). Anal. Calcd. for $C_{25}H_{31}N_3OS$: C, 71.22, H, 7.41, N, 9.97, S, 7.61 Found: C, 71.23, H, 7.43, N, 10.03, S, 7.65.

4-(1,2,2,4-Tetramethyl-1,2,3,4-tetrahydroquinoline-6-carbonothioyl)piperazine-1-carbaldehyde (3'c)

Yield = 58 %, m.p. 199-201°C. ^{1}H NMR (DMSO-d_6): δ = 1.17 (s, 3H, $(CH_3)_{2A}$-C2), 1.27 (s, 3H, $(CH_3)_{2B}$-C2), 1.28 (d, J=7.36, 3H, CH_3-C_4), 1.40 (t, J=12.81, 1H, CH_{2A}), 1.83 (dd,

J=12.98, J=4.24, 1H, CH_{2B}), 2.77 (m, 1H, CH), 2.79 (s, 3H, N-CH_3), 3.60-4.40 (bro. m, 8H, 4CH_2-piperazine), 6.49 (d, J=9.17, 1H, ArH's), 7.17 (d, J=6.60, 1H, ArH's), 7.18 9 (s, 1H, ArH's), 8.10 (s, 1H, CHO). Anal. Calcd. for $C_{19}H_{27}N_3OS$: C, 66.05, H, 7.88, N, 12.16, S, 9.28 Found: : C, 66.07, H, 7.90, N, 12.22, S, 9.30.

Piperidin-1-yl(1,2,2,4-tetramethyl-1,2,3,4-tetrahydro-quinolin-6-yl)methanethione (3'd)

Yield = 79 %, m.p. 115-117°C. ^{1}H NMR (DMSO-d_6): δ =1.17 (3H, s, $(CH_3)_{2A}$-C2), 1.26 (3H, s, $(CH_3)_{2B}$-C2), 1.27 (3H, d, J=6.59, CH_3-C4), 1.40 (1H, t, J=12.85, CH_{2A}), 1.44-1.65 (6H, bro. m., 3CH_2-piperidin.), 1.83 (1H, dd, J=13.04, J=4.44, CH_{2B}), 2.76 (1H, m, CH), 2.78 (3H, s, N-CH_3), 3.50-4.30 (4H, bro. m., 2CH_2-piperidin), 6.47 (1H, d, J=9.18, ArH's), 7.03 (1H, dd, J=6.79, J=2.16, ArH's), 7.04 (1H, s, ArH's). Anal. Calcd. for $C_{19}H_{28}N_2S$: C, 72.10, H, 8.92, N, 8.85, S, 10.13 Found: C, 72.13, H, 8.95, N, 8.91, S, 10.15.

Ethyl 1-(1,2,2,4-tetramethyl-1,2,3,4-tetrahydro-quinoline-6-carbonothioyl)piperidine-4-carboxylate (3'e)

Yield = 74 %, m.p. 110-112°C. ^{1}H NMR (DMSO-d_6): δ = 1.10-2.10 (m, 19H, 4CH_3+CH_2-THQ+2CH_2-piperidin.), 2.72-2.80 (m, 8H, N-CH_3+2CH_2-piperidin.+CH-THQ), 4.08 (q, J=7.08, 2H, -O$\underline{CH_2}CH_3$), 6.47 (d, J=8.56, 1H, arom.), 7.05 (dd, J=8.14, J=2.00, 1H, ArH's), 7.07 (s, 1H, ArH's). Anal. Calcd. for $C_{22}H_{32}N_2O_2S$: C, 68.00, H, 8.30, N, 7.21, S, 8.25 Found: C, 68.01, H, 8.34, N, 7.25, S, 8.29.

(1-Benzyl-2,2,4-trimethyl-1,2,3,4-tetrahydroquinolin-6-yl)(morpholino)-methanethione (3'f)

Yield = 84 %, m.p. 140-142°C. ^{1}H NMR (DMSO-d_6): δ = 1.24 (s, 3H, $(CH_3)_{2A}$-C2), 1.26 (s, 3H, $(CH_3)_{2B}$-C2), 1.32 (d, J=6.59, 3H, CH_3-C4), 1.64 (t, J=12.98, 1H, CH_{2A}), 1.90 (dd, J=13.03, J=4.72, 1H, CH_{2B}), 2.96 (m, 1H, CH), 3.50-4.20 (bro. m, 8H, 4CH_2-morph.), 4.26 (d, J=18, 1H, CH_{2A}-Bn), 4.78 (d, J=18.07, 1H, CH_{2B}-Bn), 6.13 (d, J=8.65, 1H, ArH's), 6.90 (dd, J=8.63, J=2.13, 1H, ArH's), 7.15-7.35 (m, 6H, ArH's).). Anal. Calcd. for $C_{24}H_{30}N_2OS$: C, 73.06, H, 7.66, N, 7.10, S, 8.13 Found: : C, 73.09, H, 7.70, N, 7.14, S, 8.14.

(4-Methylpiperazin-1-yl)(1,2,2,4-tetramethyl-1,2,3,4-tetrahydroquinolin-6-yl)methanethione hydrochloride (3'g)

Yield = 66 %, m.p. 180-182 °C. ^{1}H NMR (DMSO-d_6): δ = 1.19 (3H, s, $(CH_3)_{2A}$-C2), 1.28 (3H, s, $(CH_3)_{2B}$-C2), 1.30 (3H, d, J=7.31, CH_3-C4), 1.42 (1H, t, J=12.45, CH_{2A}), 1.85 (1H, dd, J=13.08, J=4.52, CH_{2B}), 2.75 (3H, d, J=4.55, N-CH_3-piperazin.), 2.81 (3H, s, N-CH_3-THQ), 3.08 (1H, m, CH), 4.10-4.70 (8H, bro. m., 4CH_2-piperazin), 6.50-7.35 (3H, m, ArH's), 11.25 (1H, s, HCl). Anal. Calcd. for $C_{19}H_{30}ClN_3S$: C, 62.02, H, 8.22, N, 11.42, S, 8.71, Cl, 9.63 Found: C, 62.06, H, 8.26, N, 11.46, S, 8.75, Cl, 9.67.

(1-Benzyl-2,2,4-trimethyl-1,2,3,4-tetrahydroquinolin-6-yl)(4-methylpiperazin-1-yl)methanethione hydrochloride (3'h)

Yield = 70 %, m.p. 170-172 °C. ^{1}H NMR (DMSO-d_6): δ = 1.26 (3H, s, $(CH_3)_{2A}$-C2), 1.27 (3H, s, $(CH_3)_{2B}$-C2), 1.34 (3H, d, J=6.59, CH_3-C4), 1.65 (1H, t, J=12.68, CH_{2A}), 1.92 (1H, dd, J=13.00, J=4.63, CH_{2B}), 2.73 (3H, d, J=4.56, N-CH_3), 2.99 (1H, m, CH), 4.26 (1H, d, J=18.19, CH_{2A}-Bn), 4.50-4.76 (8H, m, 4xCH_2-piperazin.), 4.80 (1H, d, J=18.23, CH_{2B}-Bn), 6.13-7.40 (8H, m, ArH's), 11.20 (1H, s, HCl). Anal. Calcd. for $C_{25}H_{34}ClN_3S$: C, 67.62, H, 7.22, N, 9.46, S, 7.22, Cl, 7.98 Found: C, 67.68, H, 7.77, N, 9.51, S, 7.27, Cl, 8.01.

General procedure for the synthesis of 5-alkyl-8-(carbonothioyl)-4,5-dihydro-4,4-dimethyl-1H-[1,2]dithiolo[3,4-*c*]quinoline-1-thiones (4a-d)

A mixture of N-alkyl-2,2,4-trimethyl-1,2-dihydroquinoline-6-carbaldehyde **1** (1 mmol), the corresponding amine (1.33 mmol), and elemental sulfur (7.33 mmol) in DMF (2 ml) was refluxed until the reaction is completed (monitoring using TLC: hexane/ethyl acetate 7:3). Up on the completion of the reaction the reaction mixture was allowed to cool overnight and 5 ml of isopropyl alcohol was added to ensure complete precipitation of the product. The solid obtained was filtered, washed with cold isopropyl alcohol followed by cold water.

4,4,5-Trimethyl-8-(morpholine-4-carbonothioyl)-4,5-dihydro-1H-[1,2]dithiolo[3,4-c]quinoline-1-thione (4a)

Light orange solid, Yield = 68 %, m.p. 105-107 °C. ^{1}H NMR (DMSO-d_6): δ =1.55 (s, 6H, C4-C$(CH_3)_2$), 2.90 (s, 3H, N-CH_3), 3.60-3.90 (6H, bro. s, 6H, morph.), 4.20-4.40 (2H, bro. s, 2H, morph.), 6.94 (d, J = 8.65, 1H, H-6), 7.39 (dd, J = 6.34 and J = 2.26, H-7), 9.24 (d, J=8.65, 1H, H-8). Anal. Calcd. for $C_{18}H_{28}N_2OS_4$: C, 52.91, H, 4.93, N, 6.86, S, 31.39 Found: C, 52.93, H, 4.90, N, 6.89, S, 31.41.

5-Benzyl-4,4-dimethyl-8-(piperidine-1-carbonothioyl)-4,5-dihydro-1H-[1,2]dithiolo[3,4-c]quinoline-1-thione (4b)

Yellow solid, Yield = 86 %, m.p. 97-99 °C. ^{1}H NMR (DMSO-d_6): δ =1.50 (bro. s, 6H, piper.), 1.67 (s, 6H, C4-C(CH3)2), 3.60 (bro. s, 2H, piper.), 4.25 (bro. s, 2H, piper.), 4.70 (s, 2H, Bn), 6.75 (d, J=8.71, 1H, H-6), 7.17 (dd, J = 8.64 and J = 2.19, 1H, H-7), 7.20-7.33 (m, 5H, Ph), 9.27 (d, J = 2.19, 1H, H-8). Anal. Calcd. for $C_{25}H_{26}N_2S_4$: C, 62.20, H, 5.43, N, 5.80, S, 26.57 Found: C, 62.23, H, 5.40, N, 5.84, S, 26.60.

5-Benzyl-4,4-dimethyl-8-(morpholine-4-carbonothioyl) -4,5-dihydro-1H-[1,2]dithiolo[3,4-c]quinoline-1-thione (4c)

Orange solid, Yield = 69 %, m.p. 110-112 °C. ^{1}H NMR (DMSO-d_6): δ =1.70 (s, 6H, C4-C$(CH_3)_2$), 3.55-3.85 (bro. s, 6H, morph.), 4.20-4.40 (bro. s, 2H, morph.), 4.71 (s, 2H, Bn), 6.76 (d, J = 8.73, 1H, H-6), 7.23 (dd, J = 8.72 and

J=2.09, 1H, H-7), 7.30-7.40 (m, 5H, Ph), 9.31 (d, J = 2.23, 1H, H-8). Anal. Calcd. for $C_{24}H_{24}N_2OS_4$: C, 59.47, H, 4.99, N, 5.78, S, 26.46 Found: C, 59.50, H, 5.02, N, 5.81, S, 26.49.

4,4,5-Trimethyl-8-(4-phenylpiperazine-1-carbono-thioyl)-4,5-dihydro-1H-[1,2]dithiolo[3,4-c]quinoline-1-thione (4d)

Light orange solid. Yield = 80 %, m.p. 90-92 °C. . ^{1}H NMR ($CDCl_3$): δ =1.25 (s, 6H, C4-C(CH_3)$_2$), 2.97 (s, 3H, N-CH3), 3.50-4.50 (m, 8H, piperazine), 6.95(d, J=8.59, 1H, H-6), 7.50-7.70 (m, 5H, Ph), 8.00 (dd, J = 8.50 and J = 2.19, 1H, H-7), 9.50 (d, J = 2.09, 1H, H-8). Anal. Calcd. for $C_{24}H_{25}N_2S_4$: C, 59.59, H, 5.21, N, 8.69, S, 26.51. Found: C, 59.63, H, 5.23, N, 8.67, S, 26.55.

RESULTS AND DISCUSSIONS

The purpose of this study is to investigate the regioselectivity in the three-component reaction of hydroquinoline-6-carbaldehydes, cyclic secondary amines and sulfur by taking 1.33 equivalent and excess of elemental sulfur.

The multi-step synthesis of the starting materials 1-alkylhydroquinoline-6-carbaldehydes **1a**, **1b**, **1'a** and **1'b** were carried out by the know methods[25-26] as represented in Scheme 2.

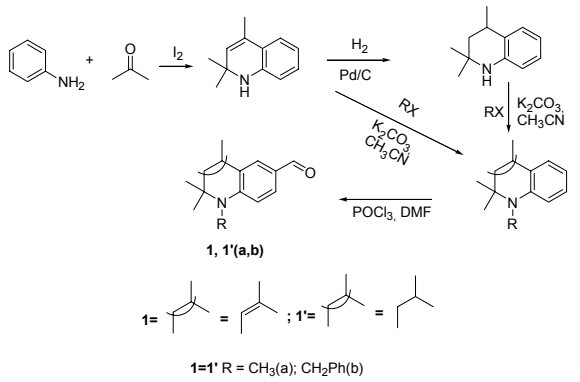

Scheme 2. Synthesis of starting materials 1-alkylhydroquinoline-6-carbaldehydes **1** and **1'**.

Brown[6] has reported the synthesis of 4,5-dihydro-4,4-dimethyl-1H-1,2-dithiolo-[3,4-c]quinoline-1-thiones from 2,2,4-trimethyl-1,2-dihydroquinoline (and its 1-methyl and 6-ethoxy-derivatives) and 4.0 equivalents of sulfur in refluxing DMF. We have extended this reaction to N-alkyl-2,2,4-trimethyl-1,2-dihydroquinoline-6-carbaldehydes (**1a, b**) and N-alkyl-2,2,4-trimethyl-1,2,3,4-tetrahydroquinoline-6-carbaldehydes (**1'a, b**). In the case of **1a** and **1b** there is a competition between the Willgerodt-Kindler reaction of formyl group in the presence of amine and formation of 1H-1,2-dithiol-1-thione cycle from the 3, 4-double bond and the 4-methyl-group.

When 1.33 equivalents of elemental sulfur is used the Willgerodt-Kindler reaction takes place exclusively for both di- and tetrahydroquinolinecarbaldehydes (**1a**, **1b**, **1'a** and **1b**) resulting in thioamides **3a-f** and **3'a-h** as shown in Scheme 3. As one would expect this regioselectivity is due to the more reactivity of formyl group as compared to the double bond 4-CH_3-C4 = C3.

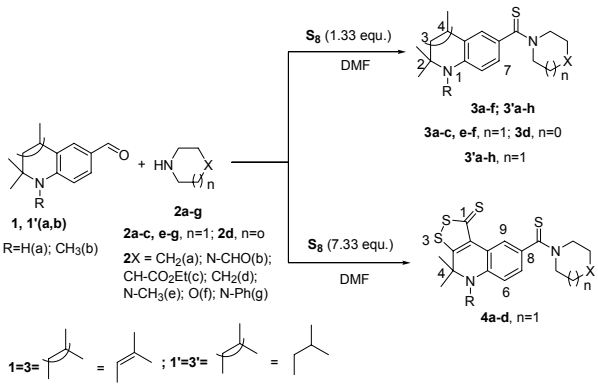

(**3a**) R=CH_3, X=CH_2; (**3b**) R=CH_3, X=N-CHO; (**3c**) R=CH_2Ph, X=CH_2; (**3d**) R=CH_3, X=CH_2; (**3e**) R=CH_3, X=NCH_3; (**3f**) R=CH_3, X=NPh; (**3'a**) R=CH_2Ph, X=CH_2, (**3'b**) R=CH_2Ph, X=N-CHO; (**3'c**) R=CH_3, X=N-CHO; (**3'd**) R=CH_3, X=CH_2; (**3'e**) R=CH_3, X=CH-COOEt; (**3'f**) R=CH_2Ph, X=O; (**3'g**) R=CH_3, X=NCH_3; (**3'h**) R=CH_2Ph, X=NCH_3; (**4a**) R=CH_3, X=O); (**4b**) R=CH_2Ph, X=CH_2; (**4c**) R=CH_2Ph, X=O; (**4d**) R=CH_3, X=NPh.

Scheme 3. Synthesis of thioamides **3a-f**, **3'a-g** and 1H-1,2-dithiol-1-thiones **4a-d**.

The ^{1}H-NMR spectra of compound **3a-f** indicated that there are singlet 4-methyl protons signals in the range of δ 1.89-1.95 ppm and singlet 3-CH-methine protons signals in the range δ 5.39-5.48 ppm. As compared to the starting materials **1a,b**, there is no formyl proton signal instead there are broad singlet signals in the range δ 1.45-1.70 ppm and δ 3.50-4.30 ppm for compounds **3a** and **3c** which are assignable for ten piperidine methylene protons.

For compounds **3b, 3e** and **3f** the eight piperazine methylene protons appeared as broad signals in the range δ 3.50-4.85 ppm. The pyrolidine methylene protons of compound **4d** are clearly seen as a pair of pentat signals at δ 1.87 ppm, J=6.73 Hz and δ 1.97 ppm, J=6.94 Hz, and two triplet signals at δ 3.60 ppm, J=6.62 Hz and δ 3.77 ppm, J= 7.02 Hz.

The 4-methyl doublet protons, 4-CH methine multiplet proton and the two diastreotropic 3-CH_{2A} (triplet) and 3-CH_{2B} (doublets of doublet) methylene protons signals of compound **3'a-h** appeared in the range δ 1.27-1.34, 1.96-3.08, 1.40-1.65 and 1.80-1.92 ppm, respectively.

In the ^{1}H NMR spectra of compounds **3e, 3'g, 3h**, isolated in hydrochloride form, the proton signals are broadened in the range of 11.20 -11.40 ppm.

Compounds **3a-f, 3'a-h** is obtained in 56-84% yields. Their colors vary from light yellow to red. They are soluble in most polar solvents (chloroform, DMF, DMSO, ethanol).

In the ^{1}H-NMR spectra of compounds **4a-d** there are no 3-CH-methine, 4-methyl- and formyl protons signals as compared to the starting materials **1a,b**. This is due the

formation of the pseudoaromatic heterocyclic ring via the 3,4-double bond and 4-methyl of N-alkyl-2,2,4-trimethyl-1,2-dihydroquinoline-6-carbaldehydes and sulfur in addition to the formation of thioamides.

An attempt that was made to synthesis 5-R-8-(carbonothioyl)-4,5-dihydro-4,4-dimethyl-1H-[1,2]dithiolo [3,4-c]quinolin-1-thione from the reaction of N-alkyl-2,2,4-trimethyl-1,2,3,4-tetrahydroquinolines **1'a,b**, secondary cyclic amine and excess sulfur was not successful. This might be due the reason that the amine catalyst is unable to facilitate the dehydrogenation reaction of C3-C4 bond to form the allylic methyl form to undergo sulfurization.

A plausible reaction mechanism for the Willgerodt-Kindler reaction of hydroquinolinecarbaldehydes with amines and elemental sulphur is shown in Scheme 4 and we propose that the reaction mechanism is analogous with the work reported in reference[27] for phenyl glyoxals. The condensation of hydroquinolinecarbaldehydes **1, 1'** with amine **2a-g** gave the iminium salt **5, 5'**. Subsequent nucleophilic addition of amine to sulphur, followed by elimination of S7, ammonium sulfide leads to **6**. Intermediate **7, 7'** is then produced by nucleophilic addition of **6** to iminium salt **5, 5'** which is finally converted into the desired thioamides **3, 3'** by the elimination of a molecule of amine.

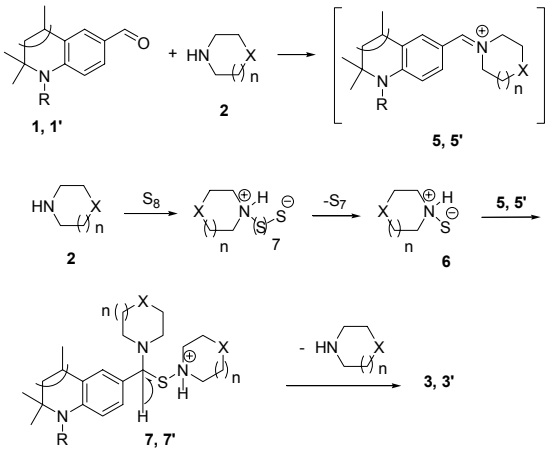

Scheme 4. Plausible Reaction mechanism for the synthesis of **3, 3'**.

Conclusions

When 1.33 equivalent of elemental sulfur is used exclusively the Willgerodt-Kindler reaction takes place both for the N-alkyl-2,2,4-trimethyl-1,2-dihydro-quinoline-6-carbaldehydes and N-alkyl-2,2,4-trimethyl-1,2,3,4-tetrahydroquinoline-6-carbaldehydes which results in the formation of thioamides. The use of excess sulfur leads to the formation of both 5-R-8-(carbonothioyl)-4,5-dihydro-4,4-dimethyl-1H-[1,2]dithiolo [3,4-*c*]quinolin-1-thione cycle and thioamide for N-alkyl-2,2,4-trimethyl-1,2-dihydroquinoline-6-carbaldehydes. In the case of N-alkyl-2,2,4-trimethyl-1,2,3,4-tetrahydro-quinoline-6-carbaldehydes the use of excess sulfur gave only the Willgerodt-Kindler thioamide product and there is no formation of 1H-1,2-dithiol-1-thione.

Acknowledgments

This work was supported by the Ministry of Education and Science of Russian Federation within the frame work of contract No. 218.N 02.G25.31.000.

References

[1]Landis, P. S. *Chem. Rev*. **1965**, 65, 237.
[2]Pedersen, C. *Th. Adv. Heterocyclic Chem.* **1982**, 31, 63 and *Sulfur Rep.* **1995**, 16, 173.
[3]Bottcher, B., and Bauer, F., *Ann*., **1950**, 227, 568, *Ber*., **1951**, 84, 458, *Ann*., 1951, 218, 574.
[4]Mollier, Y., and Lozach, N., *Bull. Soc. Chim. France*, **1958**, 651, **1960**, 700.
[5]Spindt, R. S., Stevens, D. R., and Baldwin, W. E., *J. Am. Chem. Soc*., **1951**, 73,3693.
[6]Brown, J. P., *J. Chem. Soc. (C)*, **1968**, 1074.
[7]Barreau, M., Cotrel, C., Jeanmart, C., *Chem. Abst*. **1977**, 86, 121373.
[8]Prochaska, H. J., Rubinson, L., Yeh, Y., Baron, P., Polsky, B. *Molecular Pharmacology*, **1991**, 45, 916.
[9]Kensler, T. W., Groopman, J. D., Eaton, D. L., Curphey, T. J., Roebuck, B. D. *Carcinogenesis* **1992**, 13, 95.
[10](a) Hagen, H., Fleig, H. Ger. Offen. Patent 2, 460,783, *Chem. Abst.* **1976**, 85, 123899. (b) Bader, J., Gaetzi, K. Ger. Offen. Patent 1, 278,701, *Chem. Abst*. **1969**, 70, 115147.
[11]Misra, P., Misra, S., Mohapatra, R., Mittra, A. J. *Indian Chem. Soc.* **1979**, 61, 404.
[12](a) Suzuki, Y., Yazaki, R., Kumagai, N., Shibasaki, M. *Chem. Eur. J.* **2011**, 17, 11998. (b) Suzuki, Y., Yazaki, R., Kumagai, N., Shibasaki, M. *Angew. Chem. Int. Ed.* **2009**, 48, 5026. (c) Sureshkumar, D., Kawato, Y., Iwata, M., Kumagai, N., Shibasaki, M. *Org. Lett.* **2012**, 14, 3108. (d) Koduri, N. D., Scott, H., Hileman, B., Cox, J. D., Coffin, M., Glicksberg, L., Hussaini, S. R. *Org. Lett.* **2012**, 14, 440. (e) Ogawa, T., Mouri, S., Yazaki, R., Kumagai, N., Shibasaki, M. *Org. Lett.* **2012**, 14, 110. (f) Yazaki, R., Kumagai, N., Shibasaki, M. *Org. Lett.* **2011**, 13, 952. (g) Murai, T., Ui, K., Narengerile *J. Org. Chem.* **2009**, 74, 5703. (h) Arshad, N., Hashim, J., Kappe, C. O. *J. Org. Chem.* **2009**, 74, 5118.
[13](a) Hanzlie, R. P., Vyas, K. P., Traiger, G. J. *Toxicol. Appl. Pharmacol.* **1980**, 46, 685. (b) Walter, H., Zambach, W. *Chem. Abstr.* **1996**, 125, 55871.
[14](a) Wingert, H., Sauter, H., Bayer, H., Oberdorf, K., Lorenz, G., Ammermann, E. EP 35, **1994**, *Chem. Abstr.* **1994**, 121, 533719. (b) Wei, Q.-L., Zhang, S.-S., Gao, J., Li, W.-H., Xu, L.-Z., Yu, Z.-G. *Bioorg. Med. Chem.* **2006**, 14, 7146.
[15](a) Thioamide pesticides Searle, R. J. G., Boyce, C. B. C., Bay, H. US 4,096,275, **1978**. (b) Insecticides, nematocides Fauss, R., Findeisen, K., Becker, B., Hamman, I., Homeyer, B. US 4,581,375, **1986**.
[16](a) Bandgar, B. P., Gawande, S. S., Warangkar, S. C., Totre, J. V. *Bioorg. Med. Chem.* **2010**, 18, 3618. (b) Harrowven, D. C., Lucas, M. C., Howes, P. D. *Tetrahedron Lett.* **1999**, 40, 4443.
[17]Reynard, P., Moreau, R. C., Samama, J. P. *Bull. Soc. Chim. Fr.* **1965**, 12, 3623.
[18]Jeschke, P., Harder, A., Etzel, W., Gau, W., Thielking, G., Bonse, G., Iinuma, K. *Pest Manage. Sci.* **2001**, 57, 1000, *Chem. Abstr.* **2001**, 136, 839295.
[19](a) Batjargal, S., Wang, Y. J., Goldberg, J. M., Wissner, R. F., Petersson, E. J. *J. Am. Chem. Soc.* **2012**, 134, 9172. (b) Xie, J., Okano, A., Pierce, J. G., James, R. C., Stamm, S., Crane, C. M., Boger, D. L. *J. Am. Chem. Soc.* **2012**, 134, 1284. (c) Sharma, I., Crich, D. *J. Org. Chem.* **2011**, 76, 6518. (d) Wang, L., Xu, Z., Ye, T. *Org. Lett.* **2011**, 13, 2506.
[20](a) Mason, C. R., Maynard-Atem, L., Al-Harbi, N. M., Budd, P. M., Bernardo, P., Bazzarelli, F., Clarizia, G., Jansen, J. C. *Macromolecules* **2011**, 44, 6471. (b) Deletre, M., Levesque, G. *Macromolecules* **1990**, 23, 4876. (c) Kanbara, T., Kawai, Y., Hasegawa, K., Morita, H., Yamamoto, T. *J. Polym. Sci., Part A: Polym. Chem.* **2001**, 39, 3739.
[21](a) Cao, J.-L., Qu, J. *J. Org. Chem.* **2010**, *75*, 3663. (b) Geng, X.-L., Wang, J., Li, G.-X., Chen, P., Tian, S.-F., Qu, J. *J. Org. Chem.* **2008**, *73*, 8558. (c) Chen, P., Qu, J. *J. Org. Chem.* **2011**, *76*, 2994. (d) Hernández, J. G., García- López, V., Juaristi, E. *Tetrahedron* **2012**, *68*, 92. (e) Ganesh, M., Seidel, D. *J. Am. Chem. Soc.* **2008**, 130, 16464.

[22](a) Raucher, S., Klein, P. *J. Org. Chem.* **1981**, *46*, 3558. (b) Curphey, T. J. *J. Org. Chem.* **2002**, *67*, 6461. (c) Cho, D., Ahn, J., De Castro, K. A., Ahn, H., Rhee, H. *Tetrahedron* **2010**, *66*, 5583. (d) Bergman, J., Pettersson, B., Hasimbegovic, V., Svensson, P. H. *J. Org. Chem.* **2011**, *76*,1546. (e) Smith, D. C., Lee, S. W., Fuchs, P. L. *J. Org. Chem.* **1994**, *59*, 348. (f) Pathak, U., Pandey, L. K., Tank, R. *J. Org. Chem.* **2008**, *73*, 2890. (g) Shibahara, F., Sugiura, R., Murai, T. *Org. Lett.* 2009, *11*, 3064. (h) Kaboudin, B., Malekzadeh, L. *Synlett* 2011, 2807. (i) Coats, S. J., Link, J. S., Hlasta, D. J. *Org. Lett.* **2003**, *5*, 721. (j) Kaleta, Z., Makowski, B. T., Soós, T., Dembinski, R. *Org. Lett.* **2006**, *8*, 1625.
[23]Brown, E. V. *Synthesis* **1975**, 358, and references cited therein.
[24]Webel, L. M., McNamara, D. J., Colbry, N. L., Johnson, J. L., Degnan, M. J., Whitney, B., *J. Heterocycl. Chem.*, **1979**, 16(5), 881.
[25]Krysin, M. Yu., Shikhaliev, Kh. S., Anokhina, I. K., Shmyreva, Zh. V.,*Chem. Heterocycl. Compd*., **2001**, 37, 227.
[26]Kaijun, T. H., Dehui, H. R., Shuangqing, W., Shayu, L. Y. L., Guoqiang, Y.,*Chem. Commun.*, 2011, 47, 10052.
[27]Bagher, E., Saleh, V. K., Orhan, B., *Synlett* **2013**, 24, 977.

Received: 09.06.2015.
Accepted: 30.07.2015.

SYNTHESIS AND SPECTRAL STUDIES OF OXOVANADIUM(IV) SCHIFF BASE COMPLEXES DERIVED FROM 1,1'-OXALYLDIIMIDAZOLE AND AROMATIC AMINES

Ashok Kumar Yadava[a], Hardeo Singh Yadav[a], Rajul Saxena[b] and Devendra Pratap Rao[b]*

Keywords: Schiff base, 1,1'-oxalyldiimidazole, oxovanadium(IV), chelating legends.

New Schiff base (L), derived from condensation of 1,1'-oxalyldiimidazole with o-phenylenediamine has been prepared. Five new oxovanadium(IV) complexes (one is $[VO(L)]SO_4$ and four $[VO(mac)]SO_4$) have been carried out by using *in situ* method of preparation where vanadyl ion act as kinetic template for the Schiff bases. The synthesized complexes were characterized by elemental analyses, conductometric measurements, magnetic moments, IR, ESR and electronic spectroscopy. These complexes contain VO^{2+} group and have square pyramidal geometry wherein Schiff bases act as tetradentate chelating ligands.

*Corresponding Author
E-mail: devendraprataprao@yahoo.com
[a] Department of Chemistry, North Eastern Regional Institute of Science and Technology (NERIST), Nirjuli-791109, Arunachal Pradesh, India
[b] Coordination Chemistry Laboratory, Department of Chemistry, D.A-V. P.G. College, Kanpur-208001, Uttar Pradesh, India

Introduction

In fact, Schiff base ligands are able to stabilize many different metals in various oxidation states. They controlling the performance of metals in a large variety of applications in clinical, analytical and biological in addition to catalysis.[1,2] A large number of Schiff base complexes have biological interest.[3,4] It is known that the existence of metal ions bonded to biologically active compounds may enhance their activities.[5,6] In metal coordination chemistry, Schiff bases occupy an important position as ligand due to the incorporation of transition metals into Schiff bases. This result in an increment in biological activity of the ligand and decrease in the cytotoxic effects of both ligand and metal ion on the host.[7] The progress in the field of bioinorganic chemistry has increased the interest in Schiff base complexes. The coordination behavior of vanadium complexes is of great interest due to its presence in biological system as trace element. It has been observed that oxovanadium(IV) complexes are more stable than five or six coordinated vanadium.[8] The o-phenylenediamine can form chelate ring using in-situ method of synthesis in presence of metal cation due to kinetic template effect.[9-11]

With these assumptions a new series of oxovnadium(IV) complexes were synthesized using in situ method of synthesis by condensation of β-diketones viz. acetylacetone, benzoylacetone, thenoyltrifluoroacetone and dibenzoylmethane with o-phenylenediamine in molar ratio 1:2 in the presence of VO^{2+} cation as kinetic template using 1,1'- oxalyldiimidazole. These complexes were isolated in solid state and their tentative structures have been assigned on the basis of elemental analyses, molar conductance, magnetic susceptibility measurements and spectral (IR, ESR and electronic) data.

Experimental

Materials

Oxovanadium(IV) sulfate, oxalyldiimidazole and o-phenylenediamine were procured from Aldrich. The β-diketones viz. acetylacetone, benzoylacetone, thenoyltrifluoroacetone and dibenzoylmethane were purchased from Sisco Research Laboratories Pvt. Ltd., Mumbai, India.

Analytical and physical measurements

Vanadium was estimated gravimetrically as its vanadate, after decomposing the oxovanadium complex with concentrated nitric acid.[12] Sulfur was estimated as barium sulfate.[13] The melting point (uncorrected) determination was done by using sulfuric acid bath. Toshniwal conductivity bridge, model no. CLO102A was used for measurement of conductance at room temperature. The magnetic susceptibilities of the complexes in powder form were carried out at room temperature using Gouy's balance. Mercury tetrathiocyanatocobaltate(II), $Hg[Co(CNS)_4]$, (χ_g = 16.44 x 10^{-6} c.g.s. unit at 20 ^{0}C), was used as calibrant in conductance measurement. The electronic spectra of these complexes were recorded on Beckmann DU-2 spectrophotometer in the range 2000-185 nm. The room temperature and LNT ESR spectra were recorded at RSIC, IIT, Chennai, India. The IR spectra of the complexes in the range 4000-200 cm^{-1} were recorded in KBr on Perkin-Elmer 621.

Synthesis of oxovanadium(IV) complexes

In order to prepare $[VO(mac)]SO_4$, an ethanolic solution of vanadyl sulfate (2 mmol, 1.630 g) was added gradually to a refluxing solution of 1,1'-oxalyldiimidazole (2 mmol, 0.380 g) and *o*-phenylenedimine (4 mmol, 0.432 g) in ethanol (50 mL) in RB flask (Scheme 1). The color of the reaction mixture turned into dirty green after mixture was refluxed for 2 h. Precipitate was filtered off and washed with cold ethanol. Solid product was dried under in vacuum

desicator over silica gel. Purity of the complex was checked by TLC (yield: 55 %, type I). Ethanolic mixture of type I complex further reacted for 2 h with β-diketones (such as acetylacetone, benzoylacetone, thenoyltrifluoroacetone or dibenzolylmethane) in ratio 1:1 to get macrocyclic complex (type II). The purity of the macrocyclic product was checked by TLC.

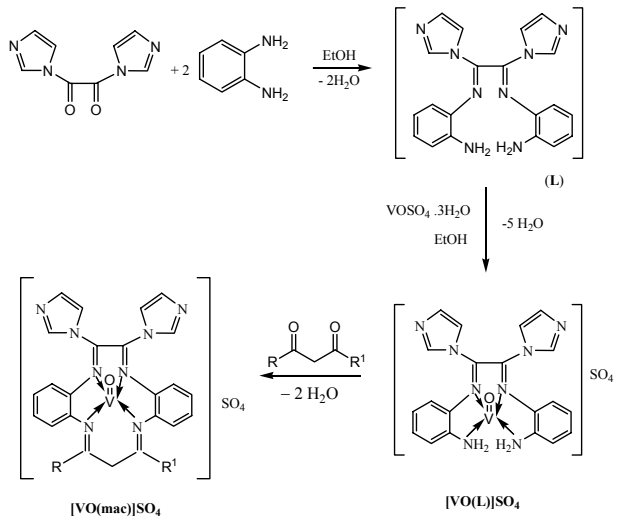

Scheme 1. Synthesis of oxovanadium(IV) complexes.

[VO(L)]SO_4

Yield 45 %. F. W. 533.42. Decomposition temp. 218 °C. IR (KBr): 1624 (C=N), 304 (V-N), 982 (V=O), 1140 (SO_4^-), 958 (SO_4^-), 608 (SO_4^-), 3350 (N-H_{asym}), 3179 (N-H_{sym}) cm^{-1}. Anal. Calcd. for $C_{20}H_{18}N_8VSO_5$: C 45.0, H 3.4, N 21.0, V 9.6, S 6.0 Found: C 44.9, H. 3.3, N 20.9, V 9.6, S 5.9. μeff. BM (300 °C): 17.6.

[VO(mac^1)]SO_4

Yield 50 %. F. W. 517.47. Decomposition temp. 221 °C. IR (KBr): 1620 (C=N), 303 (V-N), 980 (V=O), 1133 (SO_4^-), 955 (SO_4^-), 604 (SO_4^-) cm^{-1}. Anal. Calcd. for $C_{23}H_{20}N_8VSO_5$: C 48.3, H 3.5, N 19.6, V 8.9, S 5.6 Found: C 48.3, H. 3.8, N 19.5, V 8.8, S 5.5. μeff. BM (300 °C): 17.2.

[VO(mac^1)]SO_4

Yield 48 %. F. W. 633.54. Decomposition temp. 217 °C. IR (KBr): 1618 (C=N), 300 (V-N), 980 (V=O), 1133 (SO_4^-), 956 (SO_4^-), 602 (SO_4^-) cm^{-1}. Anal. Calcd. for $C_{28}H_{22}N_8VSO_5$: C 53.1, H 3.5, N 17.7, V 8.0, S 5.1 Found: C 52.7, H. 3.4, N 18.0, V 7.9, S 5.0. μeff. BM (300 °C): 17.1.

[VO(mac^3)]SO_4

Yield 55 %. F. W. 693.54. Decomposition temp. 220 °C. IR (KBr): 1622 (C=N), 302 (V-N), 982 (V=O), 1134 (SO_4^-), 955 (SO_4^-), 604 (SO_4^-) cm^{-1}. Anal. Calcd. for $C_{26}H_{17}N_8VS_2O_5F_3$: C 45.0, H 2.5, N 16.2, V 7.4, S 9.3 Found: C 44.9, H. 2.4, N 16.1, V 7.3, S 9.2. μeff. BM (300 °C): 17.2.

[VO(mac^4)]SO_4

Yield 55 %. F. W. 695.61. Decomposition temp. 229 °C. IR (KBr): 1622 (C=N), 302 (V-N), 984 (V=O), 1133 (SO_4^-), 956 (SO_4^-), 602 (SO_4^-) cm^{-1}. Anal. Calcd. for $C_{33}H_{24}N_8VSO_5$: C 57.0, H 3.5, N 16.1, V 7.3, S 4.6 Found: C 56.5, H. 3.4, N 16.0, V 7.3, S 4.5. μeff. BM (300 °C): 17.5.

where, L = Ligand derived by condensation of 1,1'-oxalyldiimidazole with o-phenylenediamine (1:2), mac^1 = macrocyclic ligand derived by condensation of L with acetylacetone, mac^2 = macrocyclic ligand derived by condensation of L with benzoylacetone, mac^3 = macrocyclic ligand derived by condensation of L with thenoyltrifluoroacetone, mac^4 = macrocyclic ligand derived by condensation of L with dibenzoylmethane.

Results and Discussion

The oxovanadium(IV) complexes were synthesized by initially refluxing the reaction mixture of 1,1'-oxalyldiimidazole with o-phenylenediamine and vanadyl sulfate in 1:2:1 molar ratio in aqueous ethanol and then reacting the products with β-diketones. The reactions appear to proceeds according to the Scheme 1. Elemental analyses of the complexes, given above, proved 1:1 molar ratio of metal to ligand stoichiometry.

Infrared Spectra

The important bands of the infrared spectra for the complexes have been given above. The oxovanadium(IV) exhibit >C=N absorption around 1624-1618 cm^{-1}, which normally appears at 1660 cm^{-1} in free ligands.[14-16] The lowering of this frequency in the complex [VO(L)]SO_4 indicate the coordination of nitrogen atoms of the azomethine groups to the vanadium.[16-18] The presence of a band around 300 cm^{-1} may be show ν (V-N) vibration.[19] The presence of >C=N band and the absence of the >C=O band at around 1700 cm^{-1} indicates the condensation of the o-phenylediamine with the keto group of 1,1'-oxalylimidazoles.[18] The band appearing at 3350 and 3179 cm^{-1} may be assigned to asymmetrical and symmetrical N-H stretching modes of the coordinated terminal amino group of the o-phenylediamine.[20] The complexes show a band at around 980 cm^{-1}, which is assigned to ν(V=O) vibration.[21] The presence of SO_4^{2-} group in the complexes is indicated by the appearance of three bands at ca. 1133-1140 cm^{-1} (ν_3), 955-958 cm-1 (ν_1) and 602-608 cm^{-1} (ν_4). The absence of a ν_2 band and non-splitting band of ν_3 band indicate the retention of tetrahedral symmetry.[22] The IR spectra of the complexes of the type [VO(mac)]SO_4 show the same pattern of bands but the asymmetrical and symmetrical N-H stretching modes of terminal amino groups disappear due to condensation of these amino groups with carbonyl groups of β-diketones in cyclization reactions.

Electronic Spectra

The electronic spectra exhibit bands in the regions 11,080 – 12,020 cm^{-1}, 15,120 - 15,900 cm^{-1} and 21,095-22,030 cm^{-1}. These spectra are similar to other four coordinate oxovanadium(IV) complexes involving nitrogen donor atoms. These spectral bands are evaluated according to an energy level scheme reported by Tsuchimoto et al[22] for distorted, five coordinate square pyramidal oxovanadium(IV) complexes.[23] The observed bands can be assigned to $^2B_2 \rightarrow {}^2E$, $^2B_2 \rightarrow {}^2B_1$ and $^2B_2 \rightarrow {}^2A_1$ transitions, respectively. One band is also observed in the region 35,200 – 35,750 cm^{-1}, which may be due to transition of the azomethine linkages.[24]

Molar Conductance

The molar conductance values (Λ_M) of the oxovanadium(IV) complexes were measured in DMF and the obtained values are between 80-110 ohm^{-1} cm^2 mol^{-1} indicating their 1:1 electrolytic nature.

Magnetic Moment

Effective magnetic moments (μ_{eff}) values of the complexes were measured at room temperature and the observed values were lie in the range 1.71-1.76 B.M. which are in agreement to a $3d^1$-system of square-pyramidal oxovanadium(IV) centre.[23]

ESR Spectra

The X-band ESR spectra of the complexes were recorded in DMSO at room temperature and at LNT (177 K). ESR spectra of the oxovanadium(IV) complexes were analyzed by the method of Mishra, Tan and Ando et al.[25-27] The room temperature ESR spectra show eight lines, which are due to hyperfine splitting originating from the interaction of the unpaired electron with a ^{51}V nucleus having the nuclear spin, $I = 7/2$. This nuclear spin confirms the presence of a single oxovanadium(IV) cation as the metallic centre in the complexes. The anisotropy is not observed due to rapid tumbling of molecules in solution at room temperature and only g-average values at about 1.902 are recorded. The anisotropy is clearly visible in the spectra at LNT and eight bands each due to $g\|$ and $g^{\perp}$ are observed at about 1.920 and 1.985 separately which are corresponds to a square pyramidal structure.[28-30] The $g\|$, $g^{\perp}$, $A\|$ and $A^{\perp}$ values are recorded from the spectra, which are in good agreement for a square-pyramidal structure. Further, g values of all very close to the spin-only value (free electron value) of 2.0020, suggesting little spin-orbit coupling. On the basis of the above studies, the tentative structures are proposed for these oxovanadium(IV) complexes of the type $[VO(L)]SO_4$ and $[VO(mac)]SO_4$ is given in the Scheme 1.

Conclusions

The present investigation demonstrates simple synthetic routes to 5 new oxovanadium(IV) complexes with tetraaza macrocyclic ligands. The spectral data suggest that the 1,1'-oxalyldiimidazole is good chelating agents having two reactive carbonyl groups capable of undergoing Schiff base condensation with o-phenylenediamine. Schiff bases prepared by condensation of 1,1'-oxalyldiimidazole with o-phenylenediamine behave as tetradentate ligands by bonding to the metal ion through the azomethine nitrogen and amino group. The analytical data show the presence of one metal ion per ligand (1:1 metal and ligand) molecule and suggest a mononuclear structure for the VO^{2+} complexes. The electrical conductance, magnetic moment values, infrared, ESR and electronic spectral data indicated a square pyramidal structure for VO(IV) complexes. X-ray crystallographic data of the synthesized oxovanadium(IV) complexes, which might have confirmed the tentative structures, could not be possible because suitable crystals were not isolated.

Acknowledgements

The authors are thankful to the Director, NERIST, Nirjuli, Itanagar, Arunachal Pradesh, India for providing laboratory facilities and Central Research Facility for microanalysis of carbon, hydrogen and nitrogen.

The author(s) declare(s) that there is no conflict of interest regarding the publication of this paper.

References

[1]Mohamed, G. G., *Spectrochim.. Acta A,* **2006**, 64, 188.

[2]Kilic, A., Tas, E., Deverec, B., Yilmaz, I., *Polyhedron,* **2007**, 26, 4009.

[3]Prakash, A., Singh, B. K., Bhojak, N., Adhikari, D., *Spectrochim. Acta A,* **2010**, 76, 356.

[4]Mourya, R. C., Rajput, S., *J. Mole. Struc.,* **2006**, 794, 24.

[5] Shi, L., Mao, W. J., Yang, Y., Zhu, H. L., *J. Coord. Chem."* **2009**, 62, 3471.

[6] Mohamed, G. G., Abd El-Wahab, Z. H., *Spectrochim. Acta A*, **2005**, 61, 1059.

[7]Travnicek, Z., Malon, M., Sindelar, Z., Dolezal, K., Rolcik, J., Krystof, V., Strnad M., Marek, J., *J. Inorg. Biochem.*, **2001**, *84*, 23-32.

[8] Selbin, J., *Coord. Chem. Rev.,* **1966**, *1*, 293.

[9]Cutler, A. R., Alleyne, C. S., Dolphin, D., *Inorg. Chem.,* **1985**, *24*, 2281.

[10]Malek, A., Fresco J. M., *Can. J. Chem.,* **1973**, *51*, 1981.

[11]Prasad, R. N., Agrawal, M., Sharma, S., *J. Serb. Chem. Soc.,* **2005**, *70*, 54.

[12]Vogel, A. I., "*A Text Book of Quantitative Inorganic Analysis*" 4th ed., Longmans Green Co. Ltd., London, **1978**.

[13]Vogel, A. I., "*A Text Book of Practical Organic Chemistry"*, 4th ed., Longman, London, **1978**.

[14]Rana, V. B., Singh, P., Singh, D. P., Teotia, M. P., *Trans. Met. Chem*., **1982**, *7*, 174.

[15]Sreeja, P. B., Kurup, M. R. P., *Spectrochim. Acta Part A*, **2005**, *61*, 331.

[16]Yadava, H. D. S., Sengupta, S. K., Tripathi, S. C., *Inorg. Chim. Acta*, 1987, 128, 1.

[17]Ferraro, J. R., "*Low Frequency Vibrations of Inorganic and Coordination Compounds*," Plenum Press, New York, NY, USA, **1971**.

[18]Nakamoto, K.., "*IR and Raman Spectra of Inorganic and Coordination Compound, Part A and B*," John Wiley & Sons, New York, NY, USA, **1998**.

[19]Sakata, K., Kuroda, M., Yanagida, S., Hashimoto, M., *Inorg. Chim. Acta*, **1989**, *156*, 107.

[20]Nonoyama, M., Tomita, S., Yamasaki, K.., *Inorg. Chim. Acta*, **1975**, *12*, 33.

[21]Samanta, S., Ghosh, D., Mukhopadhyay, S., Endo, A., Weakley, T. J. R., Chaudhury, M., *Inorg. Chem*., **2003**, *42*, 1508.

[22]Tsuchimoto, M., Hoshina, G., Yoshioka, N., Inoue, H., Nakajima, K., Kamishima, M., Kojima, M., Ohba S., *J. Solid State Chem*., **2000**, *153*, 9.

[23]Sarkara, A., Pal, S., *Inorg. Chim. Acta*, **2008**, *361*, 2296.

[24]Christos, A., Kontogiorgi, Dimitra, J., Hadjipavlou-Litina, *Bioorg. Med. Chem. Lett*., **2004**, *14*, 611.

[25]Mishra, A. P., Pandey, L. R., *Indian J. Chem. A*, **2005**, *44 A*, 94.

[26]Tan, R., Li, C., Peng, Z., Yin, D., Yin, D., *Catalysis Commun*., **2011**, *12*, 1488.

[27]Ando, R., Nagai, M., Yagyu, T., Masunobu, *Inorg. Chim. Acta*, **2003**, *351*, 107.

[28]Dodwad, S. S., Dhamnaskar, R. S., Prabhu, P. S., *Polyhedron*, **1989**, 8, 1748.

[29]Rao, S.N., Mishra D. D., Maurya R. C., Rao, N. N., *Polyhedron*, **1997**, 16, 1825.

[30]Boucher, L. J., Yen, T. F., *Inorg. Chem*., **1969**, 8, 689.

Received: 21.07.2015.
Accepted: 02.08.2015.